



**HAL**  
open science

# Améliorations de l'accès paquet en sens montant du WCDMA

Konstantinos Dimou

► **To cite this version:**

Konstantinos Dimou. Améliorations de l'accès paquet en sens montant du WCDMA. domain\_other. Télécom ParisTech, 2003. Français. NNT: . pastel-00000671

**HAL Id: pastel-00000671**

**<https://pastel.hal.science/pastel-00000671>**

Submitted on 26 Nov 2010

**HAL** is a multi-disciplinary open access archive for the deposit and dissemination of scientific research documents, whether they are published or not. The documents may come from teaching and research institutions in France or abroad, or from public or private research centers.

L'archive ouverte pluridisciplinaire **HAL**, est destinée au dépôt et à la diffusion de documents scientifiques de niveau recherche, publiés ou non, émanant des établissements d'enseignement et de recherche français ou étrangers, des laboratoires publics ou privés.

# **Améliorations de l'accès paquet en sens montant du WCDMA**

Konstantinos Dimou

April 17, 2004

To my parents Dimitrios and Morfoula and to my sister Irini.

# Acknowledgments

This Ph.D. thesis is the result of a four-year research project carried out in two institutions: the first half of it has been conducted in the Département Informatique et Réseaux of École Nationale Supérieure des Télécommunications (ENST) Paris, France and the second half has been done in the Department of Communication Technology of Aalborg University (AAU), Denmark. The work in ENST has been performed under the direction of Professor Philippe Godlewski. In AAU my work has been conducted under the direction of my main supervisor Professor Preben E. Mogensen and of my co-supervisors Dr. Troels B. Sørensen and Dr. Jeroen Wigard (Nokia Networks).

I would like to thank professors Xavier Lagrange and Jens Zander for accepting to be the reviewers of my PhD thesis. Their comments and suggestion helped to improve this thesis. A special thanks is also given to the members of the jury Prof. Bernard Fino, Dr. Claudiu Mihailescu and to the president of the jury Prof. Djamal Zeghlache.

A significant number of people has contributed to this work. First, I express my gratitude to my main supervisors Professors P. Godlewski and P. E. Mogensen for accommodating me in their groups. The work with Prof. P. Godlewski is going to be a very useful experience for my professional life. Special thanks goes to Prof. P. Mogensen for his encouragement, support and patience he has shown to me throughout our discussions.

For discussions and suggestions I would like to thank my colleagues in the Cellular Systems (CSys) group at Aalborg University and at Nokia Networks in Aalborg. Special esteem goes to T. B. Sørensen for his patience in listening me and for his wise advices. For assistance with the implementation of simulators and for simulation campaigns, I would like to thank Claudio Rosa and José Outes Carnero. For the same reason, also thanks to master students Malek Boussif and Alberto Ramos. I feel thankful to Lisbeth Larsen for facilitating my everyday life: on every request of mine regarding administrative issues, she was there always with a smile.

This work has been sponsored by the french national network of research in telecommunications (Réseau Nationale de Recherche en Télécommunications, RNRT) and by Nokia; a thanks goes to them for their financial support.

I deeply acknowledge the help of my friends throughout these years. I am particularly thankful to my friend Artur Hecker for his support and encouragement he gave me during our numerous and long discussions. I fully recognize the significance of the support that Marisa Cangelosi and Evdoxia Baniotopoulou gave me for a long period.

Finally, I express my profound gratitude to my parents Dimitrios and Morfoula and to my sister Irini for their unconditional love and support. Without their continuous encouragement, the chances of this work being accomplished would be very few. This work is dedicated to them.

## Resumé

Les systèmes de troisième génération (3G) commencent à apparaître en Europe et ailleurs. Le mode d'accès utilisé sur l'interface radio de ces systèmes est le CDMA (*Code Division Multiple Access*). En Europe, le système de 3G en déploiement est l'UMTS (*Universal Mobile Telecommunications System*), qui emploie le WCDMA (*Wideband CDMA*) pour sa partie d'accès radio.

Une évolution majeure des systèmes de 3G en comparaison avec ceux de deuxième génération (2G) est la possibilité des services de haut débit. Ceci permet l'introduction des nouveaux services et notamment des services de données. Il est envisagé que les services de données formeront la plus grande partie du trafic écoulé dans les réseaux de 3G. Il est prévu que ces services vont coexister avec la parole, déjà présente aux systèmes de 2G. Par conséquent, des scénarios de trafic mixte doivent être considérés. L'existence des différents types de trafic augmente la complexité de la gestion des ressources radios.

Dans cette thèse on étudie l'accès par paquet en UMTS. L'étude se concentre sur le sens montant de la transmission, c'est à dire du mobile (*User Equipment* ou UE) vers le réseau. En sens montant, la ressource radio rare est la puissance reçue à la station de base ou Node B (selon la terminologie UMTS). Le but de notre travail est d'améliorer certains mécanismes de l'accès par paquet afin d'optimiser l'utilisation de la puissance.

Le premier mécanisme de l'accès par paquet pour lequel un effort d'amélioration est fait, est l'adaptation du lien radio. En particulier, l'accent est mis sur le cas de la transmission multiservice. L'UE doit partager le débit global qui lui est alloué entre les différents services activés. Ces derniers sont véhiculés dans des *radio bearers* (tuyaux supports). À chaque intervalle élémentaire de transmission (*Transmission Time Interval* ou TTI), l'UE sélectionne un sous-débit pour chaque *bearer* ; ceci se fait par la sélection d'un "format de transport" à appliquer pendant la durée TTI. Cette procédure s'effectue dans la couche MAC (*Medium Access Control*) ; le résultat de la sélection est une combinaison de formats de transport (*Transport Format Combination*, TFC) utilisée par la couche physique. La procédure, nommée sélection de TFC, permet d'adapter la transmission des différents services aux conditions variables de la propagation radio : elle détermine notablement la performance de la transmission.

L'algorithme de sélection de TFC est tracé dans ses grandes lignes dans la norme. Un de ses principes est de favoriser le trafic temps réel au détriment des services des données par paquet. Cependant, le trafic temps réel peut être perturbé par le trafic données sous certaines conditions, en particulier pour les mobiles éloignés du Node B. On propose un algorithme de sélection de TFC qui limite ces perturbations et qui offre une plus large zone de couverture aux services temps réels.

Un autre type de mécanisme étudié concerne l'ordonnancement de paquets entre les différents utilisateurs. C'est une procédure qui est contrôlée par la partie fixe du réseau. Son impact sur les performances du système est étudié en détail et évalué à l'aide de simulations. Ensuite, le potentiel de trois mécanismes visant à améliorer l'ordonnancement de paquets est évalué. Un premier mécanisme est nommé *fast Variable Spreading Factor* (*fast VSF*) : les UEs distants changent rapidement leur facteur d'étalement (SF) afin de conserver une puissance de transmission constante, ce qui stabilise l'interférence intercellulaire. Un deuxième mécanisme étudié est un accès paquet décentralisé (*decentralized*

*mode*) utilisant une information en retour sur le niveau global d'interférence dans la cellule. Un troisième mécanisme nommé "*fast scheduling*" (ordonnancement rapide) raccourcit le cycle d'ordonnancement. Les résultats ont montré que sous certaines conditions, le mode décentralisé réduit le délai par paquet jusqu'à 25%. L'ordonnancement rapide augmente la capacité du système jusqu'à 10%. De plus, l'ordonnancement rapide améliore la qualité de service perçue par les utilisateurs en terme de débit par utilisateur et délai par paquet transmis.

Cette dissertation est composée de six chapitres. Le premier chapitre sert comme l'introduction générale de la thèse. Le cadre du travail est présenté : au début une description générale de l'UMTS est donnée. Elle est suivie par une description des services et des classes de services en UMTS. La notion de Qualité de Service (QoS) en UMTS est aussi présentée. La modélisation du trafic et en particulier du trafic des données par paquet joue un rôle important à notre travail. Pour cette raison, la partie suivante du chapitre traite ce sujet. Ensuite, le but du travail est manifesté : optimiser l'utilisation des ressources radios afin d'augmenter la capacité du système et d'améliorer la QoS offerte aux utilisateurs. De plus, cette partie du chapitre présente les travaux antérieurs ainsi que la littérature associée au sujet. Le chapitre termine avec une description générale de la structure du rapport de thèse.

Le deuxième chapitre comporte comme une présentation générale du réseau d'accès radio de l'UMTS (*UMTS Terrestrial Radio Access Network*, UTRAN). Le chapitre commence avec une description de l'architecture protocolaire de l'UTRAN. Les protocoles qui composent la pile protocolaire de l'UTRAN sont brièvement décrits ainsi que leurs fonctions principales. Les différents types de canaux en UMTS sont aussi présentés : les canaux logiques, les canaux de transport et les canaux physiques. La description se focalise sur les canaux de transport qui constituent une nouveauté de l'UMTS par rapport aux systèmes de 2G. De plus, ce concept de canal de transport est largement utilisé dans le travail. Les définitions du format de transport (*Transport Format*, TF), de la combinaison des formats de transport sont données. Le mécanisme de sélection du TFC est aussi décrit. La fin du chapitre est dédiée à la description d'une autre caractéristique de la couche physique de l'UTRAN qui est largement utilisée dans ce travail : le changement de facteur d'étalement. Dans le sens montant, les UEs sont autorisés à changer leur facteur d'étalement et par conséquent leur débit à chaque TTI afin d'adapter leur lien radio. Ce trait est nommé dans les normes 3GPP *Variable Spreading Factor* (VSF).

Le chapitre 3 traite le sujet de l'adaptation du lien radio à la couche MAC. Ceci s'effectue par la sélection du TFC, comme il est cité auparavant. Le chapitre commence avec une description de la couche MAC. Ensuite la configuration et le fonctionnement de la couche MAC dans le cas de la transmission multiservice en sens montant sont exposés. La sélection du TFC présente un plus grand intérêt au cas de la transmission multiservice. Ensuite, l'algorithme de sélection de TFC, tel qu'il est tracé dans les normes 3GPP est décrit ; dans le cas de transmission de plusieurs services, la sélection du TFC est basée principalement sur la priorité des services. Les performances de l'algorithme sont évaluées à l'aide de simulations. Le modèle de simulation est décrit en détail dans les paragraphes suivants du chapitre. Le scénario simulé contient trois types de trafic : i) de la voix, ii) des données par paquet et iii) de la signalisation. Parmi ces types de trafic, la voix a la plus grande priorité. Les plus importantes mesures de performance sont le taux

d'erreurs pour tous les types de trafic, le délai par paquet pour le trafic des données, le débit total de l'UE et la puissance transmise par l'UE. Les mesures sont prises en fonction de la distance entre l'UE et le Node B. Les résultats des simulations montrent que le taux d'erreur augmente très rapidement après une certaine distance entre l'UE et le Node B. Ce qui a comme résultat la perte du service de la parole. Ceci s'effectue à une distance considérablement plus courte que celle au cas où seulement la parole et la signalisation sont transmises. Ceci est dû au mécanisme du contrôle de puissance. En particulier, pendant la transmission simultanée de la parole et des données, où la puissance de transmission est assez élevée, les commandes de contrôle de puissance exigent souvent que l'UE transmette avec la puissance maximale. L'UE se rend alors incapable de suivre les commandes postérieures de contrôle de puissance et de maintenir son lien radio. Une variante de l'algorithme de sélection de TFC est proposée. Le nouvel algorithme est sur ses grandes axes similaire avec l'algorithme décrit dans les normes. L'algorithme introduit une nouvelle marge à la puissance de transmission. Cette marge est considérée uniquement au cas où la parole et les données sont transmises simultanément. Son but principal est de protéger la transmission de la parole. Les simulations ont montré que le nouvel algorithme présente des meilleures performances en comparaison de l'algorithme de la norme en terme de taux d'erreur pour tous les services, de délai par paquet, de débit total et en terme de puissance de transmission. L'algorithme est testé pour un certain scénario de trafic; néanmoins, des résultats similaires sont attendus pour d'autres scénarios de trafic.

Le chapitre 4 examine l'accès par paquet en sens montant de l'UMTS. Le chapitre commence avec la description générale de la procédure de l'accès par paquet. Ensuite les mécanismes principaux de la procédure sont décrits : i) l'envoi de requêtes des UEs vers le réseau sous la forme de reports de mesures de volume de trafic (*Traffic Volume Measurement Reports*, TVMR), ii) l'ordonnancement de paquets, sur le côté réseau et iii) la sélection de TFC, sur le côté UE. L'accent est mis à la description de l'ordonnancement de paquets. Plus particulièrement, la description suit deux axes : d'un part, l'algorithme d'ordonnancement par paquet est décrit en détail. L'algorithme essaye de faire une allocation équitable des ressources disponibles. De l'autre part, les problèmes liés à l'allocation de puissance pendant l'ordonnancement de paquets sont traités. À la suite du chapitre, le modèle de simulation est détaillé. Le modèle consiste en un réseau cellulaire de 24 cellules. Les plus importants mécanismes des couches basses y sont considérés. Le service qui est simulé est un service de jeu sur internet. Les résultats des simulations montrent que pour le modèle et pour le service simulé la capacité du système est 1.27 Mbps ; le système peut offrir une acceptable qualité de service à 20 UEs environ par cellule.

Le chapitre 5 présente les améliorations proposées de l'accès par paquet en sens montant. Ces améliorations visent à : i) augmenter la capacité du système et ii) améliorer certains attributs de la QoS offerte aux utilisateurs, par exemple, le délai par paquet transmis. Comme il est cité auparavant, les trois améliorations proposées sont : i) le changement rapide du facteur d'étalement (*fast VSF*), ii) l'accès paquet décentralisé et iii) l'ordonnancement de paquets rapide.

Le schéma *fast VSF* propose que les UE's changent rapidement leur facteur d'étalement afin de conserver leur puissance de transmission stable. Ceci résulte en une réduction de la variance de l'interférence aux cellules voisines (interférence inter-cellulaire). En revanche, la variance de l'interférence à la cellule servante (interférence intra-cellulaire) augmente.

Le compromis entre les deux tendances et son impact sur la variance de l'interférence globale du système est étudié. Une réduction de la variance de l'interférence globale permettra l'augmentation de l'interférence cible et par équivalence de la puissance reçue cible au Node B. Ceci se traduit en une augmentation de la capacité du système. Pour le modèle de simulation utilisé, les résultats ont montré que le fast VSF n'apporte pas de gain significatif. Une des raisons principales pour cela est que les différentes restrictions sur la sélection du TFC ne permettent pas aux UEs de stabiliser leur puissance de transmission et par conséquent de diminuer la variance de l'interférence aux cellules adjacentes.

En mode d'accès décentralisé, les UE ont plus de liberté à la sélection de leur TFC et par équivalence de leur débit. Les UE gardent leur *bearers* ouverts pendant toute leur session. Les UE transmettent des données en fonction de la valeur de l'interférence globale ; cette valeur est périodiquement diffusée dans la cellule. Les résultats des simulations ont montré qu' en cas de charge de trafic faible ou moyenne dans la cellule, une réduction de 25% du délai par paquet des données est atteint.

L'ordonnancement de paquets rapide consiste à allouer et désallouer des débits plus fréquemment aux utilisateurs, par rapport au cas de référence. L'ordonnancement rapide est atteint en diminuant les valeurs de temporisateurs qui le contrôlent. Alors, la détection de non-usage de ressources des certains utilisateurs est effectuée plus rapidement ainsi que l'allocation de ces ressources aux autres utilisateurs. Les résultats des simulations ont montré qu'un gain de 10% en capacité est atteint.

Le chapitre 6 contient les conclusions du travail et il propose le travail à venir sur ce sujet.

## Abstract

Third generation (3G) cellular systems implement a new multiaccess technique, the Code Division Multiple Access (CDMA). In Europe, the 3rd generation system under deployment is the Universal Mobile Telecommunications System (UMTS). It utilizes, in its radio access part, the wideband CDMA standard.

The major evolution of 3G systems is the provision of high data rate services. Moreover, 3G networks offer the possibility to their users to have more than one simultaneous service. A packet-switched mode of data transport has been included in 3G systems from the beginning of their conception. It is anticipated that internet-related applications along with voice, are going to be the main sources of traffic in these systems. Consequently, the packet-switched mode coexists with the circuit-switched one, the latter being present already in second generation cellular networks.

Considering that the most restricting part of a wireless network is the radio access part, the provision of the requested Quality of Service (QoS) to a high number of users increases the requirement for an efficient utilization of radio resources both by the network and the users.

In this thesis, we mainly investigate the performance of packet data services in the radio access network of UMTS. We try to enhance a number of radio resource management (RRM) mechanisms that have an impact on the performance of packet data services. The proposed enhancements aim at optimizing the utilization of resources, which is expected to increase system capacity and consequently to improve the offered QoS to packet data users.

In UMTS however, packet data services are expected to coexist with voice, as mentioned above. Therefore, a part of the thesis deals with the performance of both real time traffic and packet data in case of mixed traffic scenarios.

The work focuses on the uplink direction of transmission, hence the transmission from the User Equipment (UE) to the network. A mechanism for which an enhancement attempt is performed is the radio link adaptation. In particular, the case of multi-service transmission is studied. The UE schedules its total allocated data rate to its activated services, that are circulating in its radio bearers. At each transmission time interval (TTI), the UE selects a part of its total data rate for each radio bearer: this is performed through selection of a "transport format" to be applied during the TTI. This procedure is performed in the MAC (Medium Access Control) layer; its output is a combination of transport formats (Transport Format Combination, TFC) used by the physical layer. The procedure, named TFC selection, permits to adapt the transmission of the various services to the changing radio propagation conditions: it determines heavily the services performance.

The guidelines of the TFC selection algorithm in uplink are presented in 3G standards. The principle of the algorithm is that it favors the transmission of real time traffic over packet data. However, the real time service may be degraded due to packet data under certain conditions, in particular for UEs far from the Node B. We propose a TFC selection

algorithm that minimizes this degradation and offers larger coverage area for the real time services.

A second mechanism under study is the packet scheduling among users. It is a procedure that is controlled by the network. Its impact on the system performance is investigated and quantified through system level simulations. We study the potential of certain features to increase the efficiency of the packet scheduling. A first feature is named fast Variable Spreading Factor (VSF): UEs far from the Node B, change rapidly their spreading factor in order to maintain their transmission power constant, which stabilizes the other cell interference. A second feature is a decentralized uplink packet data access using feedback information on the total interference in the cell. A third feature, called "fast packet scheduling", reduces the packet scheduling cycle. Results have shown that in cases of medium and low load, the decentralized access mode reduces the delay per packet up to 25%. Fast scheduling increases the system capacity up to 10%. Moreover, it improves the QoS experienced by the users in terms of throughput per user and delay per transmitted packet.

# Contents

<b>1</b>	<b>Introduction: Packet Access and Services in Third Generation Cellular Systems</b>	<b>1</b>
1.1	Scope . . . . .	1
1.2	UMTS Context . . . . .	2
1.3	Services and QoS Concept in UMTS . . . . .	5
1.3.1	UMTS Service Bearers . . . . .	5
1.3.2	Traffic Classes and QoS Attributes in UMTS . . . . .	6
1.3.3	Targeted QoS metrics . . . . .	8
1.4	Packet Data Traffic Modeling . . . . .	8
1.5	Aim of the PhD Thesis . . . . .	10
1.6	Overview of the PhD Dissertation . . . . .	13
<b>2</b>	<b>UMTS Radio Access Network (UTRAN): Protocol Architecture and Radio Access Bearers</b>	<b>15</b>
2.1	UTRAN Protocol Architecture . . . . .	15
2.1.1	Protocol Architecture . . . . .	16
2.2	Physical Layer . . . . .	18
2.2.1	Physical Channels . . . . .	19
2.2.2	Main Functions . . . . .	19
2.3	Radio Access Bearer Architecture . . . . .	21
2.4	Transport Channels . . . . .	23
2.4.1	Transport Format (TF) . . . . .	23
2.4.2	Transport Format Combination (TFC) . . . . .	24
2.4.3	Transport Format Combination Set (TFCS) . . . . .	25
2.4.4	Transport Format Combination Set Forming . . . . .	25
2.4.5	TFCS Notification to the Transmitter Side . . . . .	27
2.5	Physical Layer Processing . . . . .	27
2.6	Variable Spreading Factor . . . . .	28
2.7	Concluding Remarks . . . . .	29
<b>3</b>	<b>Radio Link Adaptation in Medium Access Control</b>	<b>30</b>
3.1	MAC Protocol Concept in UTRAN . . . . .	30
3.2	MAC Protocol Basic Features . . . . .	31
3.2.1	MAC layer primitives . . . . .	31

3.2.2	MAC Protocol PDUs . . . . .	34
3.3	Uplink Multi-traffic Transmission . . . . .	36
3.3.1	MAC layer functions in uplink transmission . . . . .	37
3.3.2	Uplink transmission procedure in MAC layer . . . . .	38
3.4	Transport Format Combination Selection . . . . .	40
3.4.1	3GPP Compliant Algorithm . . . . .	41
3.4.2	Alternative algorithms . . . . .	41
3.5	Simulation Model . . . . .	42
3.5.1	Traffic Sources Characteristics . . . . .	43
3.5.2	Simulation Parameters . . . . .	45
3.6	Simulation Results . . . . .	46
3.7	Conclusions and Discussion . . . . .	53
<b>4</b>	<b>Uplink Packet Data Access in WCDMA</b>	<b>55</b>
4.1	Introduction and Aim . . . . .	55
4.2	General Issues . . . . .	57
4.3	Capacity Requests . . . . .	58
4.4	Packet Scheduling . . . . .	60
4.4.1	Packet Scheduler Functioning . . . . .	62
4.4.2	Ranking of Capacity Requests . . . . .	64
4.4.3	Data Rate Downgrade . . . . .	64
4.4.4	Estimation of the Available Power for Scheduling . . . . .	64
4.4.5	Scheduling Policy . . . . .	65
4.4.6	Load Control . . . . .	67
4.5	Power Issues . . . . .	67
4.6	Simulator Description . . . . .	70
4.6.1	System Model . . . . .	70
4.6.2	Capacity Requests . . . . .	70
4.6.3	Packet Scheduling . . . . .	72
4.6.4	Transport Format Combination Selection . . . . .	73
4.6.5	Traffic Modeling . . . . .	74
4.7	Performance Metrics Used . . . . .	75
4.8	Simulation Results . . . . .	77
4.8.1	Impact of the TFC Elimination Mechanism . . . . .	77
4.8.2	Uplink Packet Data Access Performance . . . . .	82
4.9	Conclusions and Discussion . . . . .	86
<b>5</b>	<b>Enhancements of the Uplink Packet Data Access in WCDMA</b>	<b>87</b>
5.1	Motivation for Enhanced Uplink Packet Data Access and Goals . . . . .	87
5.1.1	On the System Capacity Increase . . . . .	88
5.1.2	Delay Reduction . . . . .	90
5.2	Fast Variable Spreading Factor . . . . .	90
5.2.1	Concept . . . . .	90
5.2.2	Preliminary Study on the Capability of the Fast VSF to Stabilize i-factor . . . . .	91

5.2.3	Implementation . . . . .	95
5.2.4	Simulation Parameters . . . . .	96
5.2.5	Simulation Results . . . . .	97
5.3	Decentralized Uplink Packet Data Access . . . . .	100
5.3.1	Motivation For Decentralized Uplink Packet Data Access . . . . .	100
5.3.2	Decentralized Uplink Packet Data Access Concept . . . . .	100
5.3.3	Simulated Cases . . . . .	103
5.3.4	Simulation Parameters . . . . .	103
5.3.5	Simulation Results . . . . .	104
5.4	Fast Packet Scheduling . . . . .	105
5.4.1	Concept . . . . .	106
5.4.2	Simulation Parameters . . . . .	106
5.4.3	Simulation Results . . . . .	107
5.5	Conclusion and Discussion . . . . .	110
<b>6</b>	<b>Conclusions and Further Work</b>	<b>111</b>
6.1	Conclusions . . . . .	111
6.2	Future Work . . . . .	112
<b>A</b>	<b>Simulators Description</b>	<b>i</b>
A.1	Fast Power Control . . . . .	ii
A.2	Outer Loop Power Control . . . . .	iii
<b>B</b>	<b>On the capability of the fast VSF to reduce the variance of the UE transmission power</b>	<b>vi</b>
B.1	Considerations on the TTI size and UE speed in relation with the fast fading characteristics . . . . .	vi
B.2	Simulation Studies and Results . . . . .	viii

# List of Figures

1.1	General UMTS architecture. . . . .	3
1.2	Principle of the uplink packet access in UTRAN. . . . .	4
1.3	Simplified Overview of the layered QoS architecture in UMTS. . . . .	6
1.4	Generic web browsing model. . . . .	9
1.5	Plan of Dissertation. . . . .	14
2.1	Radio Interface Protocol Architecture in UTRAN. . . . .	16
2.2	User Plane protocol stack in the case of establishment of dedicated channels between the UE and the network. . . . .	18
2.3	Control Plane protocol stack when dedicated channels are established between the UE and the network. . . . .	19
2.4	Code generation tree of the orthogonal variable spreading codes used in UTRAN. . . . .	20
2.5	Configuration of an UE supporting more than one radio bearers (user plane protocol stack). . . . .	22
2.6	Physical layer processing model for the uplink. Model based on the one in [67]. . . . .	28
3.1	Use of the four types of primitives. The numbers next to the primitive names indicate the order of their transmission. . . . .	32
3.2	MAC data PDU . . . . .	35
3.3	MAC protocol during uplink multi-traffic transmission. Transmission is done on dedicated logical and transport channels. . . . .	37
3.4	Uplink transmission in MAC layer in dedicated mode (UE side). . . . .	39
3.5	FER for various distances between the UE and the Node B. . . . .	48
3.6	Speech BLER for various distances between the UE and the Node B. . . . .	48
3.7	Percentage of lost IP packet for various distances between the UE and the Node B. . . . .	49
3.8	Mean UE transmission power for various distances between the UE and the Node B. . . . .	50
3.9	Probability of selected TFC for a distance to the Node B equal to 1400 m. . . . .	51
3.10	CDF of the UE transmission power for a distance to the Node B equal to 1400 m. . . . .	51
3.11	Percentage of correct-erroneous reception per selected TFC in the case of the 3GPP compliant algorithm. . . . .	52

3.12	Percentage of correct-erroneous reception per selected TFC in the case of the alternative TFC selection algorithm. . . . .	52
4.1	Division of the total received (Rx) power in uplink between RT and NRT traffic. . . . .	56
4.2	Overview of the Uplink Packet Data Access in WCDMA Uplink. . . . .	57
4.3	Timings in the Measurement Report sending procedure. . . . .	59
4.4	Packet Scheduling Working Environment (figure inspired from corresponding figure in [40]). . . . .	61
4.5	Time intervals in the packet scheduling procedure. . . . .	62
4.6	Functioning of the PS at each packet scheduling period. . . . .	63
4.7	Packet Scheduling Algorithm. . . . .	66
4.8	Estimation of the new total received power due to the change of the load of a user. . . . .	69
4.9	Network layout consisted of three-cell sector configuration with directional antennas. . . . .	72
4.10	Transport Format Combination Selection Procedure. . . . .	74
4.11	A simple modeling approach to include closed loop transmission model. . . . .	74
4.12	Probability of selected TFC for all of the users in the system (TFC Elimination “On and “Off”, 8 users per cell, cell radius 933 m). . . . .	78
4.13	CDF of the UE transmission power (TFC Elimination “On and “Off”, 8 UEs per cell, cell radius 933 m). . . . .	78
4.14	PDF of the noise rise (TFC Elimination “On and “Off”, 8 UEs per cell, cell radius 933 m). . . . .	79
4.15	Probability of selected TFC for all of the users (TFC Elimination “On and “Off”, 8 users per cell, cell radius 1866 m). . . . .	79
4.16	PDF of the noise rise (TFC Elimination “On” and “Off”, 8 UEs per cell, cell radius 1866 m). . . . .	80
4.17	FER as a function to the distance from the serving BS (TFC Elimination “On” and “Off”, 8 UEs per cell, cell radius 1866 m). . . . .	80
4.18	CDF of the Eb/No target (TFC Elimination Mechanism “On” and “Off”, 8 UEs per cell, cell radius 1866 m). . . . .	81
4.19	PDF of the noise rise (TFC Elimination “On” and “Off”, 8 UEs per cell, cell radius 1866 m). . . . .	82
4.20	PDF of the noise rise (32 UE per cell, weighting factor for inactive users (WFIU) is set 0, 0,5 and 1 respectively). . . . .	83
4.21	Mean Cell Throughput for different number of UEs in the cell. . . . .	84
4.22	Probability of selected TFC for the cases of 8, 20 and 32 users per cell. . . . .	84
4.23	PDF of the noise rise for the cases of 8, 20 and 32 UEs per cell. . . . .	85
5.1	Basic concept of the fast VSF scheme. . . . .	91
5.2	UE at the cell border. . . . .	92
5.3	Implementation of the fast VSF scheme. . . . .	95
5.4	CDF of i-factor (fast VSF “On” and “Off”, 12 UEs per cell, traffic model scenario B). . . . .	97

5.5	PDF of the noise rise (fast VSF “On” and “Off”, 12 UEs per cell, traffic model scenario B). . . . .	98
5.6	CDF of the experienced delay per packet call (fast VSF “On” and “Off”, 12 UEs per cell, traffic model scenario B). . . . .	99
5.7	Average UE throughput during activity period (fast VSF “On” and “Off”, 12 UEs per cell, traffic model scenario B). . . . .	99
5.8	Motivation for the proposal of the decentralized scheme. . . . .	101
5.9	Packet data transmission mechanism in the decentralized scheme. . . . .	102
5.10	CDF of the experienced delay per IP packet, for the cases of the centralized and decentralized schemes (10 UEs per cell). . . . .	104
5.11	CDF of the UE transmission power, for the cases of the centralized and decentralized schemes. . . . .	105
5.12	PDF of the noise rise, for the cases of the centralized and decentralized schemes. . . . .	105
5.13	Probability of selected TFC for all of the users in the system, for the cases the packet scheduling period is 500 and 100 ms, (columns 1 and 2 respectively, 32 UEs per cell, traffic model scenario A). . . . .	107
5.14	PDF of the noise rise, for the cases the packet scheduling period is 500 and 100 ms (12 UEs per cell, traffic model scenario B). . . . .	108
5.15	CDF of the delay per packet call, for the cases the packet scheduling period is 500 and 100 ms (12 UEs per cell, traffic model scenario B). . . . .	109
5.16	Probability of selected TFC for all of the users, for the cases the packet scheduling period is 500 and 100 ms, (columns 1 and 2 respectively, 12 UEs per cell, traffic model scenario B). . . . .	109
A.1	Model of errors of the power control command . . . . .	ii
A.2	Model of the outer loop power control in uplink. . . . .	iii
A.3	General Model of the outer loop power control. . . . .	iv
A.4	Pseudo-code of the simulated model of the outer loop power control. . . . .	v
B.1	Fast fading in relation with the TTI size. . . . .	vii
B.2	Envelope autocorrelation of fast fading in Clarke’s scattering model ([55]). . . . .	viii
B.3	Standard deviation of the UE transmission power versus UE speed for the cases the fast VSF is deactivated and activated. . . . .	x

# List of Tables

1.1	UMTS traffic classes and their requirements in terms of delay and error free delivery of the information elements. . . . .	7
2.1	Example of a Transport Format Set . . . . .	24
2.2	Transport channel attributes. . . . .	25
2.3	Dynamic attributes of a Transport Format Combination Set (TFCS). . . . .	26
3.1	Parameter settings of the “Modified Gaming” traffic model. . . . .	44
3.2	Simulation main parameters . . . . .	45
3.3	Attributes of the transport channles used in the simulation. Parameter values are in line with the ones in [82]. . . . .	46
3.4	The TFCS used in the simulation. . . . .	47
3.5	Total UE throughput for the distances of 1200m to 1400 m for in case of the 3GPP compliant and the alternative TFC selection algorithms. . . . .	49
3.6	BLER for speech, percentage of lost IP Packets and mean UE throughput for the case of the 3GPP compliant algorithm and when a TFC Elimination Offset of 4 dB is applied. . . . .	53
4.1	Most important simulation parameters. . . . .	71
4.2	Capacity requests related parameters. . . . .	73
4.3	Parameters of the implemented packet scheduling function. . . . .	73
4.4	Parameter settings of the “Modified Gaming” traffic model. . . . .	75
4.5	Cell Throughput, UE throughput FER for the cases TFC Elimination is “On” and “Off”. The cell radius is 933 m and 1866 m. . . . .	81
4.6	Cell Throughput, UE throughput and FER (32 UEs per cell, WFIU is set to 0, 0,5 and 1). . . . .	83
4.7	Mean and standard deviation of the NR, Cell Throughput, UE throughput and delay per packet call for the cases of 8, 20 and 32 UEs per cell. . . . .	85
5.1	Mean and standard deviation of the received power in the serving Node B 1 and in an adjacent Node B, due to an UE at the borders of the cell. . . . .	94
5.2	Simulation parameters for the fast VSF scheme. . . . .	97
5.3	Cell Throughput, UE throughput and delay per packet call (fast VSF “On” and “Off”, 12 UEs per cell, traffic model scenario B). . . . .	99
5.4	Timing related parameters for the reference case and for the fast packet scheduling case. . . . .	106

5.5	Cell Throughput, UE throughput and delay per packet call for the cases of packet scheduling period equal to 500 ms and 100 ms, for both of the traffic model scenarios. . . . .	110
A.1	Parameters related to the fast power control function. . . . .	iii
B.1	Time required in order to have an auto-correlation equal to 0.7 and 0.5 for various UE speeds. . . . .	viii
B.2	Main simulation parameters. . . . .	ix

# Glossary

## A

AC	Admission Control
AMC	Adaptive Modulation and Coding
AMR	Adaptive Multi-Rate
AVI	Actual Value Interface

## B

BCH	Broadcast Channel
BLER	Block Error Rate
BMC	Broadcast/Multicast Control

## C

CBR	Constant Bit Rate
CCTrCh	Coded Composite TRansport CHannel
CDF	Cumulative Density Function
CDMA	Code Division Multiple Access
CN	Core Network
CPCH	Common Packet Channel
CRC	Cyclic Redundancy Check
CS	Circuit Switched

## D

DCCH	Dedicated Control CHannel
DCH	Dedicated CHannels
DSCH	Downlink Shared Channel
DU	Data Unit

## F

FACH	Forward Access Channel
FDD	Frequency Division Duplex
FER	Frame Erasure Rate

## H

HARQ	Hybrid Automatic Repeat Request
HSDPA	High Speed Downlink Packet Access
HS-DPCH	High-Speed Downlink Physical Channel

## **I**

IP Internet Protocol

## **L**

LC Load Control

## **M**

MAC Medium Access Control

MMS Multimedia Message Service

## **N**

NR Noise Rise

NRT Non Real Time

## **O**

OLPC Outer Loop Power Control

OVSF Orthogonal Variable Spreading Factor

## **P**

PCH Paging Channel

PC Power Control

PDCP Packet Data Convergence Protocol

PDF Probability Density Function

PDU Protocol Data Unit

PS Packet Scheduler

Pw Power

## **Q**

QoS Quality of Service

QPSK Quadrature Phase Shift Keying

## **R**

RAB Radio Access Bearer

RACH Random Access Channel

RAN Radio Access Network

RF Radio Frequency

RLC Radio Link Control

RM	Rate Matching
RNC	Radio Network Controller
RNTI	Radio Network Temporary Identity
RNS	Radio Network Subsystem
RRC	Radio Resource Control
RRM	Radio Resource Management
RT	Real Time

## **S**

SAP	Service Access Point
SCH	Synchronization Channel
SF	Spreading Factor
SHO	Soft Handover
SMS	Short Message Service
Std	Standard Deviation

## **T**

TBS	Transport Block Size
TBSS	Transport Block Set Size
TCP	Transmission Control Protocol
TCTF	Target Channel Type Field
TD-CDMA	Time Division CDMA
TDD	Time Division Duplex
TF	Transport Format
TFC	Transport Format Combination
TFCI	TFC Identity
TFCS	Transport Format Combination Set
TFS	Transport Format Set
TTI	Transmission Time Interval
Tx	Transmission

## **U**

UE	User Equipment
UMTS	Universal Mobile Telecommunications System
UTRAN	UMTS Terrestrial Radio Access Network

## **V**

VSF	Variable Spreading Factor
-----	---------------------------

## **W**

WAP	Wireless Application Protocol
WCDMA	Wideband Code Division Multiple Access
WFIU	Weighting Factor for Inactive Users
WWW	World Wide Web

# Chapter 1

## Introduction: Packet Access and Services in Third Generation Cellular Systems

### 1.1 Scope

A classical problem in cellular networks is the control of multiple access of users to the physical medium. Among both directions of transmission, the uplink, i.e. the direction from the user to the network is the one that exhibits the highest scientific interest.

For circuit-switched services and in particular for voice, the multiple access issue in uplink has been resolved in the first and second generation of cellular systems ([36]). For packet-switched services, which have been considered from the conception of third generation (3G) cellular systems, the multiple packet access induces specific problems; in particular, in Code Division Multiple Access (CDMA) systems, where the management of power is a very important issue ([58]). In order to meet the needs in Quality of Service (QoS) of their different services, third generation wireless networks are required to perform an efficient management of power and of other scarce radio resources ([22]).

This thesis deals with the packet data access in the uplink (UL) in Universal Mobile Telecommunication System (UMTS). The latter one is the proposed 3G system in Europe and in Japan and it utilizes the CDMA mode in its radio access part ([43]). Scenarios with (i) packet data traffic only or (ii) with a mix of packet data traffic and voice are investigated.

Among the elements with a key role in the packet data access are the Medium Access Control (MAC) protocol and the packet scheduler (PS). The MAC protocol controls the access to the physical medium. In uplink, it exhibits a higher interest, since it is semi-autonomous (it is partly coordinated by the network as it is going to be discussed later). The PS is the entity in charge of allocating resources to packet data users. One of the resources to be scheduled is the power.

This introductory chapter is organized as follows: in the next section (section 1.2) the UMTS context is presented. Therein, a brief overview of the complex UMTS architecture

is given. The discussion then focuses on the architectural layout of the uplink packet data access procedure. The approach we used in this thesis is “top-down” and therefore in the next section (section 1.3) we outline the services and the quality of service concept in UMTS. Among this range of services, packet data services are expected to be between the ones that are going to prevail in UMTS. This evolution has created a considerable research effort on the modeling of traffic that originates from packet data applications. Moreover, traffic modeling is an important part of our study here. Therefore, this issue is treated in section 1.4. In section 1.5, the aim of this thesis is presented and in section 1.6 the overview of the dissertation is given.

## 1.2 UMTS Context

The initial aim of the first and second generation cellular networks was to offer voice service. In this respect, these systems are quite successful. The constantly increasing number of their subscribers and the higher request for a better quality for the voice service, raised the demand for larger capacity. In addition, the tremendous success of internet during the last years pushed the need for wireless internet access. Third generation (3G) cellular networks are introduced with the aim to satisfy these emerging needs ([59]).

As mentioned in the previous paragraph, third generation cellular systems utilize the CDMA mode in their radio access network (RAN) part. In Europe, the proposed 3G system is the UMTS. Its standardization is still an ongoing process. Depending on the type of coverage desired, UMTS appears in two different modes: Frequency Division Duplex (FDD) and Time Division Duplex (TDD). The former one is suitable for outdoor and macro cellular areas, whereas the latter is mostly targeted for indoor and micro cellular environments. The FDD mode utilizes the Wideband CDMA (WCDMA) access technique, whereas the TDD mode applies the Time Division CDMA (TD-CDMA) scheme.

### General UMTS Architecture

It is envisaged that UMTS will offer in its maturity services with different data rates, ranging from high-speed multimedia communications, such as video calls, to low speed services such as the Short Message Service (SMS). In addition, it has to provide the voice service as well. It is expected that UMTS will allow data rates up to 2 Mbps in micro-cell and indoor environments and 384 kbps in wide areas ([43]). In order to be able to offer these services to many users, UMTS will heavily rely on packet switching. Packet switching allows several users to share the same resources. Therefore, the UMTS Radio Access Network (UTRAN) is conceived in a way that both circuit switched and packet switched traffic can be accommodated ([49]) as it shown in figure 1.1.

It has to be noted that figure 1.1, as the biggest part of the description that is related to UMTS, is based on the UMTS standards. The standardization body of UMTS is called third Generation Partnership Project (3GPP). Six releases of 3GPP standards have appeared so far. In this dissertation, the discussion is based on the release 5 of 3GPP standards, for the reason that this is the latest completed 3GPP release. The major part of the assumptions in this work are valid for previous 3GPP releases as well; an exception

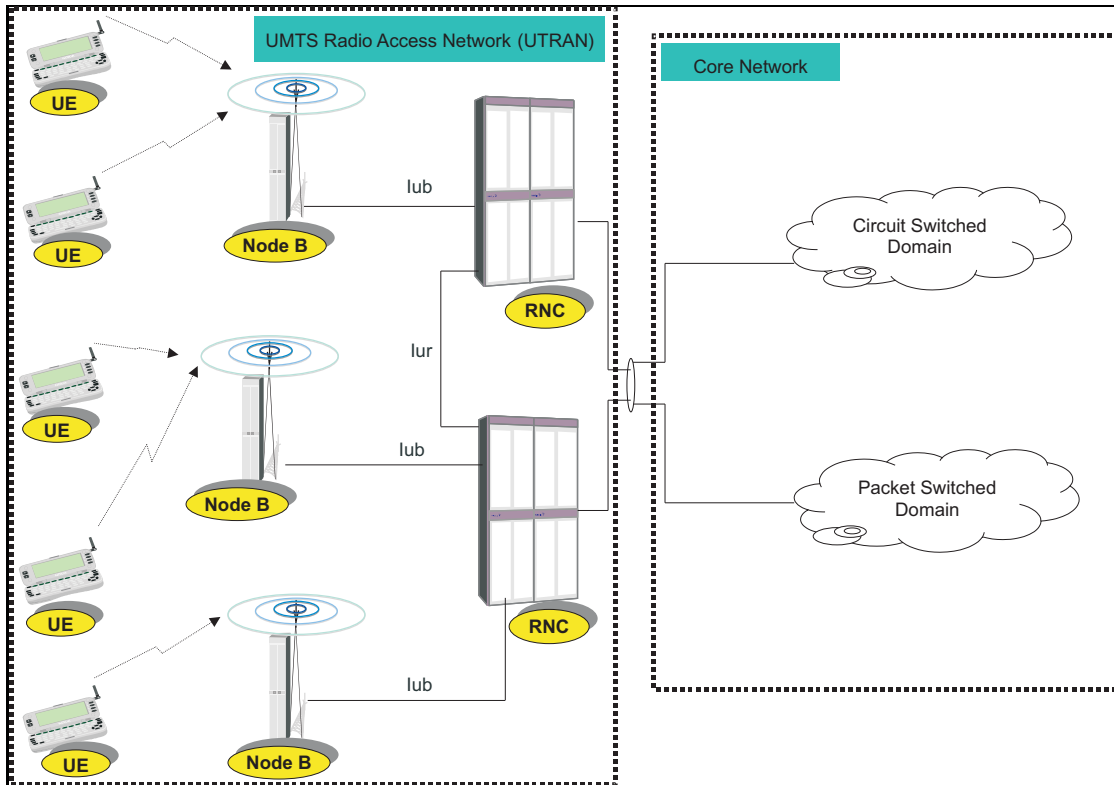


Figure 1.1: General UMTS architecture.

is the radio link adaptation mechanism in MAC layer, that is going to be discussed in chapter 3. In release 5, the description of this mechanism is more completed in comparison to previous 3GPP releases and the guidelines for the algorithm of the radio link adaptation mechanism are outlined.

Figure 1.1 illustrates the generic UMTS architecture, with the common radio access network (RAN) for both circuit switched and packet switched services. It can be seen that the core network (CN) is split into two domains: the circuit switched domain and the packet switched one, with the former one supporting circuit switched traffic and the latter packet switched traffic respectively.

### UTRAN Overview

The UMTS radio access network is the part of the UMTS that manages the transmission over the air interface, the latter named Uu. It is constituted by two types of functional components as it can be seen in figure 1.1: the Radio Network Controller (RNC) and the Node B. The RNC is the gateway to the core network (CN) and it contains the functions that control the radio resources and the mobility within UTRAN. The Node B is the entity that communicates over the air interface with the User Equipments (UEs). It is connected to a RNC through the Iub interface. Logically, it corresponds to the GSM Base

Station. A certain Node B is connected to only one RNC, while a designated RNC can be connected to more than one Node Bs; usually one RNC is connected to some tens of Node Bs. The area that is consisted of an RNC and of the Node Bs connected to it is called radio network subsystem (RNS). It is implementation dependent if RNCs are connected between them; if it is the case, RNCs are connected through the Iur interface [71].

### Uplink Packet Access in UTRAN

It is anticipated that among the range of services provided by UMTS, internet related applications and services such as web browsing and gaming, are going to be the dominant ones in some years. Hence, a significant part of the UMTS traffic is going to be packet data, originating from internet-related applications and other packet-switched services such as the Multimedia Message Service (MMS).

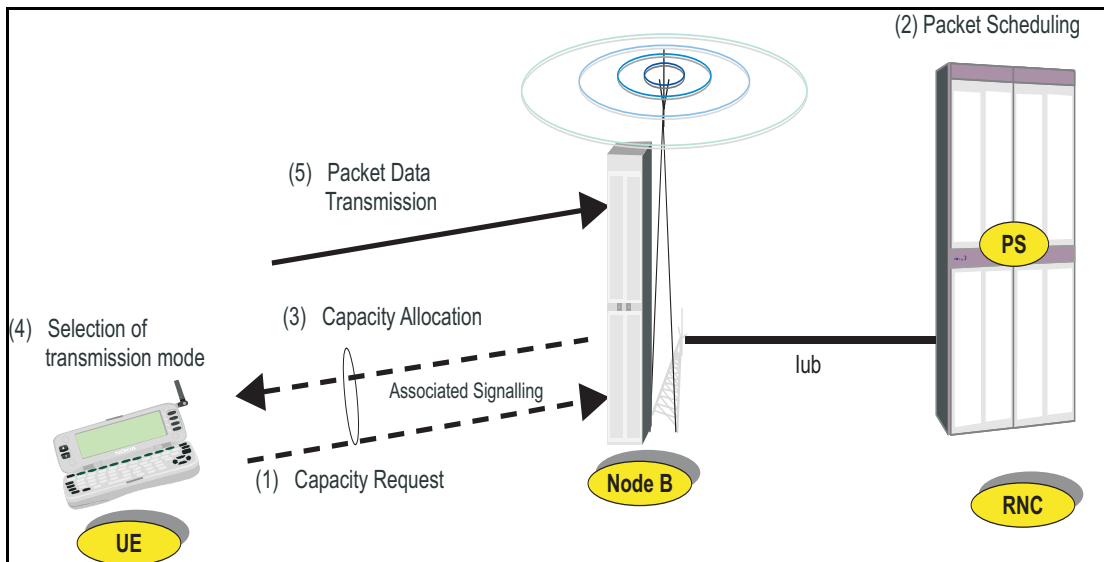


Figure 1.2: Principle of the uplink packet access in UTRAN.

The principle of the packet data access in the uplink direction of transmission in UTRAN is illustrated in figure 1.2. In the scenario presented in the figure, as in the whole thesis, we consider that a packet session is already open. We also consider that the initial access procedure has been performed and a connection has been established between the UE and the network. After the connection establishment, signaling messages can be exchanged between the UE and the network.

Even though a connection is established between the network and each UE having packet data, this connection is not the classical “circuit-connection”. The principal difference of the studied here packet access to the “circuit-connection” is that the data rate of the connection is not necessarily constant during its whole period. Due to the bursty nature of packet data traffic, a constant data rate per connection would lead to a waste of resources, therefore a dynamic control of resources is required. This control of resources

is performed by an entity called Packet Scheduler (PS). With the PS being located in the RNC, as it can be seen in figure 1.2, the packet scheduling cannot be performed on packet-by-packet basis. The principal reason for this is the delay imposed by the interfaces between the UE and the RNC (information on the delays imposed by UTRAN interfaces and by its components can be found in [22]). Therefore, the uplink packet scheduling consists in allocating a list of data rates to the UEs for a certain period.

The uplink packet data access is based on the request-response model, as it can be seen in figure 1.2. Upon data burst arrival, UEs issue capacity requests to the PS. Following the packet scheduling, the network notifies the UEs that are granted resources with a list containing the possible formats and consequently the data rates they are allowed to apply during their uplink transmission. The UE can then start the transmission of packet data. At each transmission time interval, the UE selects one of the formats in the allocated list.

### 1.3 Services and QoS Concept in UMTS

One of the major developments of third generation cellular systems, like UMTS, in comparison to the second generation ones, is the provision of new services. This became feasible in these systems mainly due to the higher data rates they can offer. Moreover, the UMTS architecture is conceived in a way that the multi-service transmission to or from a single UE is facilitated.

In UMTS, as in most of the networks, the classical issue of providing the requested QoS to users over has been considered. For this reason service bearers are introduced in UMTS. An important feature of UMTS service bearers is that a negotiation of their properties is allowed. Hence, UMTS can support a wide range of services that have different QoS and this is another advantage over GSM.

#### 1.3.1 UMTS Service Bearers

From a user standpoint, a service is considered end to end, hence from one user to the other. Consequently, the requested QoS applies for the end to end connection. If the connection lies across different networks, each network should provide the QoS over its part. In UMTS, the QoS of a connection is guaranteed by the UMTS Bearer Service. The latter one sets the mechanisms within UMTS that attempt to provide the agreed QoS; e.g. the transport of data in the user plane of the UMTS protocol stack, the control of the associated-to-data signalling and other QoS management functions. The UMTS bearer is consisted of two parts: the Radio Access Bearer (RAB) and the Core Network Bearer. The former offers the bearer service in UTRAN and the latter supports the bearer service in the Core Network (CN). Figure 1.3 represents a simplified overview of the layered QoS architecture in UMTS. (Figure is not an elaborate plan of the layered QoS architecture in UMTS, as it can be found in the UMTS standard [61]. For illustrative purposes and for the clarity of the presentation, only the elements used in this work are presented therein). In case of a connection with more than one services, a RAB per service is established. A detailed description of the UMTS bearer service and of other related issues can be found in [61]. Examples of radio access bearer configurations can be found in [82]. In chapter

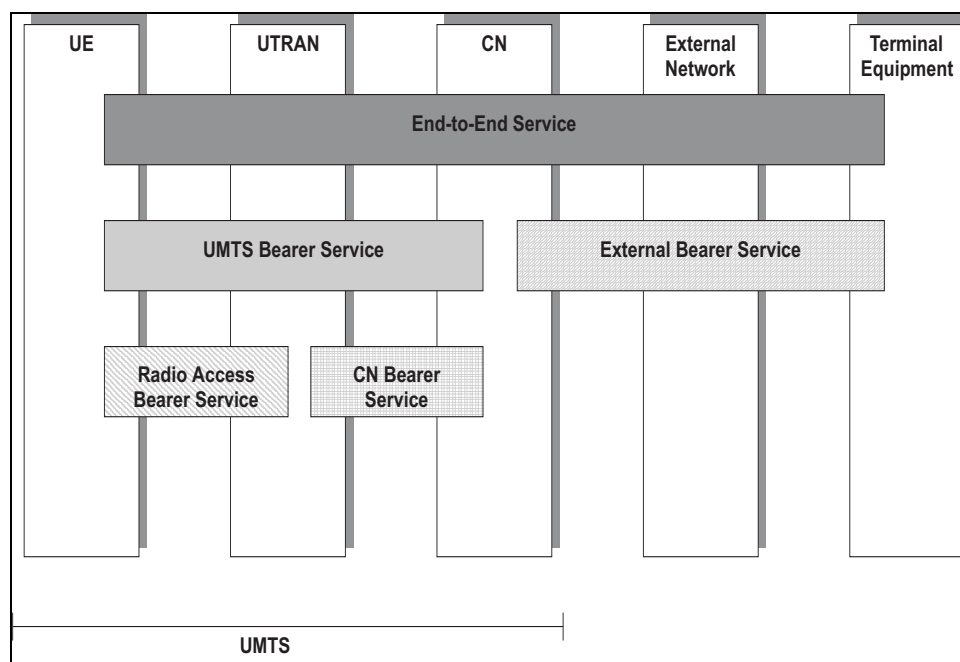


Figure 1.3: Simplified Overview of the layered QoS architecture in UMTS.

2 the way UTRAN protocols set mechanisms and communicate in order to offer a single RAB service or a mix of RAB services to an user is displayed.

### 1.3.2 Traffic Classes and QoS Attributes in UMTS

For a certain service, the properties of its service bearer are defined on the basis of the traffic of the service. Hence, different service bearer types are associated to different traffic types. In order to ensure that UMTS is capable of providing QoS in an acceptable resolution, four different service bearers are defined in UMTS. Consequently, the various types of traffic are categorized into four traffic classes.

Numerous ways to categorize traffic may be defined, e.g. unidirectional, bidirectional, symmetric, assymetric, etc. In UMTS, the principal distinctive characteristic among these traffic classes is their delay sensitivity. The UMTS traffic classes are the following:

- conversational
- streaming
- interactive
- background

Their brief description and the characteristics they differentiate them follow. Table 1.1 summarizes the UMTS traffic classes and their characteristics. Namely, the table gives

	<b>Conversational</b>	<b>Streaming</b>	<b>Interactive</b>	<b>Background</b>
Delay	Intolerant	Tolerant	Tolerant	Tolerant
Delay Jitter	Intolerant	Intolerant	Tolerant	Tolerant
Error Data Delivery	Tolerant	Tolerant	Intolerant	Intolerant
Typical Services	Speech, Face-to-face video conference	Internet streaming (radio, web cameras)	Web browsing, data retrieval from databases	email, MMS

Table 1.1: UMTS traffic classes and their requirements in terms of delay and error free delivery of the information elements.

the tolerance of the various traffic classes in delay, delay jitter and residual bit error rate. It also cites some typical services per traffic class.

### **Conversational Class**

The most known service of this class is the speech. Traditionally, it is processed as a circuit-switched application. The traffic is bidirectional and usually symmetrical.

Due to the conversational nature of the services of this class, the requirement in absolute values of delay are rigorous. In addition, almost no variance in the experienced delay of the service is tolerated, since the quality of these services is dictated by human perception. Another distinguishing property of this class is the fact that the time interval between information entities (blocks or packets) should be preserved almost constant, since a small delay in the timings of consecutive information entities would degrade significantly the quality of service perceived by humans. Hence, the requirement for delay jitter is also stringent. Other applications include, video telephony (conference) and video games.

### **Streaming Class**

Typical services of this class are the real time audio or real time video on the internet. In their majority, “streaming services are unidirectional and consequently highly asymmetric. Usually, the direction of transmission is from a network server to a user. The quality of service is also determined by human perception, since usually the receiver is a human. Delay requirements are thus strict, but since the streaming data flow is time aligned in the receiving end, the requirements in absolute delay values are not as severe as for “conversational services. This time alignment is achieved through buffering. It is of higher importance though that the inter-arrival time of consecutive information entities exhibits low variance. Hence, the delay jitter should be low. However, the time alignment in the receiver can easily “correct” the delay jitter through appropriate buffering.

### **Interactive Class**

Services where an user or a machine is on line and is requesting data from a remote server belong to this traffic class. The most widespread “interactive services are web browsing and file retrieval from data bases. The principal characteristic of this traffic

class, as of any kind of service that is based on the request-response pattern, is that the user, who is requesting data from a remote server, expects the response within a certain period [54]. Traffic of this class is heavily asymmetric, but a little bit more traffic in UL than in the streaming applications is expected.

The time elapsed from the moment the user issued a request and the moment the user has received the information requested, i.e. the so called round trip time (RTT), is one of the key features of this traffic class. It determines the satisfaction and hence the QoS experienced by the user. Depending on the service, the value of the RTT varies significantly. Another characteristic of this traffic class is that data has to be received error free at the requesting end point. The main reason for this is that these applications tolerate delay. Therefore, error correction techniques such as retransmissions are feasible.

### Background Class

This category is consisted of services where the receiving end is not expecting data. Hence, services of this class are tolerant in delay. Examples of this kind of services are email and the Multimedia Message Service (MMS) ([28]). As in the interactive class services, also for services of this class, there is a requirement of error-free delivery of data.

### QoS Class Attributes

The traffic class of a service constitutes one of its QoS attributes and as such it determines the properties of its allocated service bearer. A number of other QoS attributes has been defined in UMTS [61]. Most remarkable among them (other than the traffic class) are the maximum and guaranteed bit rate, the residual error rate, the delay, the handling of priorities and the in-order-delivery of information entities.

#### 1.3.3 Targeted QoS metrics

In this report, the work focuses on the performance of the packet data access. For this reason, we chose an interactive service in order to perform our investigation. The QoS is measured in terms of guaranteed data rate, residual error rate and the transfer delay per information entity, hence per transmitted packet.

As a real time application, the speech is chosen. Hence, a conversational class service. The QoS attribute we are interested in for speech is the residual error rate.

The definition of this QoS metrics in UMTS can be found in [61]. The way they are measured in our simulations is going to be described in the corresponding chapters. The optimization work done here aims at these QoS attributes.

## 1.4 Packet Data Traffic Modeling

Traffic modeling is very important when studying RRM algorithms and consequently in our study. Considering, that the aim here is to increase system capacity and to improve the QoS of the users, it is important to model accurately the traffic from services.

In previous generation cellular networks, the principal target was to offer speech as service. Speech traffic is traditionally model as a sequence of activity and inactivity

periods, with the activity period emulating the time a user speaks and the inactivity period emulating the silence. The data rate during activity periods is constant. This model is introduced by Brady in [8] and it is known as the ‘on-off’ model. Variations of this traffic model have been proposed for UMTS in [?] and in [78] .

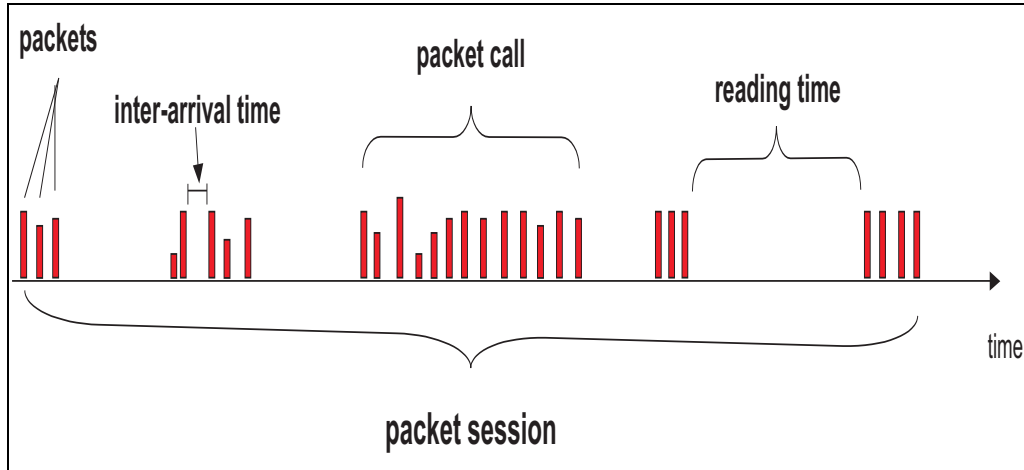


Figure 1.4: Generic web browsing model.

New services and consequently new types of traffic in 3G systems have urged a research effort on traffic modeling. The focus has been turned on the modeling of the traffic originating from World Wide Web (WWW) related applications. The initial approach has been to model WWW traffic in UTRAN, based on traffic characterizations carried out in wired networks. Although this approach seems heavily questionable, considering the limitations imposed by the air interface and the intermediate mechanisms set in order to mitigate them (e.g. the Wireless Application Protocol, WAP), it is a rather fair one, since 3G radio networks will also be used for internet access from portable computers, where ‘wired’ WWW models are applicable. Thus, on the basis of the work done in [2] and [41] the ‘web browsing’ model of [83] has emerged. Therein, WWW traffic is modeled by using ‘packet sessions’, ‘packet calls’ and ‘reading time’ periods, as it can be seen in figure 1.4. A packet session starts when a user starts WWW browsing session and ends when he stops downloading information. Each packet session is consisted of a number of packet calls. A packet call emulates the data burst originating from a web page and the reading time the inactivity period between two packet calls. This time corresponds to the period during which the user is reading the downloaded web page before sending a request for the next page. Within a packet call, datagrams, or packets, arrive at certain inter-arrival time. The above parameters, i.e. packet call duration and size, reading time, datagram size and inter-arrival time, follow certain distributions with certain statistics. In each model, these statistics and distributions are tailored in order to emulate characteristics of the service to be modeled, e.g. data rate during activity, burstiness, round trip time delays, etc. Therefore, the statistics of the web browsing models are heavily influenced by the statistics of HyperText Transfer Protocol (HTTP), since HTTP is the protocol used by web browsing applications. Measurements on HTTP traffic has shown that HTTP

traffic is characterized by “heavy-tail” distributions, which explains the important traffic variance (burstiness) even in large time scales ([38]). Therefore, the packet call size in the web-browsing model is usually characterized by heavy-tailed distributions such as Pareto. For simulation reasons however usually truncated heavy-tail distributions or fat-tail distributions such as the lognormal are used in order to describe the packet call sizes.

Moreover, these parameters can be modified in order to model traffic emanating from other than web browsing services. As an example, in [6], the described above traffic model is tailored in a way that emulates the traffic from web gaming.

A family of traffic models that are based on the web browsing model, has been created the last years, as an example in [25] and in [42]. They aim at increasing the modeling accuracy of the existing web browsing model by essentially modifying the distributions of its characteristics. These distributions result from the measured web traffic. A generic web browsing model that considers the nature of TCP traffic and its procedures (slow start, congestion algorithm, etc) has been proposed in [1].

The web browsing model however applies for the downlink. For web browsing applications, the traffic in uplink is mainly consisted of TCP layer acknowledgements, resulting thus in a low data rate. In order to study the performance of the packet data access in uplink a service resulting in higher data rates is required. Measurements and studies of uplink traffic have shown that the service that generates the highest data rates in uplink is the network gaming [60]. On the basis of the statistics of network gaming ([6]), a generic traffic model for interactive services in uplink has been proposed within 3GPP, the so-called “modified gaming model” ([78]). This model with some slight modifications has been used in our work. For the easiness of the reader, its characteristics are presented in the next chapters along with the other simulation assumptions.

## 1.5 Aim of the PhD Thesis

### Aim

In this thesis our objective is to propose methods and algorithms that optimize the utilization factor of resources allocated to packet data services in the uplink direction of transmission in WCDMA. This will improve the performance of packet data services, i.e. it will increase system capacity and it will improve the experienced QoS of users in uplink.

### Background

Current internet applications such as web browsing are characterized by the client-server model; users issue requests to remote servers for files or for any other type of data that is located in them ([56]). Hence, data is downloaded from the network to users in most of the cases. As a result, in packet switched networks the largest part of the traffic is observed in the network-to-users direction. Consequently, the downlink direction of transmission in UMTS is expected to exhibit higher load than the uplink, with the last one mainly carrying user requests for services and acknowledgements of reception. For

this reason, in the last years the research effort was primarily directed to the downlink direction of transmission with an outstanding example the implementation of the High Speed Downlink Packet Access (HSDPA).

The expected increase of load in the downlink and the introduction of new services, such as the MMS, however, raise the demand for a corresponding improvement in the uplink direction of transmission of packet data. In that respect, feasibility studies for the enhancement of the uplink packet data transmission have started in 3GPP [78]. Candidate features have been suggested in almost all of the layers and for all of the mechanisms involved in the UL packet data access for both the UTRAN and the UE. Some of the proposed features are: advanced UE transmitters and receivers, substitution of fast power control function from adaptive modulation and coding (AMC) techniques (for the maintenance of the radio link), improved coding schemes, optimization of the packet scheduling, shorter transmission time intervals and fast dedicated channel establishment and release, as well as hybrid automative repeat request (HARQ) mechanisms.

### Studied Features

Among the proposed features, improvements in the procedure of format selection for the packet data transmission and in packet scheduling are discussed here. As it is presented above, the first one is a mechanism of selection of the appropriate format, essentially of the data rate, among the allocated ones to the UE at each transmission interval. For the uplink transmission, this mechanism is located in the UE. Given that one of the criteria of a format selection are the radio propagation conditions, the TFC selection is thus a radio link adaptation mechanism. In case of multi-service transmission, the mechanism performs the scheduling of the allocated to the UE resources to its different services. In 3GPP documentation, e.g. [73], it is called Transport Format Combination (TFC) selection.

The packet scheduling in the uplink direction of UTRAN is of particular interest, as discussed above. The packet scheduler grants “capacity rights” to UEs, by allocating to them a set with possible data rates they can transmit, since scheduling on a packet by packet basis is not feasible, mainly due to delays in the radio interface. The resource to be scheduled in the uplink is the received power in the Node B ([58]).

Our goal is to improve these two procedures without applying major changes in the overall procedure of the uplink packet data access. The expected gain from the improvement in the packet scheduling is the increase in system capacity and consequently the improvement of the QoS of the packet data services. The expected gain from the improved TFC selection mechanism under discussion in this thesis is that the addition of packet data services is not degrading the performance of the existing real time ones.

The guidelines for a TFC selection algorithm for the uplink direction of transmission have been described in the 3G standard [73]. The main characteristic of this algorithm is that it favors the transmission of the highest priority real-time traffic over packet data. In the case of simultaneous transmission of a real time service and a packet data one, the probability of loss increases in comparison to the case of single real-time transmission, due to the higher requirement in the transmission power. This increase in losses affects more the real time service than the packet data one. We propose an algorithm that avoids this

effect. For this reason, a simulator emulating the uplink multi-service transmission of a single UE has been implemented.

The performance of the uplink packet scheduling has been investigated by means of system level simulations. Performance evaluation criteria are the system capacity and the offered QoS to users. We propose three features that aim at improving the efficiency of the packet scheduling and hence at increasing system capacity. In the first feature, UEs are changing rapidly the spreading code and hence the spreading factor they use for their transmission in order to minimize the variance of their transmission power. In this dissertation, this feature is called Fast Variable Spreading Factor (VSF). The second feature proposes an uplink packet data access where UEs participate more in the control of the overall procedure. Therefore, this access mode is called decentralized. The third studied feature is the faster packet scheduling.

### **Associated Work**

In order to perform our investigations, we studied and implemented packet data traffic models, we analyzed the UTRAN protocol architecture with an emphasis on the mechanisms that realize the uplink multi-service transmission. We have also implemented features related to the propagation in the physical layer such as radio channel models, power control (PC) mechanisms and receiver antenna diversity. Radio resource management (RRM) mechanisms such as load control, soft handover (SHO) control are also taken into account in our studies. Moreover, in order to assess the system performance and to analyze results we studied concepts such as cell interference and the ratio of other to own interference, the so called i-factor.

### **Related Literature**

Radio resource management in 3G cellular systems has received a lot of attention in the research community during the last years. Most of the effort however has been directed to the downlink direction of transmission. Therefore the literature related to issues studied here, such as packet scheduling, in downlink is wide, e.g. [39], [27], [9], [19], [3].

The system modeling for the study of packet scheduling algorithms both in downlink and uplink is described in [52] and in [35]. In addition, in [52] a packet scheduling algorithm based on traffic priorities is presented and its performance is assessed. In [35] various packet scheduling algorithms “are designed based on different philosophies: rate or utility optimal, fairness-based, and user-oriented”. Obtained results show that “the fairness-based approaches seem to be a good compromise and are good candidates for practical implementations in a real system”. Uplink packet scheduling and its performance have been studied also in [?], [48], [23], [16], in [57] and in [34]. The modeling of the packet scheduling is addressed also in [?]. Therein, the impact of packet data traffic on the performance of speech services is also discussed. A packet scheduling algorithm based on load and interference in the system is proposed. Packet scheduling in the case of a system with two classes of users “delay-tolerant and delay-intolerant users”. Two transmission policies for the delay-tolerant users are studied: in the first mode, users share the available resources and transmit when they wish. In the second mode, only a limited number of

users can transmit at a certain time. Results show that this time-scheduling approach affords a better cell throughput. In [23] a packet scheduling algorithm for dual traffic in UMTS is presented. Data rate allocations for the “packet traffic” are performed on the basis of interference in the cell and of user’s transmission power increases the usage of radio resources. In [34] the performance of a number of packet scheduling algorithms is assessed. The major observation is that scheduling users with good channel conditions one-at-a-time and users with bad channel conditions in larger groups offers the highest cell throughput among the studies algorithms.

Radio link adaptation through format selection in uplink has been studied in [17] and [46]. A number of TFC selection algorithms for packet data services has been discussed in [46]. Algorithms aiming at guaranting a certain data rate for a service or at maximizing the user transmitted data rate are proposed. The performance of the discussed TFC selection under different admission control policies is investigated. Different TFC selection algorithms in uplink along with other RRM functions, such as load control have also been treated in [51] and in [53]. The difference being that in [53] a scenario of mixed real and non real time traffic is studied. The selection of TFC has been discussed also in [4], with a focus on the implications of the TFC selection mechanism onto the physical layer performance.

## 1.6 Overview of the PhD Dissertation

The rest of the dissertation is organized into five chapters. The main contributions of the thesis are presented in the three chapters ranging from chapter 3 to chapter 5. In chapter 2 a brief overview of the UMTS Terrestrial Radio Access Network (UTRAN) is given. Therein, the aim is to introduce the UTRAN elements that are needed for the understanding of the next chapters. The overall conclusions of this thesis are discussed in chapter 6. Each chapter starts with a small paragraph introducing the issues to be discussed in that designated chapter and it ends with a paragraph containing conclusions. Figure 1.5 illustrates the general outline of the main body of this dissertation.

An outline of each chapter follows:

In chapter 2, a summary of UTRAN is given and its layered protocol architecture is then described. A brief overview of the physical layer is given as well. Radio bearer architecture is also discussed. In addition, the UE architecture in the case of multi-service uplink transmission is presented.

Chapter 3 gives an outline of the Medium Access Control (MAC) protocol. After the presentation of the main functions of the MAC protocol, we focus on its role in the uplink transmission; in particular, on the link adaptation issue through appropriate TFC and thus data rate selection. We study the performance of the standardized TFC selection algorithm and we then discuss alternative TFC selection algorithms. We compare the standardized TFC selection algorithm to one alternative algorithms with the help of discrete event simulations.

An analysis of the uplink packet data access follows in chapter 4. The principal mechanisms involved in the uplink packet data access are identified; their impact on the overall performance is stated. In particular, the influence of the packet scheduling on the over-

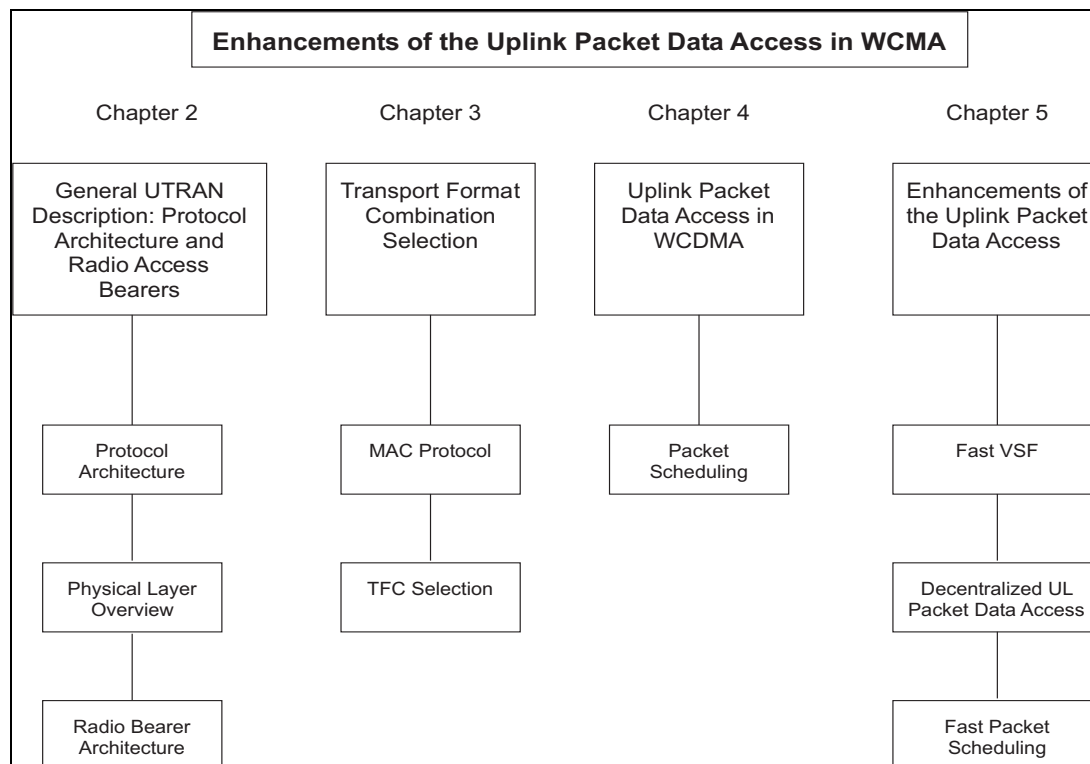


Figure 1.5: Plan of Dissertation.

all performance is discussed. System performance is evaluated by means of simulations. The network level simulator therefore built is then shortly described. Next, we list the performance metrics we use and at the end we present and analyze simulation results.

Possible enhancements in the uplink packet data access are proposed and evaluated in chapter 5. First, the fast variable spreading factor feature is discussed. Then, an alternative mode of uplink packet data transmission, where the control of the procedure is more distributed than in the standardized one is presented. Therefrom, this mode is called decentralized in this report. At the end, the improvement through faster scheduling is assessed.

The main conclusion of the dissertation and the future work are presented in chapter 6.

## Chapter 2

# UMTS Radio Access Network (UTRAN): Protocol Architecture and Radio Access Bearers

The present chapter introduces the UMTS Radio Access Network (UTRAN). The description here is based on technical specifications of 3GPP. However, the description is a synthesis and an interpretation of 3GPP standards. Its aim is not to give a detailed description of UTRAN, but to i) situate the context of the work in this thesis, which is the uplink multi-traffic transmission, within UTRAN and to ii) present the UTRAN features that are taken into account and that are implemented in our simulation tools. Therefore, for most of the cases in this chapter, we present the basic characteristics of each described feature and we omit the details. The discussion here concentrates on the FDD mode of UMTS.

This chapter is organized as follows: in the first part (section 2.1), an overview of UTRAN architecture is given. Therein, the protocol architecture is presented. In addition, the role of each protocol is outlined. In section 2.2 the physical layer along with physical channels are described. Then, the UTRAN protocol mechanisms and the inter-layer protocol procedures set in order to offer radio access bearer (RAB) services to a user are given (section 2.3). In the next section (section 2.4), transport channels are presented. Section 2.6 describes the variable spreading factor issue.

### 2.1 UTRAN Protocol Architecture

In the CN of UMTS there are two modes of processing the offered traffic: a) the classical circuit-switched mode and the b) packet switched mode, as mentioned in the previous chapter. In general, the circuit-switched handling is applied for the real time (RT) services, thus for services that belong to the conversational or streaming traffic class. The packet-switched mode is applied for internet related services, hence for services of the interactive or background traffic class. Variations can also be imagined, e.g. real time traffic that is packet switched (Voice over IP, or audio streaming over IP, etc.).



mechanisms that maintain the radio link, e.g. the power control.

Physical channels are mapped to transport channels. The latter ones define the way information is transmitted in the physical layer, e.g. they define the type of coding applied. Transport channels consist the means of communication between the physical and the MAC layer. More information on the physical layer and on the mapping of transport channels to physical channels is going to be discussed in section 2.2.

The MAC protocol mainly controls the access of traffic flow from higher layers to transport channels. It communicates with higher layers through logical channels. Hence, logical channels are the service access points (SAPs) offered by the MAC layer to RLC and they define the type of traffic that is transmitted through them. Essentially, there are two criteria that differentiate the logical channels into different groups:

- the nature of their traffic,
- the number of users the traffic is addressed to.

The traffic carried through a logical channel may be user data or associated signaling. In case the information carried on a single logical channel is addressed to (or from) a single user, then the logical channel is called “dedicated”. In the opposite case, where the carried traffic on a logical channel is addressed to a group of users or to all of the users in the cell, then the logical channel is named “common”. Consequently, a number of different logical channels is defined. All the types of logical channels and their characteristics are described in [71].

In MAC layer, logical channels are mapped into transport channels. In UMTS, the role of MAC protocol is not restricted to the control of the access to physical channels, as in other systems. It is also in charge of adapting the transmission from logical channels according to physical channel variations. It performs thus radio link adaptation. It is a subject of our study and it is going to be discussed more analytically in chapter 3.

The RLC is a typical data link control protocol containing the retransmission and the in-sequence delivery mechanisms. As such, it contains the buffers required for the operations of retransmission and in-sequence delivery of data units. The PDCP is in charge of compressing and segmenting higher layer protocol data units (PDUs), typically IP packets. The BMC is in control of information to be broadcasted or multicast to certain users in the cell. Detailed description of the above mentioned protocols can be found in [73], [74], [75], [76].

In layer 3 the RRC protocol can be found. Its principal task is to manage the network level signalling within UTRAN, making it thus the most complicated UTRAN protocol. Hence, its major functions involve handling information to be broadcasted in UTRAN, dealing with paging and mobility issues within UTRAN and managing the procedures related to the establishment, reconfiguration and release of the radio access bearers. The radio resources needed for the radio bearers are also managed by the RRC. These functions are performed in collaboration with other network layer entities, e.g. the packet scheduler (PS), the admission control (AC) and the load control (LC) entities. These entities are also located in the RNC and they form the Radio Resource Management (RRM) module. They are going to be discussed in chapter 4. Moreover, the RRC is in charge of ensuring that the requested QoS requirements per radio bearer are met. Therefore, all the related

to the radio connection measurements that are accomplished in underlying layers are reported to RRC. More detailed information on the RRC protocol can be found in [77].

In figure 2.1 it can be seen that, as in other networks, two protocol stacks are defined in the radio interface of UTRAN: the user-plane (u-plane) and the control-plane (c-plane). The first one is consisted of protocols that provide the data transfer and the second protocol stack offers the associated signalling and control.

The user plane stack contains protocols of layer 1 and layer 2. The control plane comprises protocols of layer 1 up to layer 3. Layer 1 and 2 of the control plane protocol stack are almost similar to the ones of the user plane. The difference between them is that the control stack does not contain the PDCP protocol, since signaling data units do not require compression and segmentation.

A number of possible distributions of UTRAN protocols to the UTRAN components exist, depending on the traffic type of the service and on the physical channel used. All the feasible distributions of protocols to the UTRAN entities are listed in [71].

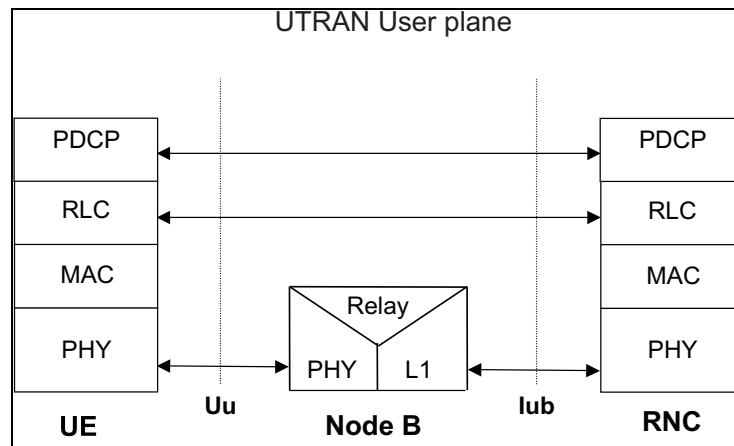


Figure 2.2: User Plane protocol stack in the case of establishment of dedicated channels between the UE and the network.

Figures 2.2 and 2.3 display an example of distribution of the user plane and control plane stack into different UTRAN components. All the UTRAN protocols can be found in the UE side, as it can be seen in these figures. Their peer protocol entities are usually located in the RNC. The Node B contains only the physical layer, serving thus as a relay between the UE and the RNC. This is another difference with GSM where the equivalent component, the base station has more functionalities than the Node B.

## 2.2 Physical Layer

The physical layer defines how the data has been structured for the transmission through the air interface. It is intended to provide highly flexible variable bit rate in both links as well as multi-service transmission through physical channels.

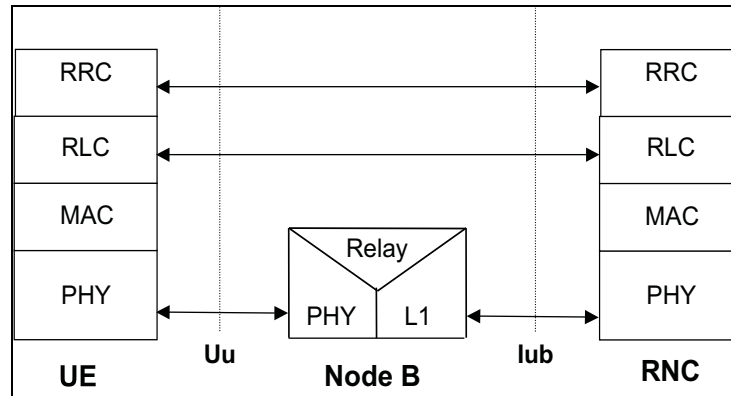


Figure 2.3: Control Plane protocol stack when dedicated channels are established between the UE and the network.

The UMTS radio interface operates with a chip rate of 3.84 Mcps and it is divided in time aligned frames. The latter ones are named radio frames. Their duration is equal to 10 ms and it is the minimum period of time over which the users' data rate cannot change. Each frame is divided into 15 slots. Hence each slot contains 2560 chips ([65]).

### 2.2.1 Physical Channels

Due to the fact the access mode in UTRAN is the WCDMA, physical channels are identified by the combination of channelization and scrambling codes. Different types of physical channels have been defined in UTRAN; examples are: the common downlink channels diffused in the entire cell, the shared channels used for the transmission by a number of users accessing them, the high speed downlink physical channel used for transmission in HSDPA and the dedicated channels (the complete list with the physical channels in UTRAN and their description can be found in [66]).

Dedicated physical channels are used in both uplink and downlink for the the transmission of data from a single user. Upon allocation of a dedicated channel to a certain user, a radio link is established between the user and the network, serving thus a circuit. Therefore, circuit-switched data are mainly transmitted through dedicated channels. In case of allocation of dedicated channels during a connection, the connection mode is called "dedicated mode". In our studies, we consider only dedicated channels. Therefore the descriptions throughout this report refer to dedicated mode.

### 2.2.2 Main Functions

The main functions of the physical layer are ([71]):

- spreading and despreading,
- modulation and demodulation,
- error detection

- measurements and reporting of Block Error Ratio (BLER), Signal to Interference Ratio (SIR), transmission power, etc.
- mapping between transport channels and physical channels

Spreading is applied to physical channels. It consists of two functions: the first one is the channelization, which transforms every data symbol into a number of chips, increasing thus the bandwidth of the signal. The number of chips per data symbol is called spreading factor (SF). Hence, the physical channel data rate,  $p$ , is the ratio of the chip rate,  $c$  and of the spreading factor,  $SF$ ,

$$p = \frac{c}{SF} \quad (2.1)$$

The second operation is the scrambling, where a scrambling code is applied to the already spread signal ([68]).

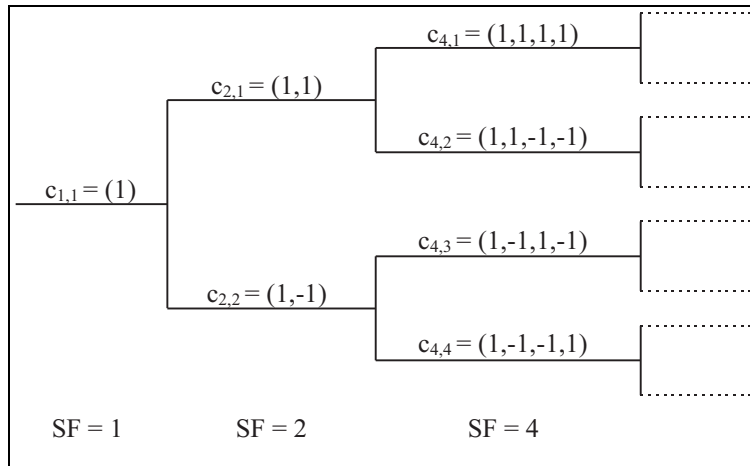


Figure 2.4: Code generation tree of the orthogonal variable spreading codes used in UTRAN.

The channelization codes used in UTRAN are Orthogonal Variable Spreading Factor (OVSF) codes. Their principal characteristic is that they preserve the orthogonality between them. The OVSF codes in UTRAN are defined by the code tree of figure 2.4.

The modulation used in UTRAN is the Quadrature Phase Shift Keying (QPSK) for all of the physical channels, apart from the synchronization channel (SCH) and the high-speed downlink physical channel (HS-DPCH) in downlink. More details on the modulation and demodulation in the UTRAN radio interface can be found in [68].

Error correction is performed in the physical layer by using the Cyclic Redundancy Check (CRC) mechanism. On the basis of the CRC output the physical layer can measure the block error rate. In addition, other measurements that are performed in the physical layer are those of the transmitted power, of the received signal to noise rise ratio and of other radio frequency (RF) related measurements ([70]).

With the mapping between transport channels and physical channels, traffic from various transport channels is directed to certain physical channels. Dedicated physical channels carry only dedicated traffic or control originating from the corresponding transport channels. Complete listing of the possible mappings between transport and physical channels can be found in [66]. The whole chain of procedures and mechanisms that direct data from transport channels to physical ones is described in the following paragraph.

## 2.3 Radio Access Bearer Architecture

Upon request of a service by a user, the network establishes a connection between the designated UE and the UTRAN. It is a logical connection between the UE and the network and this does not imply that a radio link is necessarily configured between them. Rather it implies that a user is active, that his location is known in the network and that he is able to exchange signaling messages with the network. This logical connection is an RRC layer procedure and therefore it is called “RRC connection”. The UE is then in “connected mode” ([77]). Following the RRC connection, three signalling radio bearers between the UE and the network are set up. Following this stage, the UE is eligible to exchange signalling messages with the network in order to negotiate and obtain one or more services.

For the case of an UE in “connected mode”, there are four different states that define the type of RRC connection. States are distinguished from the type of physical channel that is allocated to the UE. These four states are:

- CELL\_PCH
- URA\_PCH
- CELL\_FACH
- CELL\_DCH

In the CELL\_PCH state, there is no establishment of physical channel(s) between the UE and UTRAN and no exchange of user data takes place. However, the cell where the UE is located, is known in UTRAN and therefore the network can send page the UE, when this is needed.

The URA\_PCH state is similar to the CELL\_PCH state, with the difference that the location of the UE is not known to UTRAN on a cell level. In this state, the network is aware of the position of the UE at an area of several cells. This area is called UTRAN Routing Area (URA).

In the CELL\_FACH state, a shared or common physical channel is allocated to the UE. An exchange of user data takes place through the allocated channel. Hence, a radio link is established between the UE and the network, but it is not permanent.

In case dedicated physical channels allocation, the UE is in CELL\_DCH mode. In this case a constantly “open” radio link between the UE and UTRAN has been established and the exchange of user data is therein performed. Our studies focus on this connection mode, which is called throughout this report “dedicated mode”.

For each service of the RRC connection, a radio access bearer (RAB) is established. A RAB is bidirectional. It consists of all the UTRAN protocol elements that are set in order to provide the required service. Therefore, a RAB is comprised of a PDCP entity, an RLC entity, a logical channel, a transport channel and a physical channel, as it can be seen in figure 2.5. A single RAB is responsible for one service.

Hence, the establishment of an RAB involves the initialization of PDCP and RLC entities in both of the peer units, along with the establishment of an logical, an transport and a physical channel. The PDCP entities are initialized if segmentation and compression of the higher layer protocol data units (PDUs) are needed. All these elements cooperate in order to provide one radio access bearer service, as it can be seen in figure 2.5. The parameters of the elements that form a certain RAB define its QoS, e.g. the PDCP and RLC entity parameters, the physical channel capacity ([77]) determine the QoS of the service carried by a designated RAB.

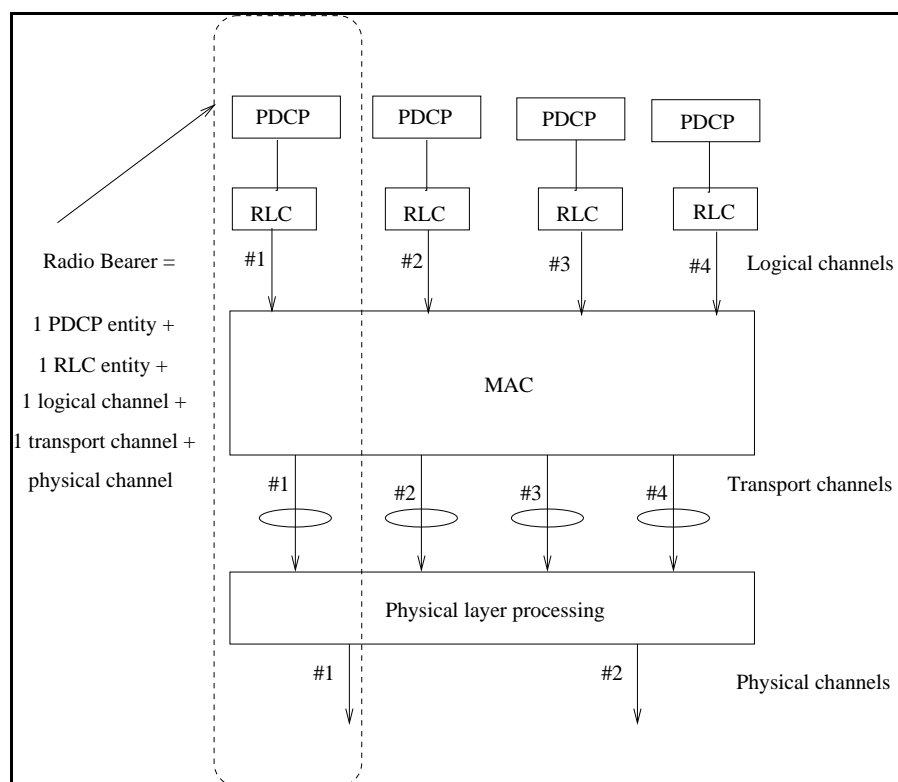


Figure 2.5: Configuration of an UE supporting more than one radio bearers (user plane protocol stack).

In case more than one RABs are established between a designated UE and the network, more than one parallel structures like the one presented above exist in both the UE and the network. Figure 2.5 displays the lower layer configuration of a UE having more than one RAB. Each RAB is then allocated a priority, which is essentially the priority of the traffic class that the RAB carries [82]. Consequently, this is the priority of the logical

channel and of the transport channel of the designated RAB.

As it can be seen in figure 2.5, in case of several active radio bearers there are more than one logical channels. The same applies for the transport channels. There can be two levels of multiplexing in that case: a) the multiplexing of logical channels to transport channels and b) the transport channels multiplexing into one or more physical channels. The first one is performed at MAC layer and the second one is performed according to the processing chain in the physical layer containing described in section 2.5). These multiplexing procedures are based on channel priorities, as it is going to be discussed in chapter 3.

## 2.4 Transport Channels

It is mentioned above that the physical layer is offering a transfer service to data coming from MAC layer by offering the transport channels. Transport channels characterize the way higher layer data is transmitted in the physical layer. Therefore, different types of transport channels are defined in UTRAN. We mention some of them: the BCH which is used for the information that is broadcasted in the entire cell, the RACH which is an uplink channel and it is used for the initial random access of UEs in the system or the PCH which is a downlink channel used for the paging (a complete list of transport channels can be found in [71]). Transport channels are categorized into common or shared ones and into dedicated ones. The common or shared transport channels either carry information that can be addressed to more than one users or they can be accessed by more than one users. Dedicated channels (DCH) carry traffic between UTRAN and a certain UE. Our studies consider only dedicated channels.

### 2.4.1 Transport Format (TF)

The format of the transport channel, named Transport Format (TF), determines the way data is transmitted in transmitted in the physical layer. A transport format is consisted of a number of transport channel attributes. Main transport channel attributes are error correction parameters such as the cyclic redundancy check (CRC), coding parameters such as the coding type and the coding rate, puncturing and repetition parameters and the number of data bits that can be transmitted during a transmission time interval (TTI) as well as this transmission interval.

More precisely, the attributes of a given transport format are ([72]):

- the Transport Block Size (TBS),
- the Transport Block Set Size (TBSS),
- the Transmission Time Interval (TTI),
- the coding type,
- the coding rate,
- the Cyclic Redundancy Check (CRC),

- the Rate Matching (RM) attribute.

A transport block is the smallest entity of data that can be transmitted from MAC to the physical layer, through a transport channel at a given transmission time interval. Its size (Transport Block Size) is equal to the MAC protocol data unit (MAC PDU) size. At a designated TTI, one transport block or more than one, a set of them (Transport Block Set), can be transmitted through a transport channel.

Coding types that can be applied are the turbo coding, convolutional coding or no coding. For the turbo coding, the coding ratio is 1/3 and for the convolutional coding the ratio can be either 1/2 or 1/3. For more information on the possible values of the other transport channel attributes, see ([67]).

Among transport channel attributes, only the transport block size and the transport block set size can change at each TTI. Therefore these attributes are called dynamic. The other attributes (TTI, coding type and rate, CRC and RM attribute) change whenever the existing transport channel configuration is modified by the network. Hence, signaling messages are required for their change. This implies that they cannot change on a TTI level and therefore they are called “semi-static” ([71]). In this respect, UMTS is a step back in comparison to General Packet Radio Service (GPRS). In the latter one, the user has the possibility to modify his coding scheme within few decades of milliseconds without prior signaling between the network and the user.

Transport Format Set							
TF	TBS	TBSS	TTI	Coding Type	Coding Rate	CRC	RM
0	320	0	40	Turbo	1/3	16	125-165
1	320	320					
2	320	640 (2 × 320)					
3	320	1280 (4 × 320)					
4	320	2560 (8 × 320)					

Table 2.1: Example of a Transport Format Set

For the period of a given transport channel configuration, a list of transport formats is allocated to a transport channel. This list is named Transport Format Set (TFS) and only transport formats that belong to the allocated TFS can be selected for the transfer through this designated transport channel.

An example of a transport format set can be seen in table 2.1. Four transport formats are defined for this set. The transport block size is equal to 320 bits. Formats differ in the number of transport blocks and thus in the total number of bits that are transmitted to the physical layer resulting therefore in data rates of 0, 8, 16, 32 and 64 kbps ([82]).

### 2.4.2 Transport Format Combination (TFC)

In case of more than one services, there are more than one activated transport channels, as it can be seen in figure 2.5. In this case, multiple transport channels are multiplexed onto one or more physical channels. A combination of transport channels is thus formed and finally transferred to the physical layer for transmission. Given that each transport

channel has its own transport format, a combination of transport formats is created at each transmission time interval; it is named Transport Format Combination (TFC).

### 2.4.3 Transport Format Combination Set (TFCS)

At each transmission time interval a TFC is selected among the existing TFCs in the TFC Set (TFCS). The last one is a list containing all the TFCs that can be applied during a period of the current configuration. Each TFC in the TFCS is identified with the aid of the TFC Identity (TFCI) field. The TFCS is allocated by the network at the configuration of low layers and it can be used till the next consecutive configuration. Typically, the time interval between two consecutive configurations signalled by the network is equal to many multiples of radio frames.

Transport Channel Attributes				
Transport Channel Attributes	Transport channel number	#1	#2	#3
	TTI	20	20	40
	Coding Type	Turbo Coding	Turbo Coding	Convolutional
	Coding Rate	1/3	1/3	1/3
	CRC	16	16	16
	RM attribute	150-195	120-160	155-185
	TB Size [bits]	640	336	148
	TB Set Sizes [bits]	0 (0 × 640)	0 (0 × 336)	0 (0 × 148)
		1280 (2 × 640)	336 (1 × 336)	148 (1 × 148)
			772 (2 × 336)	
			1544 (4 × 336)	
			3088 (8 × 336)	

Table 2.2: Transport channel attributes.

An example of a TFCS can be seen in tables 2.2, 2.3. Table 2.2 presents the attributes per transport channel of the chosen example. Table 2.3 displays the dynamic attributes, hence the various TFCs formed by the transport channels. Tables illustrate an example that applies for the uplink transmission. Three transport channels are considered; the first carries traffic from a conversational service of 64 kbps, the second from an interactive or background service with a data rate equal to 128 kbps and the third bears signaling with a data rate equal to 3.4 kbps ([82]).

The last column of table 2.3 contains the SF per transport format combination. For each combination, the resulting number of bits in the physical layer is computed. This estimation considers the physical layer processing chain presented in figure 2.6 and detailed in [67]. From the resulting number of bits in the physical layer per combination, the corresponding spreading factor is derived. (The TFCs in the list are sorted according to their total data rate).

### 2.4.4 Transport Format Combination Set Forming

The forming of the TFCS is performed in UTRAN. It is an RRC protocol task and it

Transport Format Combination Set (TFCS)					
Dynamic Attributes	TFCI	TBSS #1	TBSS #2	TBSS #3	SF
	1	0	0	0	256
	2	0	0	148	256
	3	0	336	0	64
	4	0	336	148	64
	5	0	772	0	32
	6	0	772	148	32
	7	1280	0	0	16
	8	1280	0	148	16
	9	0	1544	0	16
	10	1280	336	0	16
	11	0	1544	148	16
	12	1280	336	148	16
	13	1280	772	0	8
	14	1280	772	148	8
	15	1280	1544	0	8
	16	0	3088	0	8
	17	0	3088	148	8
	18	1280	1544	148	8
	19	1280	3088	0	4
	20	1280	3088	148	4

Table 2.3: Dynamic attributes of a Transport Format Combination Set (TFCS).

takes place during the transport channels establishment or reconfiguration.

Upon transport channel (re)-configuration, transport channels attributes, such as the possible data rates, the coding type and coding rate per transport channel and consequently all the transport formats per transport channel are defined. One of them is the transport block size of each transport channel,  $tbs_i$ . It is determined by the other transport channel attributes. In the description below, the index  $i$  denotes the transport channel. For the setting of the transport block size two options exist:

- for circuit-switched services where the transmission is done only at one bit rate, the transport block size of the transport channel,  $tbs_i$ , is given by:

$$tbs_i = r_i * TTI_i \quad (2.2)$$

where  $r_i$  and  $TTI_i$  are the transport channel bit rate and transmission time interval respectively.

- The second option for the transport block size applies for packet-switched services. In this case, a certain number of possible data rates used for the transmission through a transport channel has been defined. The lowest non zero data rate determines the transport block size in this case ([82]).

An example of an resulting thus TFCS can be seen in table 2.3.

### 2.4.5 TFCS Notification to the Transmitter Side

After the forming of TFCS, the latter one has to be transmitted to the MAC layer of the transmitter side. If the direction of transmission is downlink, the TFCS is transferred from the RRC protocol to the MAC protocol through the control service access point (SAP) connecting them (see figure 2.1). In case of uplink transmission, the TFCS is signalled to the RRC protocol of the UE, which then notifies it to the UE MAC protocol. The UE starts applying the new transport formats after a number of TTIs ([77]).

This procedure can take place also in the case of a TFCS restriction. The latter one is a mechanism, where the network prohibits the transmission of a number of TFCs of the TFCS, due to the fact that their estimated required transmission power exceeds the maximum. In that case, a sublist of TFCS, as it mentioned is permitted and the UTRAN sends the new maximum TFC of the TFCS that can be applied. In addition, it also sends the period during which the restriction applies ([77]).

## 2.5 Physical Layer Processing

The physical layer processing is presented in this paragraph. For both transmission and reception, the complete processing chains are defined in 3GPP standards, [67], [62], [63]. In the transmitter side, the physical layer processing involves among others coding, interleaving, mapping of transport channels to physical channels spreading and modulation procedures. In the receiver side, the processing contains mainly demodulation, despreading and decoding procedures as well as application of error detection mechanisms and mapping of physical channels to transport channels.

In this work the physical layer processing is modeled in its whole apart from the modulation and demodulation procedures. For this reason, in this report the term physical layer processing is used for the processing chain that performs the mapping between transport channels and physical channels.

As an example, the physical layer processing in uplink in the transmitter side, hence in the UE, is displayed in figure 2.6. This model is in accordance with the guidelines imposed in [67].

At the input of the chain transport blocks are arriving from the MAC layer. A transport block is the smallest information entity that can be transmitted through a transport channel and it corresponds to a MAC PDU. An error correction code (cyclic redundancy check (CRC) code) is added per transport block that arrives from MAC. Then, if the size of the transport block plus the CRC bits is exceeding a predefined maximum code block size, the sequence of information bits is segmented to code blocks, which enter the coder. Once the coded blocks are generated they are segmented to smaller parts, in a way that each one of them can be transmitted within a single radio frame (radio frame segmentation in figure 2.6). The data entities thus formed per transport channel are ready to be interleaved and multiplexed into the coded composite transport channel (CCTrCh). Before this procedure however, some bits per transport channel need to be punctured or repeated. This “fitting” operation is necessary because the bits contained in CCTrCh are mapped to one or more physical channels. In the case of one to one mapping (one CCTrCH mapped to a single physical channel) the physical channel capacity is defined

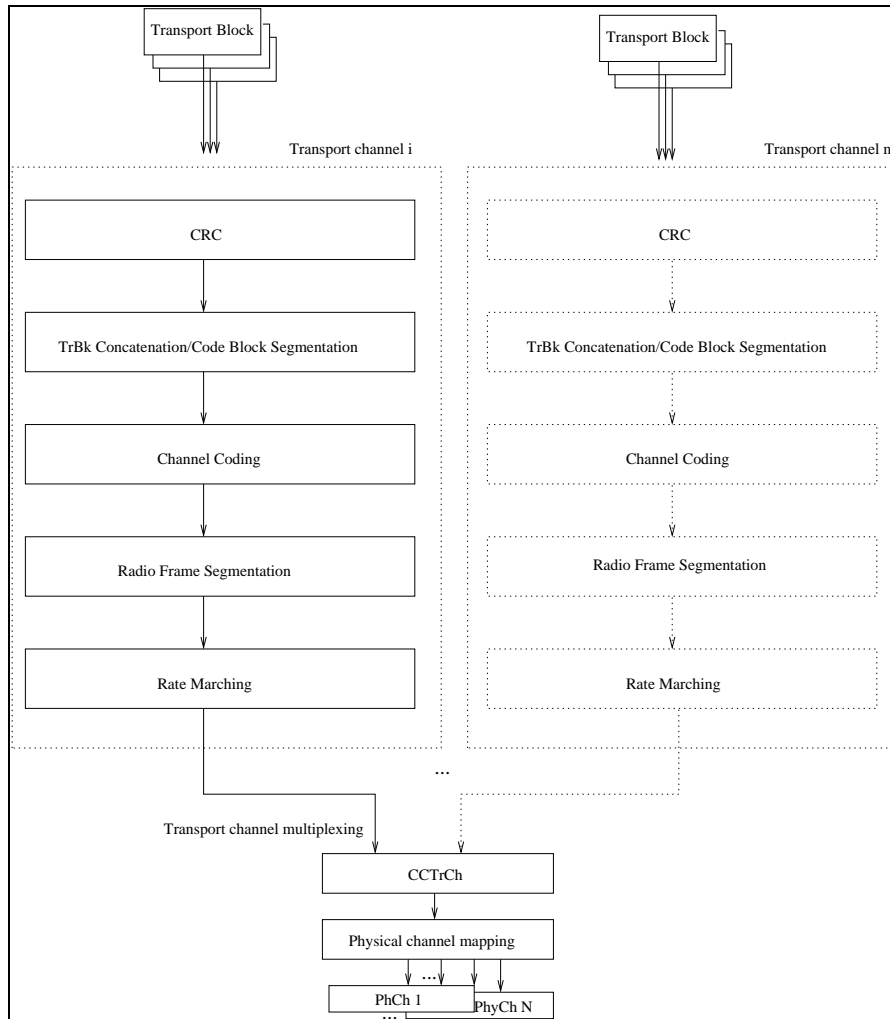


Figure 2.6: Physical layer processing model for the uplink. Model based on the one in [67].

as the number of bits in CcTrCh. The physical channel capacity however can have only certain discrete values due to physical layer parameters such as spreading.

## 2.6 Variable Spreading Factor

It could be seen in the previous paragraph that within a single TFCS different spreading factors exist. Each TFC has its associated SF. It can thus be argued that the SF is a “dynamic TFC attribute”.

During transmission, one TFC and essentially one data rate of the list is selected. (The TFC selection is a MAC protocol procedure and it is going to be discussed in chapter 3.

The data rate modifications resulting thus from the TFC selection, require a physical

channel with dynamically varying capacity. Given that the physical channel data rate,  $p$ , is the ratio of the chip rate,  $c$  and of the spreading factor,  $SF$  (see formula 2.1) and that the chip rate is always constant in UMTS, it derives that data rate modifications through TFC selection lead to a dynamically varying spreading factor. In uplink transmission the SF can change dynamically without prior signalling between the UE and the network.

As an example, we can imagine an UE that has been allocated the TFCS with the parameters of tables 2.2 and 2.3. In case no data is arriving from the conversational service and from the interactive services, the UE is transmitting only associated signalling at a data rate of 3.4 kbps. This means that the TFCI 2 is transmitted by applying a SF equal to 256. Upon arrival of traffic from both the conversational and the interactive service, the UE transmits with its maximum allocated data rate of 195.4 kbps by applying the TFCI 20. This new TFCI requires a SF equal to 4 and hence a change in the SF is performed.

## 2.7 Concluding Remarks

The present chapter has aimed at building understanding in issues such as UTRAN protocol architecture, multi-traffic transmission in uplink and transport channels.

After a brief introduction of the UTRAN protocol architecture, the protocol configuration of an UE during uplink multi-traffic transmission is presented. It is shown that each service requires an radio bearer and consequently an transport channel. This results in the multiplexing of more than one transport channels into physical channel(s).

At each transmission interval a combination of formats of the active transport channels (TFC) is selected for the transmission. The UE selects the TFC among the ones in its allocated list of TFCs, the TFCS. Each TFC results in a different total data rate and consequently it requires a different spreading factor. Hence, uplink multi-service transmission involves a dynamically varying spreading factor.

## Chapter 3

# Radio Link Adaptation in Medium Access Control

In this chapter the radio link adaptation in MAC (Medium Access Control) layer of the UMTS is discussed. The function that realizes the radio link adaptation in this layer is the Transport Format Combination (TFC) selection, already presented in chapter 2. The discussion focuses on a scenario of multi-service transmission in uplink (UL).

In the first sections of this chapter the TFC selection is described. Then, the simulator used for these studies is described and the end of this chapter simulation results are presented.

The description of the TFC selection is divided into two logical parts. In the first logical part, the implementation of the TFC selection as a protocol mechanism is described. The second part deals with the algorithmic part of the TFC selection.

The first logical part of the description starts with a brief description of the MAC protocol. The concept of MAC protocol in UMTS along with a presentation of its basic features, such as MAC PDUs and MAC primitives are given in sections 3.1 and 3.2 respectively. The MAC layer functioning in the UE side during multi-service uplink transmission is then presented in 3.3.

The second logical part starts with section 4.6.4. Therein, we present the principles of the TFC selection procedure. We also describe the 3GPP compliant algorithm for the TFC selection in uplink. We then discuss alternative algorithms.

The simulator built in order to assess the performance of the TFC selection algorithms is described in section 3.5. Simulation results are presented in section 3.7.

### 3.1 MAC Protocol Concept in UTRAN

The principal function of the MAC protocol is to provide traffic from higher layers access to the physical medium, in the transmitter side. In reception, MAC layer is expected to deliver the physical layer data units received to higher layer entities ([28]). In UTRAN, due to the multi-service capability offered to users, MAC protocol usually controls the access of traffic from more than one simultaneous radio access bearers to the physical medium (both in the UE and the network side). The part of the transmission chain of a

radio bearer that is controlled by the MAC layer is the transmission of traffic from logical channels to transport channels, as it can be seen in figure 2.5. Therefore, an additional task of MAC in UMTS is the mapping between logical and transport channels.

The radio channel is affected by considerable fluctuations and changes, resulting thus in a physical channel with dynamically varying capacity. In this case, a selection of the transport channels, that are going to access the physical channel(s) at each transmission interval, has to be made dynamically in the MAC layer. This is done by the TFC selection mechanism (see section 2.4.3). Hence, one of the major roles of the MAC layer is to adapt traffic from radio access bearers to the actual state of the physical channel(s), to perform thus radio link adaptation through TFC selection.

From the above description, it results that MAC plays an active role during the transmission. This is a new characteristic of the MAC protocol in UMTS in comparison to second generation MAC protocols, e.g. MAC in GSM.

From architectural point of view, the MAC protocol is composed of a number of entities, each one of them handling different type of transport channels. In the network side of the protocol, these entities are distributed in the RNC and in the Node B. The architecture of MAC protocol is thoroughly presented in [73].

More details about major implementation, design options for 3G MAC protocols and about their role in achieving higher data rates can be found in [37], [5], [18].

## 3.2 MAC Protocol Basic Features

In the present section (3.2) a short description of the primitives and PDUs of the MAC protocol is given. Their knowledge is very useful for the understanding of the TFC selection procedure.

### 3.2.1 MAC layer primitives

Primitives are the messages used for interlayer communication. The description is based on the OSI model and therefore the OSI terminology is adopted. In the OSI model, primitives are sent between protocols of adjacent layers. Therefore, MAC protocol is exchanging primitives with the physical layer and with the RLC protocol. This restriction imposed by OSI is not entirely respected in UMTS. Primitives are also exchanged between MAC and RRC. These primitives are mainly used for the control and configuration of MAC by RRC. For their transmission a specific SAP between MAC and RRC has been defined. It is the “control” SAP that can be seen in figure 2.1. A detailed description of the MAC primitives that are involved in the uplink multi-service transmission is given below.

In UMTS four primitive types are used. They are adopted by the OSI model ([56]). They are:

- Request (REQ)
- Indication (IND)
- Response (RSP)

- Confirm (CNF)

The request is sent when a higher layer is requesting a service from its lower layer. The indication is sent by a lower layer to its higher layer in order to inform it about the service it is offering. The response type primitive is sent by the higher layer to the lower one in order to inform the latter that the previously indicated service has been completed. The confirm primitive is sent by the lower layer that provides the service to its higher layer stating that the requested service has been offered. The use of different types of primitives is displayed in figure 3.1 (Primitives response and confirm can have a different usage in certain cases). When a designated service is requested to a lower layer by its higher layer, the order in which primitives are exchanged is defined. It is the order of their presentation here. It can also be seen in figure 3.1.

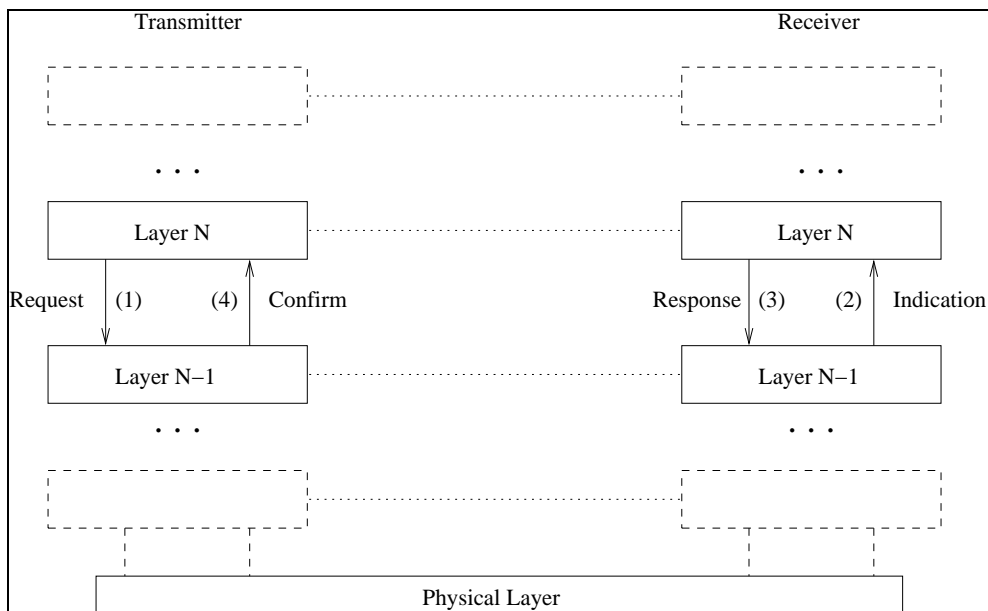


Figure 3.1: Use of the four types of primitives. The numbers next to the primitive names indicate the order of their transmission.

### Primitives between physical layer and MAC

Primitives between the physical layer and MAC are mainly used during the transfer of data units from one layer to the other and when the physical layer needs to indicate the state of the physical channels to the MAC layer.

The primitives between physical layer and MAC are:

- PHY-ACCESS(-REQ/CNF)
- PHY-CPCH\_STATUS(-REQ/CNF)
- PHY-DATA(-REQ/IND)

- PHY-STATUS-IND

The first four primitives, PHY-ACCESS(-REQ/CNF) and PHY-CPCH\_STATUS(-REQ/CNF) are used for the control of the common transport channels RACH and CPCH. Primitives PHY-ACCESS(-REQ/CNF) are exchanged during the access to a RACH or a CPCH. Primitives PHY-CPCH\_STATUS(-REQ/CNF) are sent whenever information concerning the actual state of a CPCH needs to be shared between MAC and physical layer. Their implication in the uplink multi-traffic transmission is insignificant, therefore their detailed description is omitted here. Details on these primitives can be found in [73].

The PHY-DATA-REQ primitive is sent by the MAC layer to the physical one in order to request the transmission of MAC Service Data Units (SDUs). In this case, SDUs are the transport blocks. A PHY-DATA-REQ primitive is submitted every TTI (Transmission Time Interval) for each transport channel.

The PHY-DATA-IND primitive is sent by the physical layer in order to transfer to MAC a number transport blocks. A PHY-DATA-IND primitive is submitted within a period of one TTI for each transport channel.

Both of the previous primitives contain as parameters the “Data Units” (DUs) to be transmitted, which are the transport blocks in this case, along with their TFI (Transport Format Indicator).

The PHY-STATUS-IND primitive is sent by the physical layer to MAC in order to inform the latter one about physical channel conditions.

The implication of the last three primitives in the uplink transmission procedure is discussed in section 3.3.2.

### Primitives between MAC and RLC

Primitives between MAC and RLC are basically exchanged during the transmission procedure. They are mainly used for the transfer of data units between layers. The primitives between MAC and RLC are:

- MAC-DATA(-REQ/IND)
- MAC-STATUS(-IND/RSP)

The primitive MAC-DATA-REQ is sent by the RLC protocol to MAC every time data (transport blocks) are transmitted from RLC to MAC. It contains the RLC PDUs transmitted. This primitive can also be used by an RLC entity in order to inform MAC about its buffer state (actual size, mean size or variance of the buffer size in number of bytes).

The primitive MAC-DATA-IND is sent by MAC to RLC whenever data (RLC PDUs) received in MAC layer shall be submitted to RLC.

The primitive MAC-STATUS-IND is sent by MAC whenever a change in MAC protocol happens. It indicates the RLC PDU size and the number of RLC PDUs that the RLC entity can submit to MAC during the next TTI. It may also be used by the MAC layer in order to initiate the transmission of a MAC-STATUS-RSP primitive from RLC to MAC.

The last one contains the actual buffer state. In that case, the primitive MAC-STATUS-IND contains no parameters. This primitive may also be sent during transmission on RACH or CPCH in order to inform the RLC layer that a transmission on these channels was requested by the MAC layer or, when an attempt to transmit on these channels has failed.

In addition to the previously described functionality, the primitive MAC-STATUS-RSP is sent in order to inform the MAC layer about the state of the RLC protocol, e.g., the state where the exchange between peer RLC entities is suspended for a reason.

The use of the last four primitives during the uplink transmission procedure is presented in section 3.3.2.

### Primitives between MAC and RRC

These primitives are sent with a lower frequency than the other groups of primitives. They are essentially transmitted when RRC requests the configuration (or the reconfiguration) of the MAC layer and in case the MAC layer needs to inform the RRC about its status.

The primitives between MAC and RRC are:

- CMAC-CONFIG-REQ
- CMAC-MEASUREMENT(-REQ/IND)
- CMAC-STATUS-IND

The primitive CMAC-CONFIG-REQ is sent every time the MAC protocol is (re)configured. It contains information concerning the mapping between logical channels and transport channels, logical channel priorities. In addition it carries the TFCS. (It is also used for other reasons, that are out of scope here, e.g., notify to MAC protocol parameters related to the RACH, CPCH channels and ciphering parameters).

As discussed above, MAC layer performs traffic volume measurements by keeping track of the RLC buffers sizes. These measurements are reported to the RRC layer. The primitive CMAC-MEASUREMENT-REQ is sent by the RRC in order to define the way the reporting of MAC layer measurements should be accomplished. It specifies thus if the measurement report should be periodic or event triggered. In the second case, it indicates to MAC the trigger values.

The primitive CMAC-MEASUREMENT-IND is sent by MAC. It contains the measurements requested by the RRC.

The primitive CMAC-STATUS-IND is sent by MAC in order to notify RRC about an abnormal situation (e.g. maximum number of attempts to access to the RACH channel achieved).

### 3.2.2 MAC Protocol PDUs

As discussed above a MAC PDU is a transport block in UMTS. Two groups of MAC protocol PDUs exist. The first group of PDUs is used for the transmission on the HS-DSCH and the second is used for the transmission on all the other types of channels. The

transmission on HS-DSCH is out of the scope here, therefore the description of MAC-PDUs for HS-DSCH is omitted.

A MAC protocol data unit (PDU) consists of one optional MAC header and a MAC Service Data Unit (MAC SDU), as it can be seen in figure 3.2.

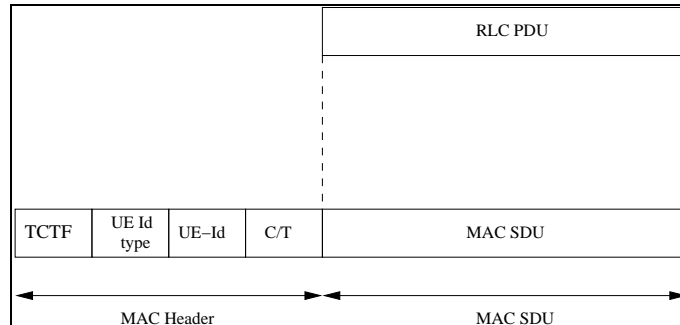


Figure 3.2: MAC data PDU

### Mac header

A MAC header, when it exists, may be consisted of one or a combination of the following fields:

- TCTF (Target Channel Type Field)
- UE Id Type
- UE Id
- C/T

### TCTF field

This header is used on the FACH and RACH transport channels. As it can be seen in [71], FACH or RACH may transport information originating from (or sent to) different types of logical channels. The TCTF is used in order to identify the logical channel type (control or data) to which the transport channel is mapped.

### UE Id related fields

The second and third header fields provide UE identification in common transport channels. There can be two different types of UE-Ids:

- U-RNTI, UTRAN Radio Network Temporary Identity
- C-RNTI, Cell Radio Network Temporary Identity

The C-RNTI is used whenever an identification of the UE inside a cell is needed. The U-RNTI provides an identification of the UE in a radio network subsystem (RNS). (This happens when an UE is logically connected to the network, but it is not allocated dedicated channels. Hence, the RNS where the UE is located, is known in UTRAN, but its exact cell is not known, [77]).

The header UE-Id type is used in order to specify which of the two above described UE-Id is going to be used in the current MAC-PDU.

### C/T field

The C/T field is used in the case of multiple logical channels being multiplexed in one transport channel. It provides an identification of the logical channel.

A detailed description of the size and coding of the previous header fields can be found in [73].

## 3.3 Uplink Multi-traffic Transmission

In this paragraph the MAC protocol functioning in case of multi-service transmission is explained. The description concentrates on the transmitter's side, thus the UE side.

As discussed before, in the multi-bearer transmission chain, there are two levels of multiplexing at MAC layer: the first one consists in multiplexing different logical channels onto one transport channel and the second one involves the transport channel multiplexing onto a single physical channel. These two levels of multiplexing can be seen in figure 3.3. This figure illustrates an example of MAC layer functioning in uplink multi-bearer transmission. The transmitter, hence the UE, is displayed. The UE is in "dedicated mode". Logical and transport channels of the figure are thus dedicated. The case of logical channels being multiplexed onto a single transport channel can be seen: logical channels #1 and #2 are multiplexed onto transport channel #1. All transport channels are multiplexed onto a single physical channel. Data units originating from RLC layer, RLC PDUs, arrive from RLC through the different logical channels. A MAC header is added to each RLC PDU, coming through logical channels #1 and #2. The C/T header (see section 3.2.2) is added in this case; no additional header fields exist due to the fact that logical channels are dedicated. The RLC PDU and the MAC header form the MAC PDU. A MAC PDU is equivalent to a transport block.

During the uplink transmission procedure, the actual state of the physical channel(s) is known to MAC layer; information regarding the physical channel(s) condition is sent to the MAC layer with the aid of the PHY-STATUS-IND primitive. Based on the actual capacity of the physical channel, the following procedures are performed in the MAC layer, at each transmission time interval:

- the selection of the logical channel to access the transport channel (in case of more than one logical channels being multiplexed to a single transport channel)
- the selection of transport channels that are allowed to transmit traffic (originating from logical channels) to the physical channel(s)

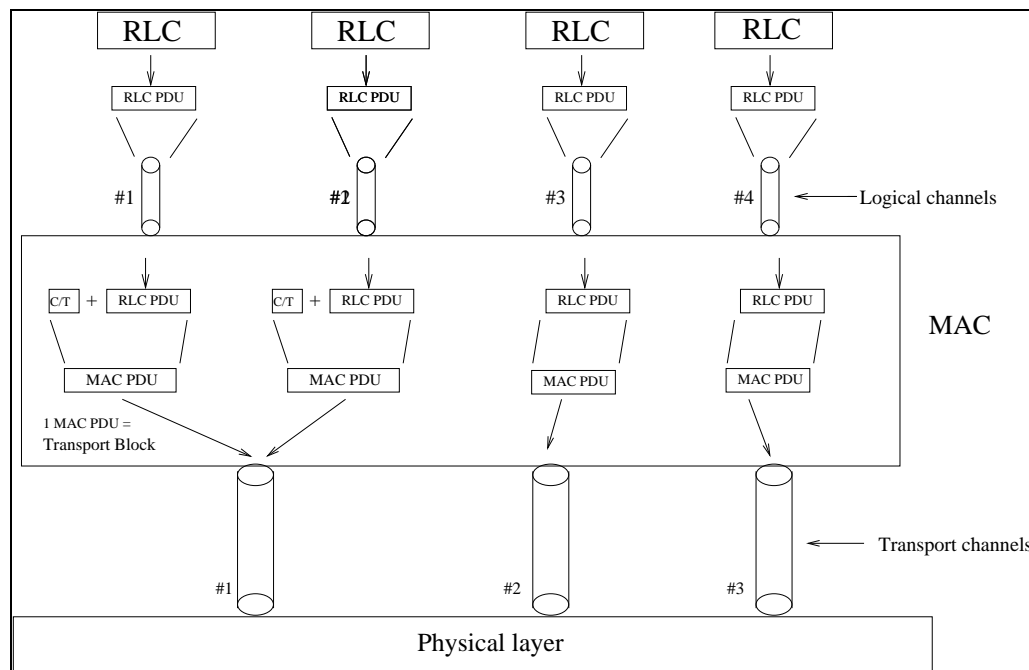


Figure 3.3: MAC protocol during uplink multi-traffic transmission. Transmission is done on dedicated logical and transport channels.

- the decision of the amount of traffic that each selected transport channel is permitted to transmit to the physical channel

The first selection of the above list is based on the priorities of the logical channels. It is controlled by the RRC layer, since logical channel priorities are therein allocated.

The last ones are parts of the Transport Format Combination selection, as it is named in the 3GPP standards.

In addition, MAC protocol is constantly aware of the RLC buffers occupancy, since this information is provided by the MAC-DATA-REQ primitive. Buffer sizes are reported to RRC with the aid of the CMAC-MEASUREMENT-IND primitive. (This information may be then transmitted to the RRC entity in UTRAN, serving thus as an implicit capacity request, as it is going to be discussed in chapter 4).

### 3.3.1 MAC layer functions in uplink transmission

In the previous section, we described the actions undertaken by MAC protocol in the UE side during uplink multi-service transmission, when the UE is in dedicated mode. Two time scales can be distinguished to characterize these functions. Functions of the longer time scale apply for the procedures of MAC protocol (re)configuration, while the second ones apply for procedures that take place at each TTI (10, 20, 40 or 80 ms).

### Longer time-scale functions

In the first group of functions belong:

- the mapping of logical channels to transport channels,
- the allocation of priorities to logical channels
- the allocation of a TFCS list (or sublist) to the current configuration.

All these functions are performed under the guidance of the RRC protocol.

### Shorter time-scale functions

In the second group of functions belong:

- the selection of the appropriate Transport Format Combination (TFC),
- the reporting of the size of RLC buffers to RRC.

#### 3.3.2 Uplink transmission procedure in MAC layer

The procedure of uplink transmission follows the next steps (see figure 3.4):

1. At the initialization phase, RRC protocol requests the configuration of the MAC layer by sending the CMAC-CONFIG-REQ primitive. RRC protocol sets the configuration about: a)the mapping of logical channels onto transport channels, b)logical channel priorities, c)the TFCS list that MAC is allowed to use during the designated configuration.
2. The primitive MAC-STATUS-IND is sent to the RLC layer in order to request the RLCs Buffer Occupancy (BO) values.
3. RLC entities send the primitive MAC-STATUS-RSP. They indicate thus their RLCs BO values to MAC protocol.
4. After the selection of the appropriate TFC for the next radio frame, MAC layer sends the primitive MAC-STATUS-IND to RLC entities whose traffic is chosen for transmission during the next TTI. This primitive contains information about the size of the RLC PDU and the number of RLC PDUs that the RLC entity may transmit during the next TTI.
5. RLC entities send through their corresponding logical channels, the primitive MAC-DATA-REQ. It contains the number of RLC PDUs to be transmitted during the next TTI, along with information about the size the RLC buffer.
6. A MAC header is added to RLC PDUs, in case this is needed.
7. The PHY-DATA-REQ primitive is sent to the physical layer by MAC layer. This primitive contains the Transport Blocks to be transmitted by the physical layer. It contains also the Transport Format of the transport channel.

8. The primitive PHY-STATUS-IND is sent from the physical layer to MAC in order to inform the last one about the level of the transmitted power. In addition, it is transmitted in the case of an abnormal event in the physical layer, e.g. maximum uplink transmission power has been reached, minimum allowable transmission power has been reached.

Steps 2-8 are repeated at the next shortest TTI boundary.

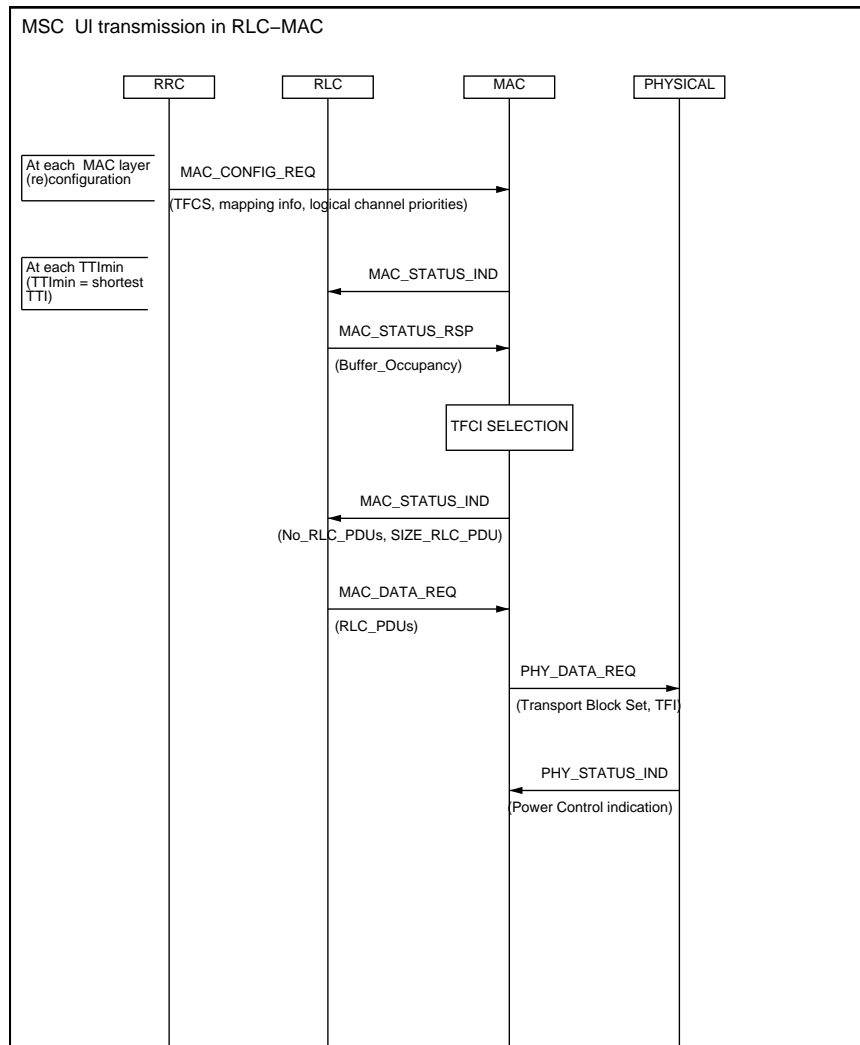


Figure 3.4: Uplink transmission in MAC layer in dedicated mode (UE side).

### 3.4 Transport Format Combination Selection

As discussed in previous sections, an important task of MAC layer is the radio link adaptation through the selection of the appropriate Transport Format Combination (TFC) among the existing ones in the allocated TFCS at each radio frame. This selection is mainly based upon:

- available physical layer resources
- transport channel priorities
- RLC buffers occupancy at the input of logical channels

With the term physical layer resources, we mean the maximum data rate of the TFCS that can be transmitted under the current radio propagation conditions.

In the 3GPP specifications ([73], [64]) mechanism that considers the physical layer conditions during TFC selection has been defined. We call it throughout this report ‘TFC Elimination’. It involves the restriction of the TFCs in the TFCS whose transmission power exceeds the maximum transmission power.

At each time slot, the UE measures its transmission power. In addition, the data rate transmitted at each TTI is also known in the MAC layer. Based on this information, MAC layer can compute the transmission power required for all of the TFCs in its TFCS. This computation is achieved through the formula that relates the user data rate,  $r$ , with the total received power  $P_{Total}$  ([22]):

$$\frac{E_b}{N_0} = \frac{w}{r} \frac{P_r}{P_{Total} - P_r} \quad (3.1)$$

where  $\frac{E_b}{N_0}$  is the energy per bit to noise density ratio of the user detected in the Node B (after demodulation),  $w$  is the chip rate and  $P_r$  is the received power from the user. Considering that:

$$P_r = GP_t \quad (3.2)$$

where  $P_t$  is the transmitted power of the user. Without introducing a big uncertainty, we omit the term  $P_r$  from the denominator. Equation 3.1 can then be written as:

$$\frac{E_b}{N_0} = \frac{w}{r} \frac{P_t G}{P_{Total}} \quad (3.3)$$

Assuming the same  $\frac{E_b}{N_0}$  for all of the data rates, the estimated transmitted power,  $P_{t,i}$  of a data rate  $r_i$  is obtained as a function of the currently transmitted power,  $P_{t,0}$  and data rate  $r_0$  by the formula:

$$\frac{P_{t,i}}{P_{t,0}} = \frac{r_0}{r_i} \quad (3.4)$$

In the above mentioned specifications, three parameters have been defined: X, Y and Z. If the required transmission power of a certain TFC in the TFCS exceeds the maximum

transmission power  $X$  slots during the last  $Y$  slots, then it cannot be selected (it is thus “eliminated”) for the next  $Z$  slots. Usually an offset,  $TFC E_{offset}$ , is considered for the “TFC Elimination” and a TFC is considered if its computed transmission power is higher than the maximum transmission power,  $P_{max}$ , minus the offset:

$$P_{thr} = P_{max} - TFC E_{offset} \quad (3.5)$$

### 3.4.1 3GPP Compliant Algorithm

In the release 5 of the 3GPP specification [73], the guidelines for the TFC selection algorithm are presented (these changes are then incorporated in the latest version of previous releases as well). The principal criteria for the appropriate format selection are the logical channel priorities, in this algorithm. Based on available physical resources, the algorithm aims at providing the highest possible data rate to the service (or equivalently transport channel) of highest priority. The selection algorithm runs at the beginning of the shortest configured TTI. It runs as follows:

1. Form the (sub)list  $L$ , with all the allowed TFCs at that TTI.
2. Select the transport channel with the highest priority,  $P_1$ .
3. Form the sublist  $L_1$  of  $L$  containing the TFCs that offer the highest bit rate to the selected transport channel.
4. If  $L_1$  contains only one TFC, choose this TFC and exit.
5. If  $L_1$  contains more than one TFCs,  $L = L_1$ .
6. Select the transport channel with the next highest priority  $P_2$ .
7. Go back to step 3.

The procedure is repeated till  $L_1$  contains only one TFC.

As an example, consider that at a given moment the TFCS list presented in tables 2.2, 2.3 is allocated to MAC layer. Priorities of transport channel 1, 2, 3 are 0, 1, 2 respectively. At that moment, none of their RLC buffers is empty and the state of the physical channel (notified to MAC with the PHY-STATUS-IND primitive) allows the transmission of the first 16 TFCs. So the list  $L$  contains the first 16 TFCs of the table 2.3. The transport channel selected is the first one, since it carries the traffic with the highest priority. At the end of the first iteration, the list  $L$  contains the TFCs 7, 8, 10, 12-15. Next, the transport channel 2 is selected. The new list  $L$  contains now only the TFC 15. The TFC 15 is chosen for transmission in the coming TTI.

### 3.4.2 Alternative algorithms

The 3GPP compliant algorithm favors the transmission of high priority traffic. Various TFC algorithms can be conceived. As an example, in [11] and in [46] a number of TFC selection algorithms has been discussed. In [11] a fair algorithm and an algorithm that

prioritizes the traffic with the highest buffer occupancy are presented. In [46], algorithms that aim at guaranteeing or maximizing the data rate of a service are proposed. Numerous other TFC algorithms may be defined. However the flexibility in the conception of TFC algorithms reduces in scenarios with real time traffic, due to the stringent delay requirements of the latter one.

Considering the traffic priorities in UMTS [82], in case of multi-traffic transmission from a real time service and from a packet data service, real time conversation services are privileged over interactive packet data ones. Under unfavorable radio propagation conditions, both of the services are experiencing losses. In these cases, the block error rate (BLER) of the real time service and the delay of the packet service are increasing. It is likely that the packet data traffic will suffer more heavily. The QoS requirement of the real time traffic being more stringent than the one of the packet data, the impact on the QoS of the real time service is going to be more important in case of unfavourable radio propagation conditions and it may lead to loss of the call.

In case a packet data service is added to a real time one, the probability the UE is in shortage of transmission power increases. Consequently, the coverage area is reducing.

### Modified TFC Selection Algorithm

A modified TFC selection algorithm is discussed here. Its aim is to increase the coverage area for the real data services. It mainly aims at scenarios with a mix of real time and packet data traffic. Its principal characteristic is that it attempts to split in time the transmission of real time traffic from the transmission of packet data, if the correct transmission of their combination is not feasible.

The operation of the algorithm is similar to the 3 GPP compliant one; the selection of appropriate formats is also performed on the basis of traffic priorities. In case, real time traffic is selected for transmission in the current TTI, packet data is also selected for transmission, only in the case the required power for the transmission of the combination of the services is below a certain threshold,  $P_{thr}$ . For this reason a power offset,  $P_{offset}$  has been defined, such as:

$$P_{thr} = P_{max} - (TFC E_{offset} + P_{offset}) \quad (3.6)$$

where  $P_{max}$  stands for the maximum transmission power of the UE.

## 3.5 Simulation Model

In order to investigate the performance of the above mentioned TFC selection algorithms, a simulator is built.

The simulator is essentially emulating the operation of the MAC protocol during uplink transmission. The MAC functions that have been implemented apart from the TFC selection are the mapping between logical and transport channels and the allocation of priorities to logical channels. For simplicity reasons, only the case of one to one mapping between logical and transport channels has been considered. Therefore, when priorities are discussed, a radio access bearer priority is equivalently its logical and transport channel priority.

In order to assess the performance during multi-service transmission in uplink, the implementation of functions of other layers is required. In the description of the multi-traffic transmission in uplink (section 3.3.2), it is mentioned that MAC is configured by RRC. In addition, MAC layer is constantly receiving information about RLC buffers size from the RLC protocol and information about the available radio resources from physical layer. For this reason, the RLC buffering is simulated. In addition, RLC layer re-transmissions are also considered. The physical layer transmission through the radio interface have been considered as well in the simulator.

Inputs of the simulator are the initial RLC and MAC configurations, i.e. the number of active RABs and their parameters such as the type of traffic the data rate per radio bearer. Attributes per transport channel are also inputs of the simulator.

The main outputs of the simulator are the chosen for transmission TFC per TTI, along with its transmission power and its total bit rate. Traces concerning the percentage of blocked packets per logical channel and the delay of packets for logical channels supporting non real-time data traffic are also kept.

The execution of the simulation basically consists of three parts. The first part is the initialization phase. The implemented segments of RLC, MAC and physical layer are configured. The Transport Format Combination Set (TFCS) of the UE is formed in this part. In the next step, the uplink transmission in low layers is simulated. The sequence of events, as it described in figure 3.4, is implemented. The major task of this procedure is the selection of the appropriate TFC at each transmission time interval. In parallel, procedures necessary for the emulation of the physical layer, such as the radio propagation, the fast power control and the outer loop power control (OLPC) ([22]) are performed. In addition, the update of RLC buffers is also accomplished. In the final step, results of the uplink transmission analysis are post processed.

Results focus on the QoS measures of the various services, i.e., the BLER for the real time services, delay per packet for the packet data services. In addition, the FER is also traced, the mean transmitted power of the UE along with its mean data rate.

Issues related to the physical layer modeling, such as the radio propagation model, the fast and outer loop power control are not described here, since they do not consist the most important part of the study. These features are thoroughly discussed in numerous books and articles, as an example, details about radio propagation modeling can be found in [47], [50]. A concise presentation of the fast and outer loop power control can be found in [22]. Their modeling in the simulator under discussion is described in appendix A.

### 3.5.1 Traffic Sources Characteristics

In this section, we describe the traffic models applied for the different types of traffic in our simulations. The scenario we investigate three traffic types: (i) CS speech, (ii) signaling and (iii) packet data originating from an interactive service (more detailed description on the services of the simulated scenario, can be found in the next section). Therefore, the traffic source modeling involves three different models.

### Speech Traffic Model

The traffic model used for the speech is based on the “On-Off” model cited in chapter 1. Parameters of the model are the ones of [83]. Both the activity (On) and the inactivity (Off) periods are exponentially distributed. The mean On period is equal to 3 seconds, whilst the mean Off period is set to 3 seconds as well. This model results thus in a 0.5 activity factor for the voice.

### Signalling Traffic Model

For the signalling, the source traffic model used is the “On-Off” model, as for the speech, with the On period emulating the moments of arrival of RRC layer signaling. The mean ‘On’ period is 0.3 seconds and the mean ‘Off’ period is set to 0.7 sec.

### Interactive Service Traffic Model

The traffic that is generated from the interactive service is modeled according to the “web browsing model” that is already presented in chapter 1. Hence, the periods of activity and inactivity are modeled by using “packet calls” and “reading time” periods respectively.

In these studies, the packet call session has an indefinite duration, thus it lasts till the end of the simulation. Therefore, no packet session arrival process has been specified.

The distributions characterizing the packet call arrival process and the datagram arrival process are inspired from the ones in [6]. Therein, these distributions are derived empirically from measurements in “gaming” applications through the network, hence this model is called “Modified Gaming Model”.

The parameters for the traffic model are summarized in table 3.1. Parameters are modified comparing to the ones in [6], in order to emulate future services with high data rates and burstiness. The packet call duration is exponentially distributed with a mean equal to 5 seconds. The reading time is also characterized by the same distribution, with the mean reading time being equal to 5 seconds. The inter-arrival time between datagrams follows a log-normal distribution with a mean equal to 40 ms and standard deviation equal to 38 ms. The datagram size is fixed and it is set to 576 bytes, which is a typical value for an IP packet size ([56]). These settings result in a mean data rate during packet call equal to 115 kbps.

Parameters of the Modified Gaming Traffic Model			
	Parameter	Distribution	Values
Packet Call	Duration	exponential	5 s (mean)
	Reading Time	exponential	5 s (mean)
Datagram	Inter-arrival Time	log-normal	40 ms (mean), 38 ms (std)
	Size	deterministic	576 bytes
	(Resulting) Data Rate during Packet Call	-	115 kbps

Table 3.1: Parameter settings of the “Modified Gaming” traffic model.

This traffic model is very generic and it can easily provide various levels of data rates and of burstiness by tuning its parameters. Parameters having an influence in the burstiness of the model are mainly the datagram inter-arrival time, the reading time and the packet call duration, whilst the offered data rate is primarily influenced by the datagram size and the mean datagram inter-arrival time.

Generated IP datagrams (or packets) are stored in RLC buffers. They are removed from the buffers either upon their correct reception or upon their expiry. Upon correct reception of an IP datagram in the Node B, an immediate acknowledgement is sent to the UE and the IP datagram can be removed from the RLC buffers.

### 3.5.2 Simulation Parameters

The simulation time is 18 minutes. The time step of the simulation is equal to a radio frame duration, thus 10 ms. For each simulation, the UE is placed at various distances from the Node B. The UE is supposed to move cyclically around the Node B, so as its distance to the Node B is constant. The total received power (or equivalently the interference) in the cell is constant and it is equal to -100 dBm. The propagation model chosen is the Okumura-Hata model in a metropolitan area ([36]). The UE maximum transmission power is 21 dBm ([62]). Each IP datagram (packet) of the interactive service remains in the UE buffer for 6 seconds. After the expiration of this period, it is removed from the UE buffer.

The ‘‘TFC elimination mechanism as it is described in [73] has been implemented, with the parameters X, Y and Z equal to 1, 30 and 30 slots respectively. The offset considered for the TFC elimination ( $TFC E_{offset}$ ) is set to 1 dB. For the modified TFC selection algorithm, the transmission power offset,  $P_{offset}$ , is set to 3 dB.

A list with the most important simulation parameters can be seen in table 3.2.

Simulation time	18 [minutes]
Chip Rate	3.84 [Mcps]
UE Max Tx Power	21 [dBm]
UE Min Tx Power	-50 [dBm]
TFC Elimination Offset	1 [dB]
$P_{offset}$	3 [dB]
Path loss with distance d km	$147.3 + 38.3\text{Log}_{10}(d)$ [dB]
$I_{total}$	-100 [dBm]

Table 3.2: Simulation main parameters

The traffic models used, are described in detail in the previous paragraphs.

As discussed before, the UE supports three services: (i) a real time one, (ii) signalling and (iii) a packet data service. The real time service is the speech. It is modeled according to the description in the previous paragraphs. The same applies for the traffic model of the packet data service. Speech has the highest priority among the services and the one with the second highest priority service is the signaling.

A CS radio bearer of 12 kbps is allocated for the speech, a signalling radio bearer of 4 kbps for the signalling and a packet switched bearer of 128 kbps for the interactive

	Transport Channels		
	#1	# 2	# 3
TTI [ms]	20	40	20
Coding type	Convolutional	Convolutional	Turbo
Coding rate	1/3	1/3	1/3
CRC	12	16	16
Transport Block Set Sizes [bits]	0	0	0
	240	160	160
			2 · 160
			4 · 160
			8 · 160
			16 · 160

Table 3.3: Attributes of the transport channels used in the simulation. Parameter values are in line with the ones in [82].

packet data service. The transport channel attributes of the corresponding radio bearers are listed in table 3.3. They are in conformance with the ones in [82]. It can be noticed in table 3.3 that the Adaptive Multi-Rate (AMR) feature ([81]) is not considered for the speech.

The combination of the transport channels form the TFCS of table 3.4. This table represents the transport block set sizes per transport format combination. In addition, the SF applied for the transmission of each TFC and the resulting total data rate are also displayed. Combinations are ranked in ascending order of total data rate and hence of required transmission power.

### 3.6 Simulation Results

The performance of both the 3GPP compliant algorithm and of the modified one is compared. The comparison is performed for various distances between the UE and its serving Node B.

Criteria for the performance evaluation are the QoS of the UE's services. The QoS measurement for the speech is the block error rate (BLER). It is defined as the ratio of the erroneously received transport blocks of speech to the total number of transmitted blocks of speech. For the packet data service, the QoS is measured in terms of percentage of lost IP packets. Considering that the retransmission of IP packets is possible, lost IP packets are the ones that are removed from RLC buffers after their expiry.

In addition, we look at the Frame Error Rate (FER) and the UE transmission power. The FER is defined as the ratio of the erroneous received physical layer (radio) frames to the total number of transmitted frames.

The focus is placed on the performance of the speech. The reason for this is that it is the service of the highest priority and the most difficult to handle, due to its stringent QoS requirements. According to 3GPP specifications, for speech it is required that the BLER is maintained up to 2% ([78]). Therefore the FER target needed for the operation of the outer loop power control is set to 2%.

TFCS					
TFCI	Transport Bloc Set Size per Transport Channel [bits]			SF	Total Data Rate [kbps]
	# 1	# 2	# 3		
1	0	0	0	256	0
2	0	160	0	256	4
3	0	0	160	128	8
4	0	160	160	64	12
5	240	0	0	64	12
6	0	0	320	64	16
7	240	160	0	64	16
8	0	160	320	32	20
9	240	0	160	32	20
10	240	160	160	32	24
11	240	0	320	32	28
12	0	0	640	32	32
13	240	160	320	32	32
14	0	160	640	32	36
15	240	0	640	16	44
16	240	160	640	16	48
17	0	0	1280	16	64
18	0	160	1280	16	68
19	240	0	1280	8	76
20	240	160	1280	8	80
21	0	0	2560	8	128
22	0	160	2560	8	132
23	240	0	2560	8	140
24	240	160	2560	8	144

Table 3.4: The TFCS used in the simulation.

In the following, we mainly present statistics for various path losses experienced by the UE. For simplicity reasons, the different path loss values are mapped to the distances they correspond. Hence, throughout this section when the discussion is about distance, the latter one stands for the distance that corresponds to a certain radio path loss.

Figure 3.5 displays the FER versus various distances. The two TFC selection algorithms and the case where only speech and signaling are transmitted (“speech only”) are displayed. It can be seen that when the 3GPP compliant algorithm is applied, the UE is able to preserve the FER to 2% till a distance of around 1100 m to the Node B. On the contrary, in the case of the modified TFC selection algorithm the FER is maintained to 2% till the distance of 1400 m.

This has an impact on the BLER for speech as it can be seen in figure 3.6.

The same behaviour is observed for the percentage of lost IP packets. Figure 3.7 shows that approximately no losses of IP packets occur till the distance of 1100 m and then the percentage of losses increases to very high levels. These losses have an impact on the total UE throughput (with this term we mean the total data rate that is successfully transmitted

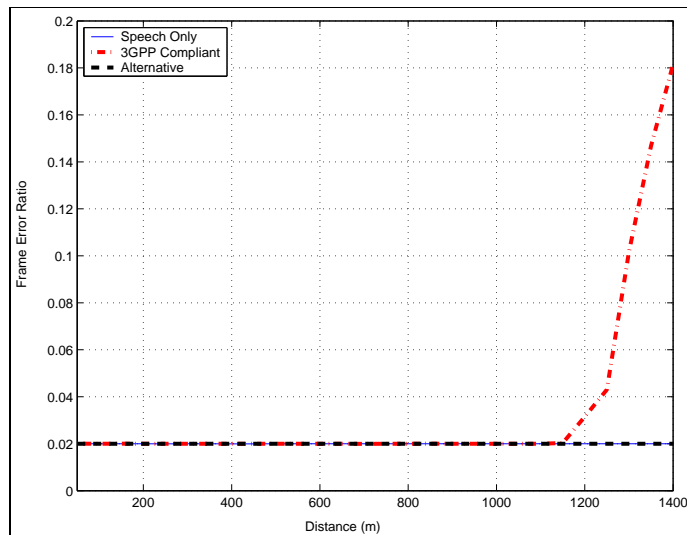


Figure 3.5: FER for various distances between the UE and the Node B.

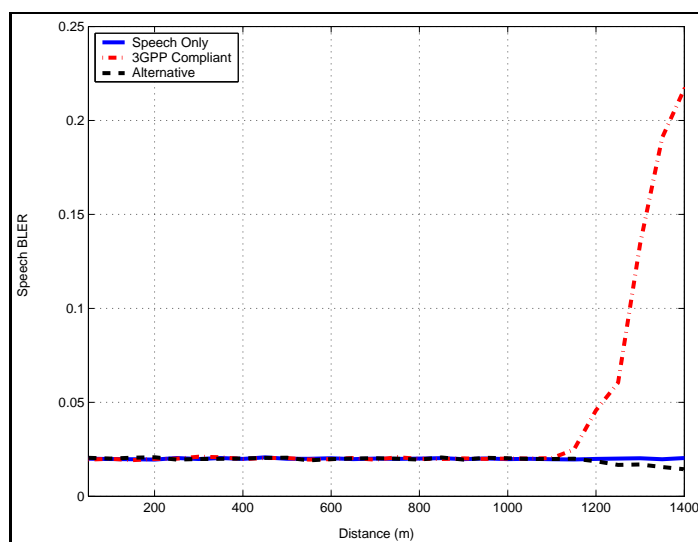


Figure 3.6: Speech BLER for various distances between the UE and the Node B.

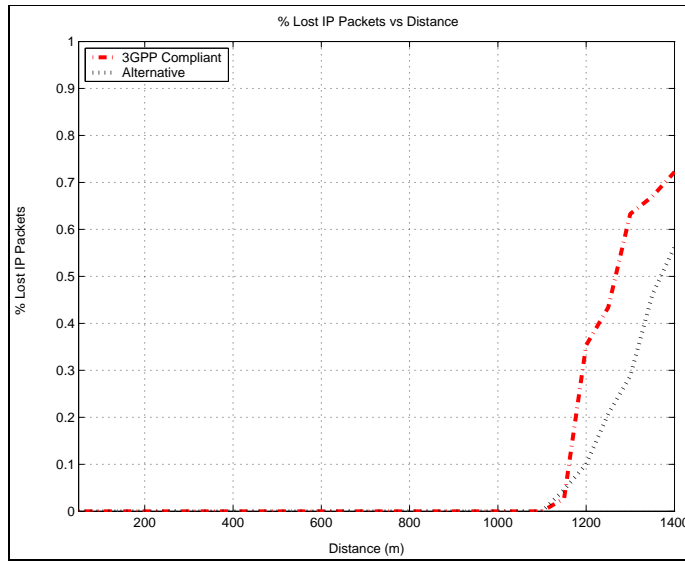


Figure 3.7: Percentage of lost IP packet for various distances between the UE and the Node B.

UE-Node B Distance [m]	UE Throughput [kbps]	
	3GPP Compliant	Alternative
1200	40.4	47.31
1300	29.09	38.06
1400	23.68	26.8

Table 3.5: Total UE throughput for the distances of 1200m to 1400 m for in case of the 3GPP compliant and the alternative TFC selection algorithms.

by the UE). Table 3.5 shows the total data rate that is successfully transmitted in case of the 3GPP compliant and of the alternative algorithms. It can be seen that the UE throughput is higher when the alternative TFC selection algorithm is applied.

Table 3.5 displays the values for the distances of interest, hence for distances higher than 1200 m. Although, the values in the table correspond to specific distances, the observed trend is general. This improvement in the so called total UE throughput is however achieved with the specific value of the  $P_{offset}$ . Higher values are expected to result in reduced UE throughput.

These results show that in the case of 3GPP compliant algorithm, the services can be guaranteed up to a distance of approximately 1100m. For higher distances, services cannot be guaranteed because the UE is in shortage of transmission power. Figure 3.8 shows the mean transmission power versus distance for both of the algorithms and for the case of “speech only” transmission. It can be seen that for distances higher than 1100 m, the mean transmission power is close to the maximum power, in the case of the 3GPP compliant algorithm. Hence, upon each TFC selection, at the beginning of each TTI,

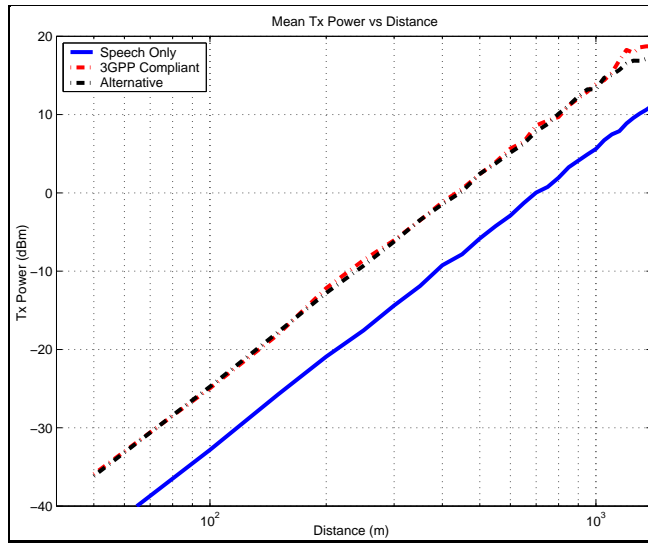


Figure 3.8: Mean UE transmission power for various distances between the UE and the Node B.

the transmission power is close the maximum. This increases the probability of the UE reaching the maximum transmission power, as a result of it following fast power control commands. As a result, the probability of losses increases.

In the same figure (figure 3.8), it can be seen that for high distances the mean transmission power is lower in the case of the alternative algorithm. This mainly derives from the fact that this algorithm reduces the probability that both speech and high data rate packet data are transmitted simultaneously; the transmission of such a combination requires a high amount of power.

Figure 3.9 shows the probability of selection of one TFC of the TFCS of table 3.4 for both of the TFC selection algorithms. The distance to the Node B is 1400 m. The figure shows that in the case of the 3GPP compliant algorithm the UE selects to transmit with the TFC 24 for approximately 14% of the time. The selection of TFC 24 involves the simultaneous transmission of speech, signaling and packet data of 128 kbps. In the case of the alternative algorithm the probability that the TFC 24 is selected for transmission is reducing. The UE in this case usually selects to transmit high data rate packet data separately. Hence an increase in the number of times TFCs 21, 17, and 12 are selected is observed.

The attempt to transmit speech and high data rates of packet data simultaneously in the case of the 3GPP compliant algorithm increases the transmitted power. Figure 3.10 shows the CDF of the transmission power for both algorithms. It can be seen that in the case of the 3GPP compliant algorithm, the UE transmits approximately 20% of the time at the maximum transmission power.

Figures 3.11 and 3.12 show the percentage of correct and incorrect reception per TFC, for all of the TFCs in the TFCS of table 3.4. It can be seen that in the case of the 3GPP compliant algorithm, when the TFC 24 is selected for transmission, approximately 67%

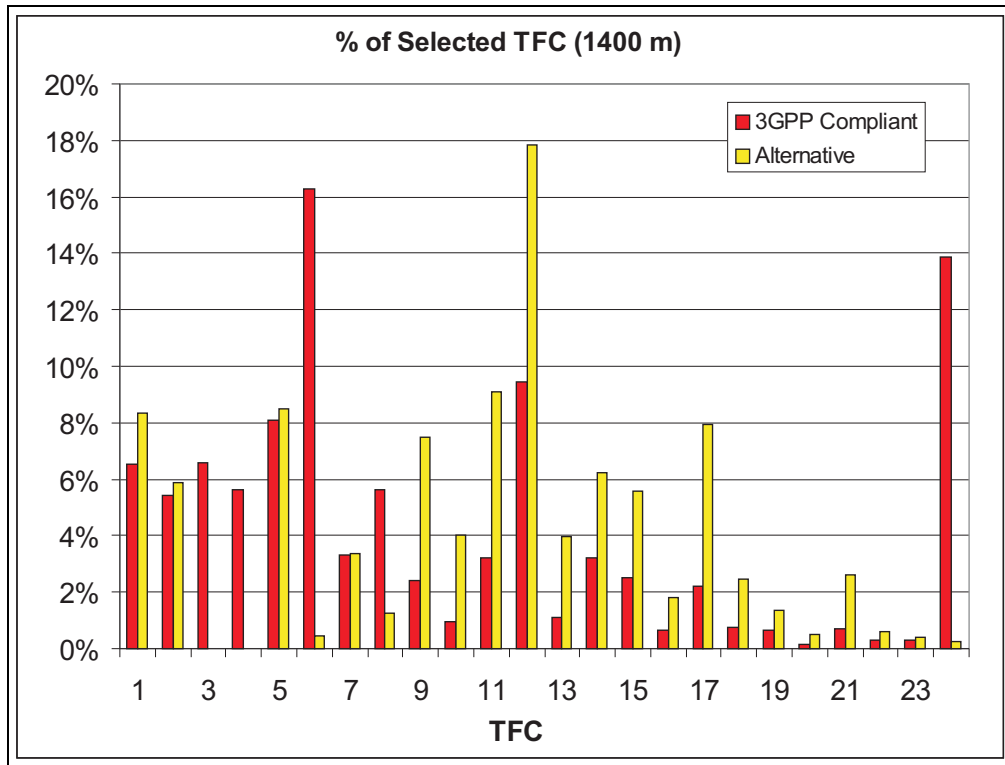


Figure 3.9: Probability of selected TFC for a distance to the Node B equal to 1400 m.

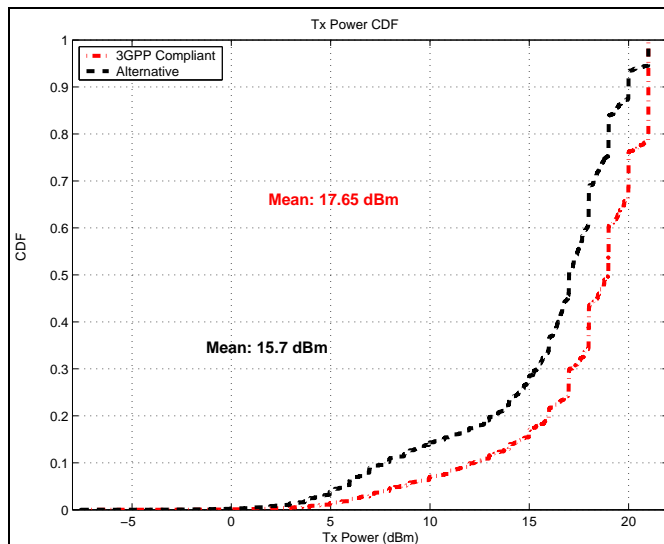


Figure 3.10: CDF of the UE transmission power for a distance to the Node B equal to 1400 m.

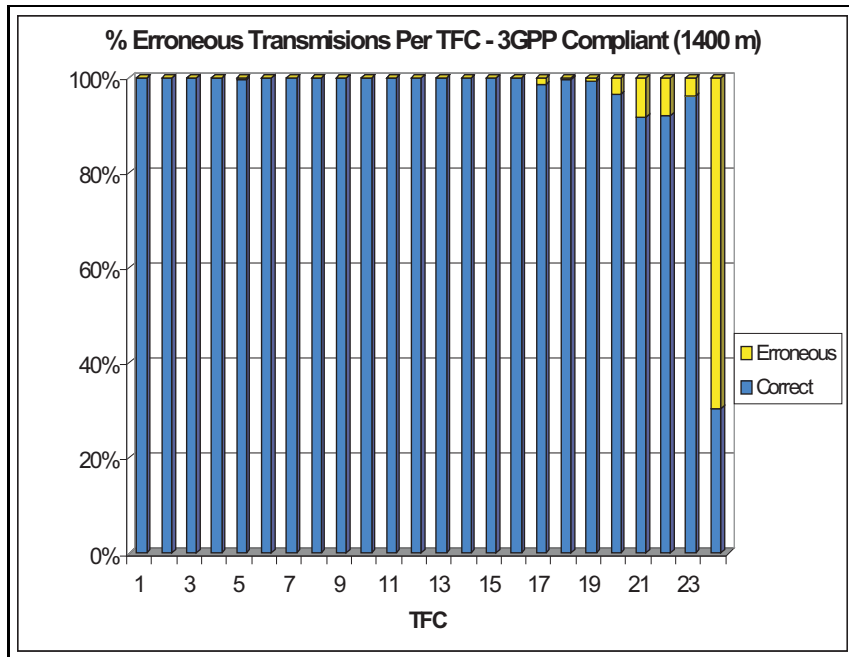


Figure 3.11: Percentage of correct-erroneous reception per selected TFC in the case of the 3GPP compliant algorithm.

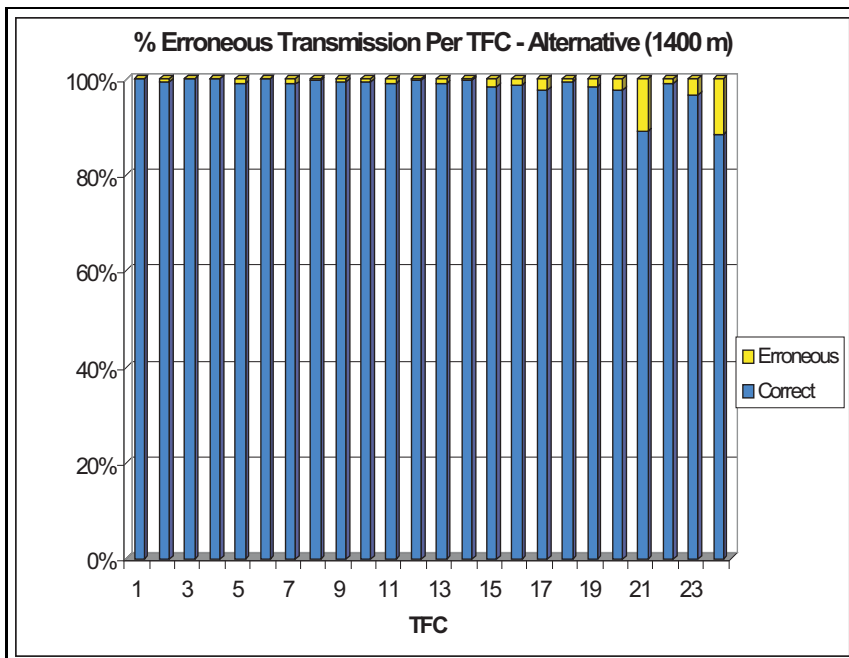


Figure 3.12: Percentage of correct-erroneous reception per selected TFC in the case of the alternative TFC selection algorithm.

of the times it fails. It could be easily argued that these failures occur when the UE is transmitting with the maximum power.

In the case of the alternative algorithm, there is an increased probability of erroneous reception in the case high data rate packet data is transmitted (TFCs 21 and 24).

Results have shown that the so-called “alternative” TFC selection algorithm outperforms the 3GPP compliant one. This is the impact of the addition of a margin whenever speech is transmitted, that leads to the separation of transmission of speech and packet data. The increase of the already existing TFC Elimination margin (‘TFC Elimination Offset’) will not bring the gain presented here.

In order to certify this argument, simulations with an increased margin for the TFC Elimination Offset are conducted. The value of the ‘TFC Elimination Offset’ is set to 4 dB. This value is the sum of the ‘TFC Elimination Offset’ used before (1 dB) and of the additional offset,  $P_{offset}$  (3 dB).

Table 3.6 summarizes some of the obtained results: the BLER for speech, the percentage of lost IP Packets and the mean UE throughput. The distances for which the TFC Elimination mechanism is in effect are displayed, hence distances equal or higher than 1200 m. From table 3.6, it can be seen that the BLER for speech is insignificantly improving in comparison to the case of a TFC Elimination Offset equal to 1 dB (see figure 3.6). However, it is still above the requirement of 2%. The increase of the TFC Elimination margin has an effect on the percentage of lost IP packets and consequently on the effective UE throughput as it can be seen in table 3.6: they are significantly reducing. The reason for these results is that the increased TFC Elimination Offset leads to a conservative algorithm that blindly eliminates the high data rate TFCS independently of the type of traffic they support. Hence, it does not lead to separated transmission of speech and packet data, as it was achieved in the case of the alternative TFC selection algorithm.

UE-Node B	Speech	% Lost	UE
Distance [m]	BLER	IP Packets	Throughput [kbps]
1200	5.3	36.87	31.85
1400	16.43	85.13	15.97

Table 3.6: BLER for speech, percentage of lost IP Packets and mean UE throughput for the case of the 3GPP compliant algorithm and when a TFC Elimination Offset of 4 dB is applied.

## 3.7 Conclusions and Discussion

In this chapter the radio link adaptation in the MAC layer during uplink multi-service transmission has been discussed. Radio link adaptation in MAC layer is performed through appropriate TFC selection.

The present chapter has started with a description of the TFC selection as a protocol mechanism. Then, the algorithmic part of the TFC selection is studied. An algorithm of TFC selection that is based in the guidelines imposed by 3GPP specifications has been

---

implemented and tested through simulations. A scenario with a combination of speech, signaling and an interactive service has been investigated. Results have shown that the addition of a packet data (interactive) service to speech “shrinks” the coverage area. The tested services can be guaranteed of a distance to the Node B approximately equal to 1100 m.

An alternative TFC selection algorithm has been proposed. Its aim is to guarantee the voice service for even higher distances in comparison to the case the 3GPP compliant algorithm is applied. This is achieved through the introduction of an additional margin that is considered only when speech is transmitted. A side effect of the algorithm is that simultaneous transmissions of speech and high data rate packet data that require high transmission power are avoided. Simulation results show that speech can be guaranteed for even higher distances when the proposed TFC Selection algorithm is applied. Moreover, the total UE throughput increases upon application of the proposed algorithm, without increasing the mean UE Tx power. This is a direct consequence of the reduction of losses and hence of retransmissions. With these assumptions, the proposed algorithm improves the utilization factor of the UE Tx power.

## Chapter 4

# Uplink Packet Data Access in WCDMA

In this chapter the packet data access in the uplink direction of UMTS is discussed. The mechanisms involved therein are presented and their influence in the system performance is quantified. A procedure having a major impact on the overall performance of the packet data access is the packet scheduling; therefrom, the description focuses on this procedure. Simulations have been performed with a network simulator implemented for this purpose and results are presented.

The chapter is organized as follows: the aim of this chapter along with a brief introduction to the packet data access in UMTS is given in sections 4.1 and 4.2. The main procedures participating in the uplink packet data access and important related issues are listed in section 4.2. They are described in detail in the next sections, 4.3, 4.4 and 4.5. Simulation campaigns have been carried out in order to assess the performance of the uplink packet data access. A system level simulator consisted only of packet data users is therefore implemented. The system model used for the simulations along with the simulation parameters are detailed in section 4.6. A listing of the performance evaluators used follows in section 4.7. Simulation results are presented and analyzed in section 4.8. Conclusions and some discussion on the simulation results follows in section 4.9.

### 4.1 Introduction and Aim

#### Introduction

In UTRAN, packet data access applies mainly to non real time (NRT) traffic, thus to interactive and background traffic classes. It could be used also for real time (RT) traffic, such as streaming or conversational, but only in specific cases, e.g. voice over IP.

The uplink direction of transmission in UMTS, as in other CDMA systems is interference limited. Thus, the scarce radio resource directly influencing the uplink capacity and hence the one to be scheduled is the received power in the Node B ([58]). Therefore, scheduling algorithms where the received power in the Node B is shared among UEs are

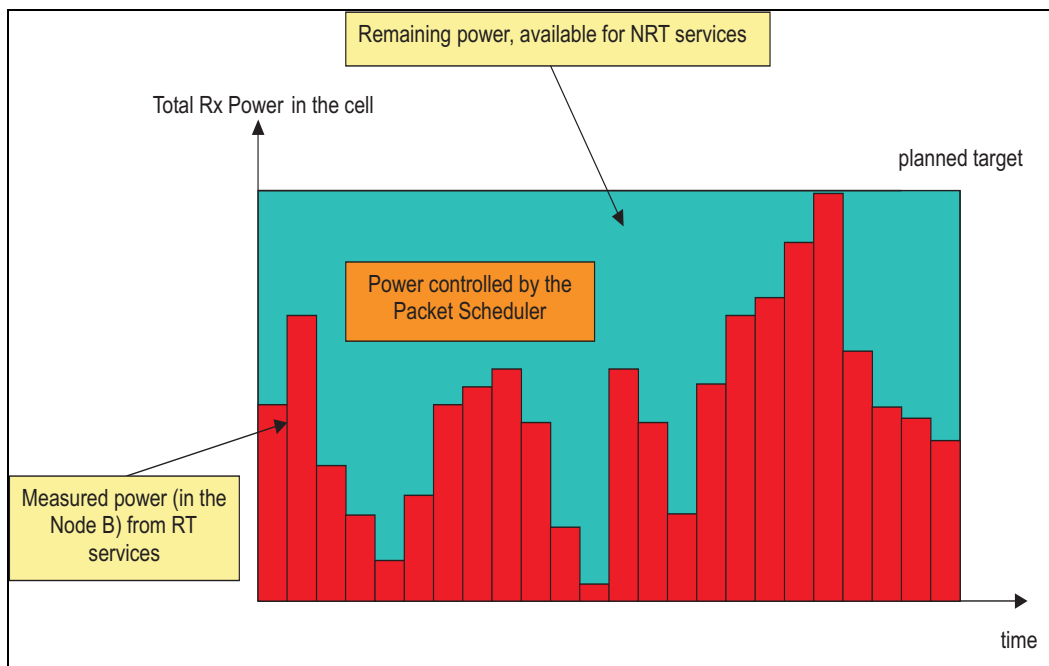


Figure 4.1: Division of the total received (Rx) power in uplink between RT and NRT traffic.

proposed in several articles, e.g. in [10], [32] and [23]. Therein, the term “uplink interference” is used in order to denote the total received power in the Node B. Here, both of the terms are used and they stand for the total received power in the Node B.

In a single cell, there is a unique power budget (i.e. the total received power) that has to be shared among the RT and the NRT traffic. As RT traffic has higher priority over NRT traffic, the power that is allocated to the NRT traffic is the one that is not used by the RT one.

Packet data transmission can be performed either on (i) common and shared channels or on (ii) dedicated ones. We discuss here the packet data transmission on dedicated channels, which ends up to be a variable bit rate circuit-switched transmission. Hence, the requirement for efficient packet scheduling on these channels is more stringent.

The power allocated for the transmission of NRT type traffic is controlled by the packet scheduler (PS), which is traditionally located in the RNC.

### Aim

The aim here is to assess the performance of the uplink packet data access through dedicated channels. Therefore, we choose a quite representative packet scheduling algorithm: the ‘fair throughput sharing’ one. We also aim at finding parameters having an impact on the overall system performance and tune them accordingly.

## 4.2 General Issues

Figure 4.2 illustrates an overview of the uplink packet data access in UMTS. We can approximate that the packet data transmission in uplink is characterized by the request-response model, as already mentioned in 1.2. First, UEs that have packet data in their RLC buffers, report the amount of data waiting in their buffers to the PS. The last one performs data rate allocations based on these measurement reports, which it interprets as capacity requests. At each scheduling interval, capacity requests previously received in the PS are ranked according to the scheduling policy applied. For each processed request, it is tested whether a possible data rate allocation to the UE (from which the request originates), results in an estimated total received power above the planned target. If this constraint is satisfied, the UE is allocated data rates, otherwise the request remains in the PS buffer. At the end of the requests processing, the network notifies the UEs that are granted resources with their new TFCS that contains the maximum TFCI (and equivalently data rate) they can apply during their uplink transmission. (In case the UE is not connected to the network, hence it is not already allocated a RAB, the network sends a RAB configuration message that contains the new TFCS. In our studies however, we consider that all UEs are already connected to the network, as mentioned in chapter 1). Then, UEs transmit by selecting one of the TFCIs within their TFCS.

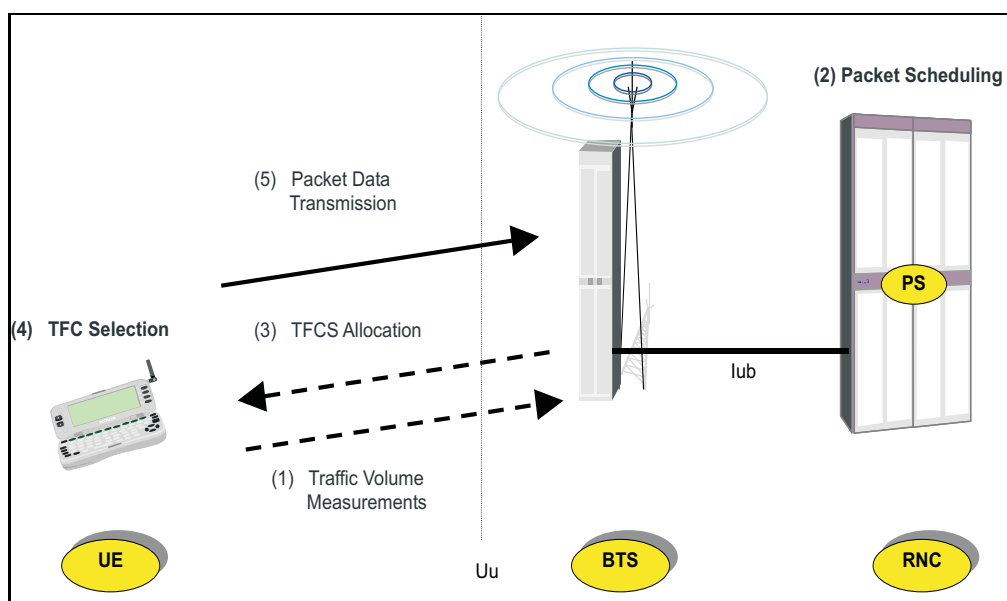


Figure 4.2: Overview of the Uplink Packet Data Access in WCDMA Uplink

From figure 4.2 and from the above description, the uplink packet scheduling in UMTS is a combination of centralized and distributed (UE autonomous) packet scheduling.

In the following section, the traffic volume measurements reporting and the packet scheduling procedures are described in detail.

### 4.3 Capacity Requests

As discussed above, an UE is implicitly sending a capacity request to the network when it transmits a traffic volume measurement report. The traffic volume measurement reporting consists an important procedure in the uplink transmission of packet data. It is not of the same importance in case of constant bit rate (CBR) services. In the latter ones, measurement reports are transmitted only once at the beginning of the service session, since the traffic flow remains constant during the whole session. Hence, the network can easily model this traffic and allocate resources accordingly ([79], [16]). To the contrary, in the case of packet data transmission, measurement reports have to be sent several times within a packet data session, mainly due to the bursty nature of traffic. For this reason also, the PS removes capacity requests from its buffer after a certain period.

With these messages UEs inform the network about the buffer size of the RLC entity connected to a certain transport channel. Hence, in case of multi-traffic transmission, where there is more than one transport channel carrying packet data traffic, a measurement report per transport channel is transmitted ([77]).

Traffic volume reporting is performed either (i) periodically or (ii) upon detection of a certain event. The latter is called “event-triggered” and it results in a periodic measurement report during activity periods, as it is going to be explained in the following.

In case of periodical measurement report transmission, the time interval between two consecutive messages may vary from 250 ms to 64 seconds ([77]). The choice of the measurement reporting period is done in a way that the reporting is frequent enough, so as the PS can perform appropriate allocations, while at the same time the signalling overhead is kept low. This value should also consider the maximum lifetime of a capacity request in the PS buffer.

In the periodical measurement reporting, the UE either reports the current RLC buffer size in number of bytes, or the mean RLC buffer size along with its variance.

For the case of “event-triggered” measurement reporting, the UE reports its RLC buffer size when the last one exceeds a predefined threshold during a certain time interval. Two thresholds for the RLC buffer size are defined: a high one and a low one. A measurement report is transmitted when (i) the RLC buffer size is larger than the high threshold and when (ii) it is smaller than the low threshold. The threshold value for the RLC buffer size ranges from few bytes to some hundreds of kbytes. In this case, the UE notifies to the network the identity of the detected event ([77]).

The “event-triggered” reporting is controlled by two timers, as it can be seen in figure 4.3. (The figure represents the case of the high threshold. The same procedure applies also for the low threshold). The first timer is called “time to trigger”. It starts upon event detection (moment  $t_1$  in figure). Upon its expiration (moment  $t_2$ ), it is tested if the RLC buffer size is bigger than the high threshold. A report is transmitted only in the case the condition is satisfied. In the case the RLC buffer size is not anymore bigger than the high threshold, the timer stops. The “time to trigger” interval can be seen in figure 4.3. It is the time period  $t_s$ . Its value may vary from 0 to few seconds ([77]). This time period is mainly introduced in order to avoid reports triggered by small discontinuous bursts whose transmission does not require additional resources. The choice of this timer has to be made in a way that unwanted measurement reports are avoided, while the transmission of

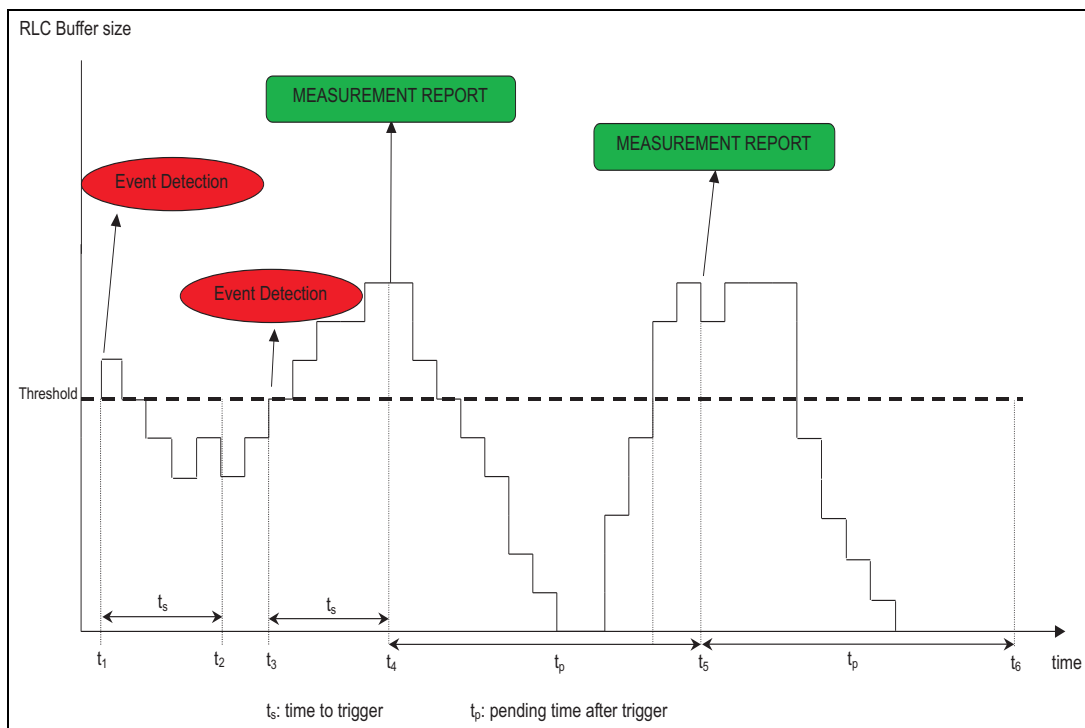


Figure 4.3: Timings in the Measurement Report sending procedure.

the measurement report is not considerably delayed.

Figure 4.3 shows another timer that controls the measurement reporting. It is the “pending time after trigger” timer ( $t_p$  in figure 4.3). Following the transmission of a measurement report (moment  $t_4$  in figure 4.3), this timer starts. A new measurement report is transmitted only if the event is still detected upon expiry of the timer (moment  $t_5$ ). When the “pending time after trigger” is active, the “time to trigger” timer is not considered, as it can be seen in figure 4.3. Hence, the “pending time after trigger” has somehow “higher priority” than the “time to trigger” timer. The value of the “pending time after trigger” timer ranges from 250 ms to 16 seconds ([77]).

The choice of the value of the “pending time after trigger” has to be based on the same principles that characterize the selection of the period of the transmission of measurement reports, in case of periodical reports sending.

Among these two options of transmitting measurement reports, the periodical one is creating a higher amount of signalling overhead comparing to the “event-triggered” mode, if the measurements are sent at short periods.

## 4.4 Packet Scheduling

In uplink, the resource to schedule among users is the total received power in the Node B, as mentioned above. Therefore, the scheduling is based on power. It is performed by an entity called Packet Scheduler (PS), which is located in the RNC.

From architectural point of view, the packet scheduler is a part of the Radio Resource Management (RRM) module of the UTRAN (see figure 4.4). As it can be seen in this figure, the packet scheduler communicates with the RRC and MAC protocols and other RRM entities. It receives capacity requests (in form of traffic volume measurement reports) from the RRC protocol and then transmits to RRC the allocated TFCS of the users that are allocated power at the end of the packet scheduling.

From the Load Control (LC) module the packet scheduler receives information regarding the total received power in the cell, the received power from RT traffic. The LC entity communicates with the Node B. The latter one provides periodically to the LC the mean values of the above mentioned entities over an observation window. In addition, it receives the value of the planned target for the received power.

The PS receives from the MAC layer information about inactive users, i.e. for users who have been allocated resources but they are not making use of them.

These information is important for the estimation of the available for scheduling power, as it is going to be discussed in the following.

The packet scheduler operates at each “packet scheduling period”, which is typically much longer than an UMTS radio frame. The latter one being equal to 10 ms ([72]) and as discussed in chapter 2.

Not all of the packet data users can be allocated data rates at a designated packet scheduling period; for each user a “modification period” has been defined. The modification period is the same for all of the users. It is the minimum time interval between two consecutive data rate modifications to a specific user.

The role of the packet scheduling and modification period can be seen in figure 4.5.

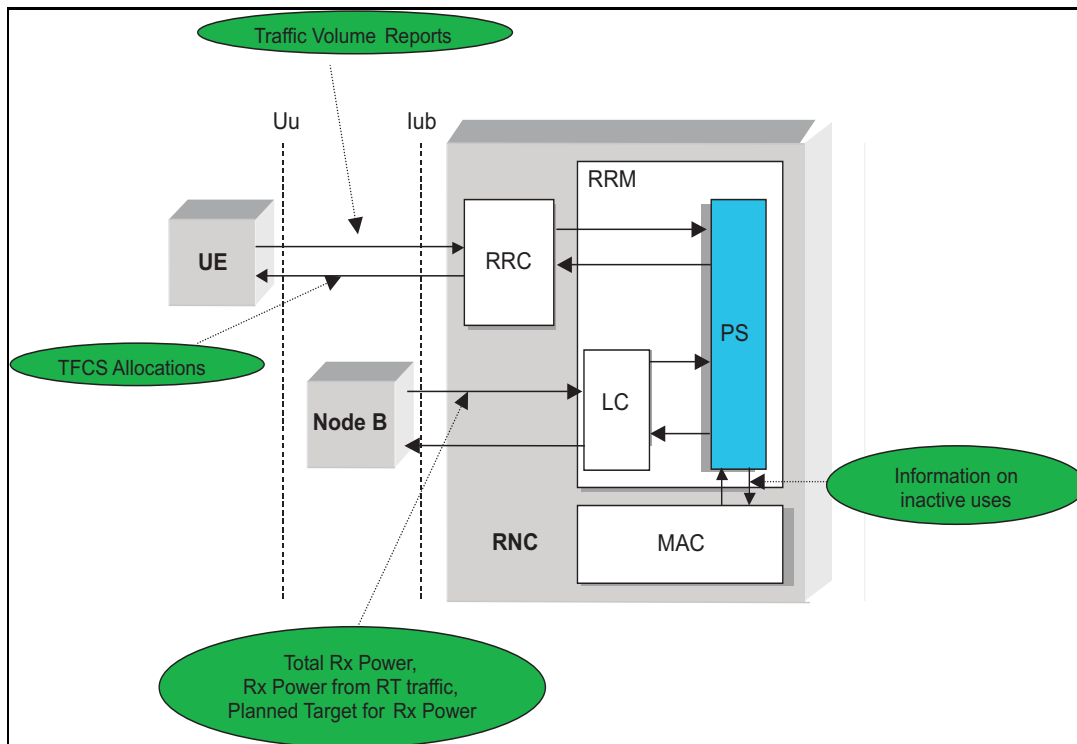


Figure 4.4: Packet Scheduling Working Environment (figure inspired from corresponding figure in [40]).

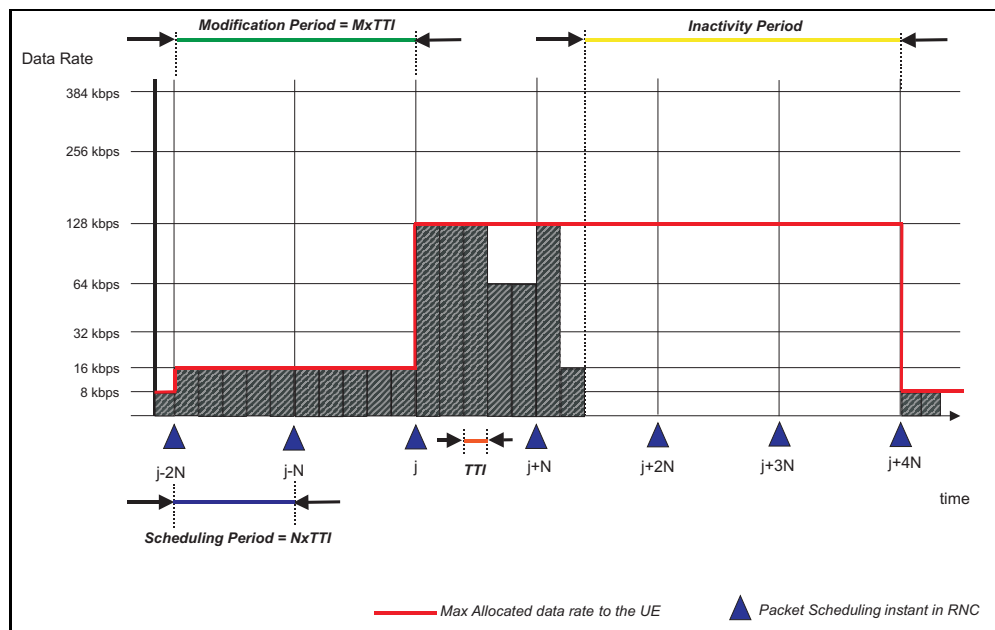


Figure 4.5: Time intervals in the packet scheduling procedure.

This figure illustrates an example of data transmission from a single UE. Therein, the time intervals involved in the transmission of a single user, such as TTI, PS period and modification period can be seen.

In the same figure, another time interval of the packet data transmission of a user can be seen. It is the “inactivity period”. It is the interval during which a user that has been allocated data rates is not transmitting. This implies that the user’s RLC buffer is empty. Upon detection of inactivity in the receiver side (in the RNC), a timer, the “inactivity timer”, is launched. Upon its expiry, resources are released.

These intervals define how dynamic is the functioning of the PS. They have a considerable impact on the performance of the packet scheduling and hence on the overall system performance, as it is going to be discussed in chapter 5.

#### 4.4.1 Packet Scheduler Functioning

At each scheduling period, capacity requests originating from users that can be allocated data rates at this certain moment, i.e. it is permitted by their modification period, are gathered. They are then ranked. Next, UEs that have been inactive for longer than the inactivity period, are downgraded to lower data rates. Then, it is tested whether the total received power is below the planned target. If it is the case, the PS starts the allocation of data rates to UEs according to the scheduling policy we are going to describe below. In the case the total received power is above the planned target, the load control function is performed.

Figure 4.6 illustrates the functioning of the packet scheduler at each packet scheduling period.

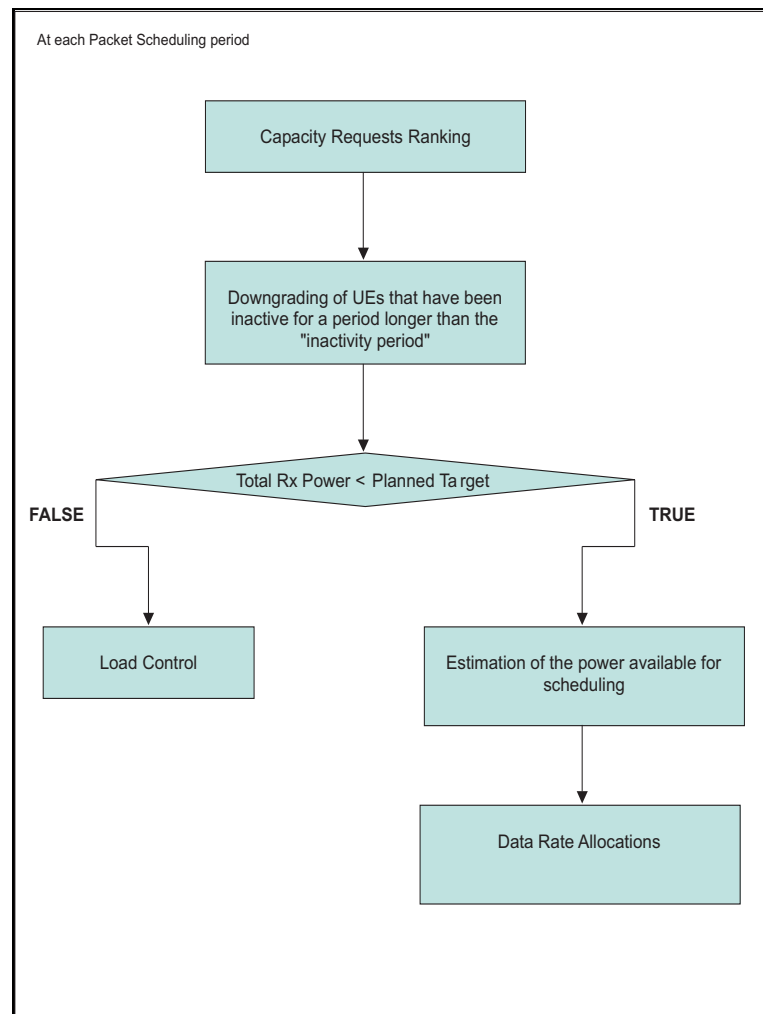


Figure 4.6: Functioning of the PS at each packet scheduling period.

### 4.4.2 Ranking of Capacity Requests

A number of queuing policies may be defined ([30]). Common policies are the First In First Out (FIFO), Last In First Out (LIFO), etc.

It has to be noted that the queuing policy is directly related to the whole packet scheduling policy. Considering that the implemented packet scheduler aims at performing fair throughput sharing, we choose to sort capacity requests in ascending order of allocated data rates, i.e. requests from UEs that have been allocated the lowest data rates are placed first. For requests originating from UEs that have been allocated the same data rate, the FIFO criterion is applied.

### 4.4.3 Data Rate Downgrade

From the description above, it derives that another task of the PS, apart from the allocation of data rates to UEs, is to downgrade data rates of different UEs. In various PS implementations, e.g. in case the PS aims at making an allocation of equal throughput to UEs, the PS may downgrade the bit rate of an UE in order to upgrade the data rate of another UE.

In addition, a reason for which an UE is downgraded to a lower data rate is when it is detected that this designated UE has been inactive for a time interval longer than the “inactivity period”.

In both of these cases, the UE can be downgraded to the next lower data rate from the one it has been allocated or to even lower data rates.

In the implementation here, the PS is downgrading the data rate of an UE only upon detection of an inactivity longer than the “inactivity period” for this UE. In this case, the UE is downgraded to the minimum possible data rate.

### 4.4.4 Estimation of the Available Power for Scheduling

At each packet scheduling period, the power available for scheduling at each Node B is obtained; originally, it is the difference between the planned target for the received power and the previously total received power. The PS is aware of both of these two values, since the received power threshold is radio network planning parameter and the mean total received power is notified to the PS by the load control entity (figure 4.4).

However, an additional margin (in the available power) for the previously inactive users has to be considered. In the last measurement of the total received power (that is transmitted from the LC entity to the packet scheduler), the contribution of non-transmitting users is zero. The possibility that some of the previously inactive users, may start transmitting with their allocated data rate and increasing thus the total received power in the next period has to be taken into account. Therefore, the power that is available for scheduling,  $P_{av}$ , is:

$$P_{av} = P_{target} - P_{Rx} - WFIU * P_{inact} \quad (4.1)$$

where  $P_{inact}$  is the estimation of the transmission power of the inactive users, in case they start transmitting at their allocated data rate and  $WFIU$  stands for the Weighting Factor

for Inactive Users. It is a weighting factor of the estimated power due to the users, that have been inactive during the previous period. It ranges from 0 to 1 and its value defines how preemptive the packet scheduler functioning is, as it is going to be shown later.

It has to be noted here that the margin due to inactive users refers only to UEs that have been inactive during the last period of measurement of the total received power in the Node B. It does not refer to UEs that have been detected inactive for an interval longer than the “inactivity time” and that have been downgraded to the lowest data rate.

#### 4.4.5 Scheduling Policy

For CDMA systems, the most common packet scheduling policies are the fair throughput scheduling, the best C/I and the time scheduling, as it is described in [22]. In the fair throughput scheduling, it is attempted to divide the available throughput equally to users, whilst in the best C/I scheduling, users that experience the best C/I ratio are the ones with higher priority on data rate allocation. In the time scheduling, resources are allocated to a single user for a time period.

Based on these main group of scheduling policies, numerous others have been proposed, e.g. in [3], [35] and [9].

In our simulation we choose the “fair throughput sharing” policy. Its aim is to share the available throughput to UEs that request for it, in a way that they have as equal throughput as possible. This scheduling policy is close to the “fair throughput” one.

Reasons for this choice are that this scheduling is

- a quite representative scheduling policy for the uplink packet data access, since it is easy to be implemented and it requires less signalling than the fair throughput scheduling and
- it results in a fairly uniform behavior of all of the users in the simulated network, making thus the collection of statistics from all the users a reliable option for the assessment of the system performance.

Figure 4.7 illustrates the packet scheduling policy. For each capacity request, it is attempted to allocate the next higher data rate to the UE. As mentioned above, the scheduling is done on power. Therefore, for each processed request the resulting total received power due to the allocation of this certain data rate upgrade is estimated. If the new resulting power is below the planned target, the UE is granted the higher data rate.

Following the allocation of a higher data rate to an UE, the (estimated) values of total received power and available power for packet data are updated.

Then, it is tested if the new allocated data rate to the designated UE is equal to the maximum data rate the system can offer. If it is the case, the request is discarded from the PS buffer. Otherwise, it is placed back to the PS buffer with the updated value of TFC.

The procedure ends when the PS buffer is empty or when the available power for scheduling has been exhausted.

Due to the fact that requests are ranked in ascending order of the currently allocated data rate, UEs having been allocated the lowest data rate are firstly upgraded to the next

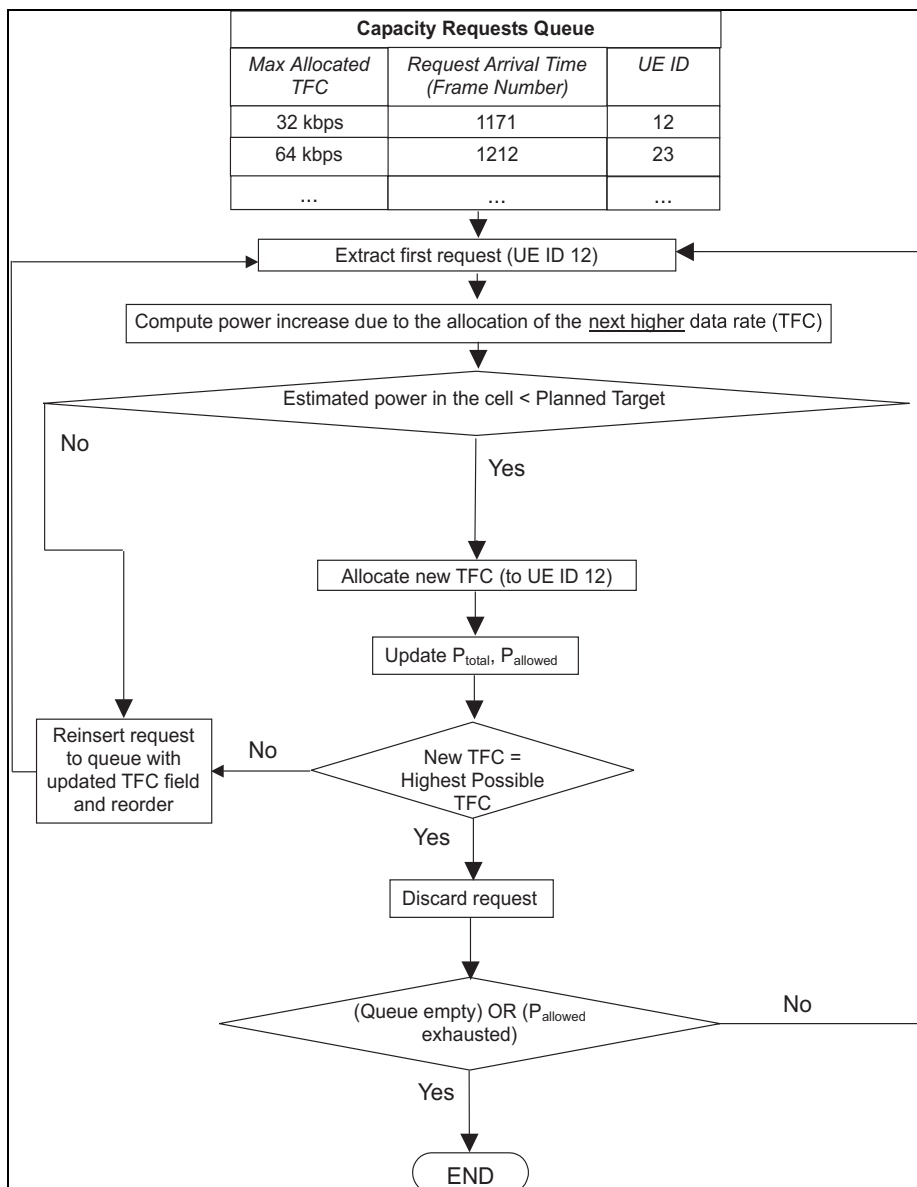


Figure 4.7: Packet Scheduling Algorithm.

higher one. Upon upgrade of all of the UEs with the lowest data rates, the second group of UEs is formed. This second group consists of (i) UEs having been allocated the next higher data rate and of (ii) the UEs that have been upgraded from the lowest data rate to this one. For UEs of this second group it is attempted to allocate the next higher data rate and so on, till there is no more available power.

#### 4.4.6 Load Control

As described in [22], the load control (LC) is an RRM mechanism, whose task is to ensure that the system does not become overloaded. Hence, it maintains the system in a stable state. If the packet scheduling and the admission control mechanisms have been designed accurately, the system is supposed to operate within the desired load range. However, the admission control and the packet scheduling are based on estimations and predictions of the load in the system and therefrom errors are introduced.

The load control is undertaken whenever the air interface load (which is the total received power in uplink) exceeds a certain threshold. Upon triggering of the load control, the data rates of a number of users are downgraded in order to bring the total received power level in a cell back to the allowed level.

The load control operates in collaboration with the packet scheduler, (figure 4.4), therefore it has been included in the implemented simulator.

In the implemented LC function, users are downgraded to the next lower data rate. For each data rate downgrade the resulting received power is estimated; the power modification estimator described above is applied. The LC stops when the total received power is set back to the target. Users that have been allocated the highest data rates are downgraded first.

### 4.5 Power Issues

Upon an upgrade or downgrade of the data rate of a user, the total received power in Node B changes. Therefore, the new total received power in the Node B that results from a data rate allocation or removal to a certain UE has to be estimated. On the basis of this estimation, the PS makes the allocation of data rates as discussed above.

In the following we describe the estimator of the new total received power, that is used in our studies.

For the easiness of the reader, we rewrite the formula that relates the user data rate,  $r_j$ , with the total received power  $P_{Total}$  is ([22]):

$$\frac{E_b}{N_0} = \frac{w}{r_j} \frac{P_j}{P_{Total} - P_j} \quad (4.2)$$

where  $\frac{E_b}{N_0}$  is the energy per bit to noise density ratio of the user detected in the Node B (after demodulation),  $w$  is the chip rate and  $P_j$  is the received power from the user.

Note: Formula 4.2 can be found in related literature in more complicated formats, e.g. in [29]. Therein, receiver imperfections and interference generated by other channels of the same UE are considered. Our physical layer model is not taking into account the above mentioned and similar features. We assume that the non simulated physical layer features exhibit an ideal behavior. Hence, we use the formula 4.2.

By defining the user load,  $L_j$ , as the ratio between the power received at the Node B due to this designated user,  $P_j$  and the total received power,  $P_{Total}$ , it derives from (4.2) that:

$$L_j = \frac{P_j}{P_{Total}} = \frac{1}{1 + \frac{w}{(E_b/N_0) \cdot r_j}} \quad (4.3)$$

The total received power at the Node B,  $P_{Total}$ , excluding the thermal noise,  $P_N$ , is the sum of power received from UEs in the cell,  $P_{own}$  and of the power received from UEs from other cells,  $P_{other}$ :

$$P_{Total} - P_N = P_{own} + P_{other} \quad (4.4)$$

In [58] and in [22], the ratio between the power received at a Node B from users outside the cell,  $P_{other}$ , to the power received from users inside the cell,  $P_{own}$ , has been defined as the i-factor,  $i_f$ :

$$i_f = \frac{P_{other}}{P_{own}} \quad (4.5)$$

Taking into account formula 4.5 and considering that the received power from users in the cell,  $P_{own}$ , can also be written as the sum of the per user received powers, formula 4.4 becomes:

$$P_{Total} - P_N = (1 + i_f) \sum_{j=1}^M P_j \quad (4.6)$$

where  $M$  is the number of UEs in the cell.

By dividing the formula 4.6 with  $P_{Total}$  and by using equation 4.3, the former one becomes:

$$P_{Total} = P_N \cdot \frac{1}{1 - (1 + i_f) \cdot \sum_{j=1}^M L_j} = P_N \cdot \frac{1}{1 - \eta} \quad (4.7)$$

where  $\eta$  is the total uplink load “seen” in the cell:

$$\eta = (1 + i_f) \cdot \sum_{j=1}^M L_j \quad (4.8)$$

Two estimations of the change in the total received power,  $\Delta P_{Total}$ , due to the load increase/decrease  $\Delta L$  are introduced in [21]. They are further discussed also in [22]. Therefore, we adopt their terminology.

The first estimation is obtained from the derivative of equation 4.7. In [21], it is called the “derivative” method and it gives  $\Delta P_{Total}$  as:

$$Derivative : \Delta P_{Total} = \frac{\Delta L}{1 - \eta} P_{Total} \quad (4.9)$$

The second estimation is the so-called “integrative” (in [21]). It is obtained from the integral of 4.9. It is:

$$Integrative : \Delta P_{Total} = \frac{\Delta L}{1 - \eta - \Delta L} P_{Total} \quad (4.10)$$

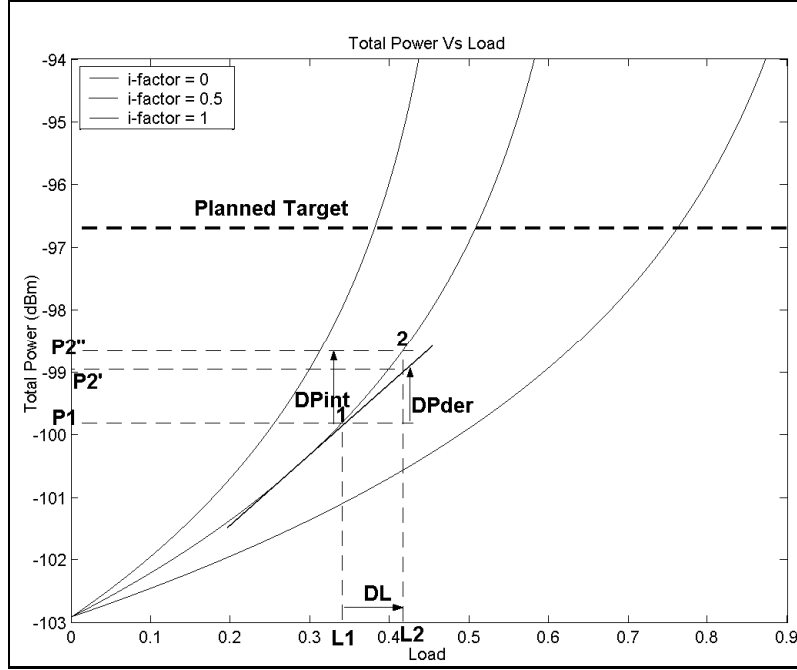


Figure 4.8: Estimation of the new total received power due to the change of the load of a user.

Figure 4.8 illustrates the principle of the estimation of the new total received power, due to the change in the total load by  $\Delta L$ . The case of the increase in the uplink interference due to the addition of a load  $\Delta L$  is displayed. Point 1 marks the current “load state” (before data rate allocation), where the total load in the cell is  $L_1$  and the total received power is equal to  $P_1$ . Upon an allocation of a certain data rate to an UE, the load increases by  $\Delta L$ . The estimated value of the resulting total received power by applying the “derivative” method is equal to  $P_2'$ . The “integrative” method gives the value  $P_2''$ .

It can be seen that the “derivative” method is giving an underestimation of the power increase. To the contrary, the “integrative” method is usually an overestimation of the the power increase. It assumes that the i-factor remains constant upon allocation of data rates to a user and therefore the same i-factor curve is used. This is somehow pessimistic since the allocation of data rate to an UE in the cell is very likely going to increase more the “own cell” received power,  $P_{own}$ , than the “other cell” received power,  $P_{other}$ . Hence, the i-factor decreases and therefore another load curve has to be used for the estimation of the power increase.

For this reason, it is suggested in [21] to apply a weighed sum of these two methods at each load modification. This approach is adopted for our simulator:

$$\Delta P_{Total} = \alpha \frac{\Delta L}{1 - \eta} P_{Total} + (1 - \alpha) \frac{\Delta L}{1 - \eta - \Delta L} P_{Total} \quad (4.11)$$

We set  $\alpha$  equal to 0.5. The term  $\Delta L$  corresponds to the difference between the new load

of the user,  $L_{new}$  and the previous one,  $L_{previous}$  ([22]):

$$\Delta L = L_{new} - L_{previous} = \frac{1}{1 + \frac{w}{(E_b/N_0) \cdot r_{new}}} - \frac{1}{1 + \frac{w}{(E_b/N_0) \cdot r_{previous}}} \quad (4.12)$$

where  $r_{new}$  is the data rate of the user after allocation and  $r_{previous}$  is the previous data rate of the user (before allocation).

## 4.6 Simulator Description

In this section the parameters of the simulator are listed. In addition, the modeling and the implementation choices for the features discussed before in this chapter are presented.

### 4.6.1 System Model

The network area is consisted of 24 cells placed in a cell grid configuration with three-cell sites and directional antennas. The network layout is displayed in figure 4.9; the cell radius is equal to 933 meters. Users are uniformly located in the network and each user is moving at 3 km/h on a designated direction during the whole simulation. The wrap-around technique ([24]) is implemented in order to ensure the presence of the users in the network area during the whole simulation.

The number of users remains constant during the whole simulation, therefore no admission control mechanism is implemented. The attenuation between a UE and a Node B is modeled according to the ITU Vehicular A test environment [78], including path loss, long-term fading (shadowing), short-term time-dispersive fading, and sectorized antenna pattern. (Additional information on the propagation model used can be found in [80]; the antenna pattern used in the simulations is detailed in [78]).

The above mentioned timers are considered in the packet scheduler implemented; the packet scheduling period is set to 500 ms, the modification period is set to 500 ms for all of the users and the inactivity timer is equal to 2 seconds. In the simulator however, upon detection of inactivity for a certain UE equal to 2 seconds, resources are not entirely released, but the UE is downgraded to the minimum allocated data rate, which is 8 kbps.

The Node B is assumed to deploy two-branch antenna diversity with ideal RAKE processing of the received signals. This procedure is called uncorrelated Maximum-Ratio Combining, MRC. Its explanation can be found in [26]. The simulator implements the soft handover (SHO) algorithm described in [22]. The closed and outer loop power control mechanisms are compliant to the ones standardized in 3GPP and they are described in appendix A. The settings of all of the features mentioned above are listed in table 4.3.

### 4.6.2 Capacity Requests

In the simulator implemented, measurement reports are transmitted on an “event-triggered” basis. Only the high threshold has been considered. A traffic volume measurement report is transmitted to the network, whenever the size of an RLC buffer of the UE exceeds the size of 32 kbits. The “time to trigger” value is set to 0 seconds and the

<b>Simulation Parameters</b>		
Cell layout	Grid size (hexagonal)	24 - cells (8 sites with 3 sectors)
	Grid configuration	Wrap around
	Cell radius	933 m
	Receiver antennas per cell	2
	Receiver antenna gain	14 dBi
	Receiver antenna gain pattern	70 degree (-3dB)
		20 dB front-to-back ratio
	UE antenna gain	0 dBi
Propagation	Path loss with distance d km	$128.1+37.6 \log_{10}(d)$ dB
	Carrier frequency	2.0 GHz
	Shadow fading standard deviation	8 dB
	Shadow fading de-correlation distance	25 m
	Fast fading channel model	Vehicular A, 3 km/h
	Fast fading model	Jakes Spectrum [26]
	Noise level per receiver antenna	-102.9 dBm
Soft Handover	Active set size	2
	Add threshold	2 dB
	Drop threshold	4 dB
	Drop Timer	200 ms
	Replace Threshold	2 dB
Power control	Fast Closed Loop PC step size	1 dB
	Outer Loop PC step size	0.3 dB
	Outer Loop PC update interval	1 TTI
	Outer Loop FER target	10 %
	Maximum Tx Power	+21 dBm
	Time resolution	Slot (1/1500 s)

Table 4.1: Most important simulation parameters.

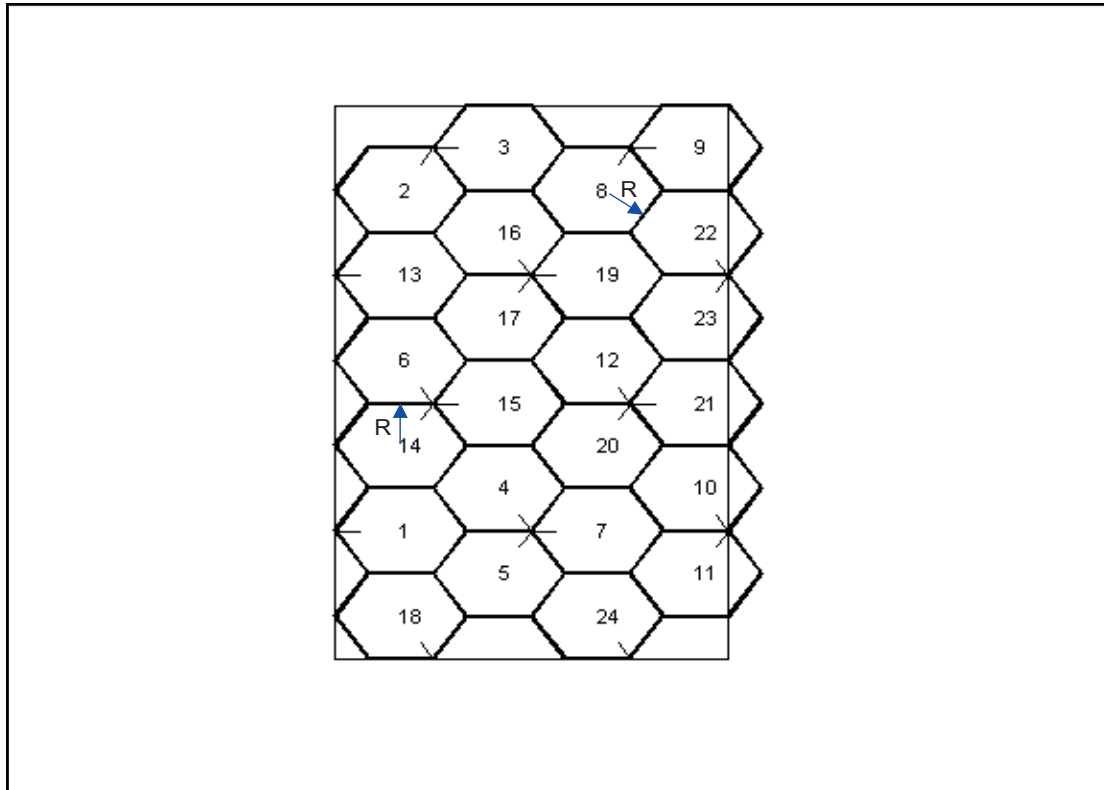


Figure 4.9: Network layout consisted of three-cell sector configuration with directional antennas.

“pending time after trigger” to 2 seconds. Table 4.2 summarizes the parameters related to capacity requests.

### 4.6.3 Packet Scheduling

The packet scheduling period has to be sufficiently short, so as the packet scheduler operates frequently enough in order to respond to capacity requests. However, a very short packet scheduling period has to be avoided due to the high amount of signalling overhead that it is going to generate.

The same criteria apply for the choice of the modification period. In the simulator, both of these parameters are set to 500 ms.

The inactivity timer needs to be long enough in order to avoid unnecessary recurrent resource releases and allocations. In order to be totally aligned with the fair throughput policy, we could define different values of the inactivity timer for different data rates, i.e. for lower data rates, the value of the timer should be higher. For simplicity reasons however, a unique value is applied for all of the data rates and it is set to 2 seconds.

The UEs in the system have only one active radio access bearer. It carries packet data. The minimum data rate of the packet data radio access bearer is 8 kbps and the maximum

Capacity Requests Parameters	
Transmission mode	“event-triggered”
Threshold	32 kbits
Time-to-trigger	0 sec
Pending-time-after-trigger	2 sec

Table 4.2: Capacity requests related parameters.

Packet Scheduling Parameters	
Scheduling principle	“Fair throughput sharing”
Packet Scheduling Period	500 ms
Modification Period	500 ms
Noise Rise target	6 dB
Noise Rise Offset (Load control)	1 dB
Minimum allocated data rate	8 kbps
Maximum possible data rate	384 kbps
Inactivity timer	2 s
Maximum lifetime of a capacity request in the PS queue	2 s

Table 4.3: Parameters of the implemented packet scheduling function.

is equal to 384 kbps. A list with the parameters related to the packet scheduling is given in 4.3.

Data rates of the packet data service are 0, 8, 16, 32, 64, 128, 256 and 384 kbps.

#### 4.6.4 Transport Format Combination Selection

The TFC selection procedure is also included in the simulator. It is performed every transmission time interval (TTI). The latter one is set to 10 ms. In addition, it contains a “TFC Elimination” mechanism as it is described in chapter 3.

The principle of the TFC selection here, as also in chapter 3, is that the UE attempts to transmit at each TTI with the maximum “non-blocked” data rate if the amount of data in the UE RLC buffers is sufficient; otherwise, the UE selects the TFC that fits to the remaining amount of bits in the UE RLC buffers.

As mentioned above, in the simulator each UE is having a single packet data radio access bearer. As a result, the TFCS of each user can be simply modeled as a list with all the possible rates of the packet data that the UE can apply. Hence, the TFC selection mechanism consists in selecting the appropriate rate for the packet data service among the non-blocked rates (figure 4.10).

Figure 4.10 illustrates an example of a TFC selection, as it can be found in the simulator. An UE is allocated a maximum data rate of 256 kbps. Due to the current radio propagation conditions however, the TFC elimination has restricted the maximum data up to 128 kbps. The buffer occupancy of the UE is such that all data in its buffer can be transmitted by selecting a TFC that corresponds to 32 kbps.

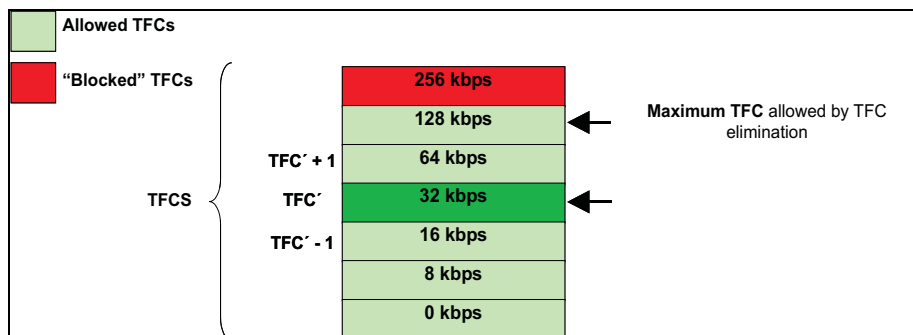


Figure 4.10: Transport Format Combination Selection Procedure.

#### 4.6.5 Traffic Modeling

The traffic model for the packet data service used here is the same as the one presented in the previous chapter. The main difference is that in this model, the reading time starts only after the RLC buffer is emptied, hence after the correct reception of the last datagram of the previous packet call (figure 4.11), modeling thus the fact that the UE is awaiting for an acknowledgement from its peer entity in the network, as it can be met in a number of internet based applications. With this mode of transmission, which is known as “closed loop”, the excessive accumulation of datagrams in the buffers and hence continuous-like transmission is avoided. This ensures a level of burstiness in the offered traffic in the system during the simulation.

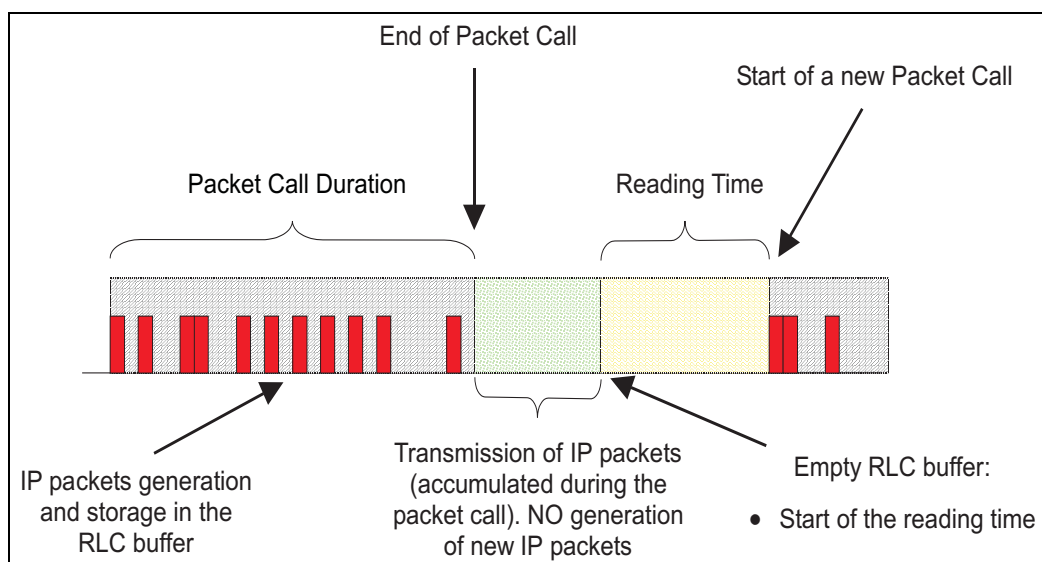


Figure 4.11: A simple modeling approach to include closed loop transmission model.

The distributions characterizing this model have already been presented in the previous

chapter. For the easiness of the reader, they are reproduced here, in table 4.4. As it can be seen in the table, two parameter settings resulting in two different mean data rates during packet call have been defined. The first parameters setting, is similar to the one used for the simulations in the previous chapter.

Parameters of the Modified Gaming Traffic Model			
	Parameter	Distribution	Values
Packet Call	Duration	exponential	5 s (mean)
	Reading Time	exponential	5 s (mean)
Datagram	Inter-arrival Time	log-normal	40 ms (mean), 38 ms (std)
	Size	deterministic	576 bytes (1152-Set B)
	(Resulting) Data Rate during Packet Call	-	115 kbps (230-Set B)

Table 4.4: Parameter settings of the “Modified Gaming” traffic model.

The second parameter setting differs from the first only in the datagram size, which is now set to the double size of the one before (1152 bytes), resulting thus in the double average data rate during packet call (approximately 230 kbps).

Generated datagrams are buffered in RLC layer buffers and stored there until their correct reception. Typical RLC mechanisms, such as ARQ or IP packet discarding after the lifetime of the IP packets in the buffers have not been implemented.

## 4.7 Performance Metrics Used

In this paragraph, the measured parameters used in order to assess the system performance and to quantify the impact of some procedures in the overall packet data service are listed. As the wrap-around technique ([24]) is used in the simulator, the following measurement are collected from all of the cells in the simulated system.

The measurement mainly used here to evaluate system performance is the cell throughput and its statistics. At each simulated radio frame (10 ms), the average cell throughput per cell (in kbps) is obtained as:

$$C = \frac{b}{N \cdot T_{RF}} \quad (4.13)$$

where  $b$  is the total number of correctly received data bits in all the Node Bs of the system,  $N$  is the number of cells in the simulation and  $T_{RF}$  is the radio frame duration.

For the assessment of the user performance, mainly two of its QoS attributes are used here: the user throughput during activity periods and the experienced delay per packet call.

The delay per packet call (in sec) is measured for all of the packet calls of all the users in the system. It is defined as the time difference between the moment of the successful reception at the Node B of the last datagram of the packet call,  $t_{rx\_end}$  and the moment of arrival of the first datagram of the packet call in the UEs buffer,  $t_{tx\_arr}$ :

$$D = t_{rx\_end} - t_{tx\_arr} \quad (4.14)$$

The user throughput during packet calls (in kbps) is obtained as the ratio between the number of bits in a packet call,  $pcb$  and the delay per packet call  $D$ :

$$U = \frac{pcb}{D} \quad (4.15)$$

It has to be noted here that this definition of user throughput is possible only when the delay per packet call,  $D$ , does not contain delays due to signalling.

Results concentrate also in the noise rise (NR) statistics. The noise rise in the cell has been defined in [22] as the ratio of the total received power,  $P_{Total}$  and the noise power,  $P_N$ :

$$NR = \frac{P_{Total}}{P_N} \quad (4.16)$$

The NR per cell is stored at each simulated radio frame. Apart from the mean and standard deviation values, the percentile outage values are also of importance. Often the requirement for a system is to operate under a certain value of NR for a percentage of the time.

From equations 4.16 and 4.7 it can be seen that the NR is a measurement of the load,  $\eta$ , in the system. To a certain load target in the system a NR target corresponds. In our simulations, the system capacity is defined as a function of the NR target and the cell throughput: the maximum observed cell throughput for a certain NR target corresponds to the system capacity for the designated NR target.

At each radio frame the i-factor of all the cells is obtained. For each cell,  $P_{own}$  is the sum of the power received by all of the users in the cell, whilst  $P_{other}$  is the sum of the powers received by all of the users in the system not belonging to the cell.

The i-factor statistics have to be read as a complement to the NR ones. The i-factor is a measurement of the isolation of the cell from the interference received from other cells and therefore an indicator of the level of control of the received interference. Hence, upon view of a certain NR distribution in the system, the i-factor distribution helps to identify if the NR distribution is the unbiased result of the packet scheduling, or if it is considerably influenced by interference originating from other cells.

The transmission power for each user in the system is also collected. For each UE, it consists the output transmission power measured at its antenna. It is measured every simulated time slot.

Other measurements used, are the Frame Error Rate (FER) and the Eb/No target. The FER of each user is the ratio of the number of erroneous frames to the total number of frames in the simulation. The FER statistics of the system are obtained by gathering the per user FER statistics. However, in some cases the FER statistics of the system are almost similar when comparing a number of configurations. In this case, the Eb/No target distributions give a better insight in the ability of the users in the system to preserve their radio link. Hence, the FER statistics along with the Eb/No target distributions are the indicators of the radio link quality in the system.

The probability of selected TFCs of all the users in the system is also largely used when displaying results. The probability of selection of a certain TFC from a certain user is obtained as the ratio of the number of the TFC selection and of the total number of TTIs in the simulation. Statistics from all UEs are gathered in order to obtain the system statistics. This measure gives a picture of the data rates UEs are trying to transmit. Implicitly, it gives an indication about the allocated data rates to the UEs by the packet scheduler.

## 4.8 Simulation Results

In this paragraph, the most representative results portraying the performance of the uplink packet data service in UMTS are displayed and commented. In addition, the impact of the TFC Elimination mechanism in the overall system performance is displayed, at the beginning.

### 4.8.1 Impact of the TFC Elimination Mechanism

The case of 8 users per cell in average is examined. Two simulation scenarios are compared: in the first one, the TFC elimination mechanism is activated (“TFC Elimination On”) whilst in the second one, it is deactivated (“TFC Elimination Off”). For the TFC Elimination mechanism parameters X, Y, Z (explained in Chapter 3) are set to 15, 30, 30 slots respectively. A number of combinations for the values of X, Y and Z are also tested; the change in the obtained results is insignificant. The other parameters are set to the values listed in table 4.3.

Figure 4.12 shows the probability of selected TFC for all the users in the system in cases the TFC Elimination is activated and deactivated (column 1 and 2 respectively). The probability of selection of a certain TFC is similar in both cases, implying thus that in the case the TFC elimination mechanism UEs are not restricting the higher data rates since their transmission does not require transmission power higher than the maximum.

Figure 4.13 certifies this statement. Users are almost always transmitting with a power that is below the maximum one.

The similar behavior of the UEs in the tested cases, results in the same air interface load in the system. Figure 4.14 shows that the noise rise in the system is almost similar in both cases.

Obtained results with regards to cell throughput, user throughput and FER (see table 4.5) confirm the discussed trends.

Next, the same scenarios are tested, with the difference that the cell radius is the double (1866 m) than in the above discussed cases. In this case however, the “TFC Elimination” algorithm is applied due to higher distances between users and their serving BSs. Figure 4.15 displays the probability of selected TFC for the cases the TFC Elimination mechanism is activated and deactivated (columns 1 and 2 respectively). Users attempt to transmit 384 kbps less frequently in the case of active TFC elimination. Instead, users try to transmit with lower data rates (e.g. 128, 64 kbps).

The elimination of the high data rates leads to a decrease in the percentage of transmission with the maximum transmission power, as it can be seen in figure 4.16.

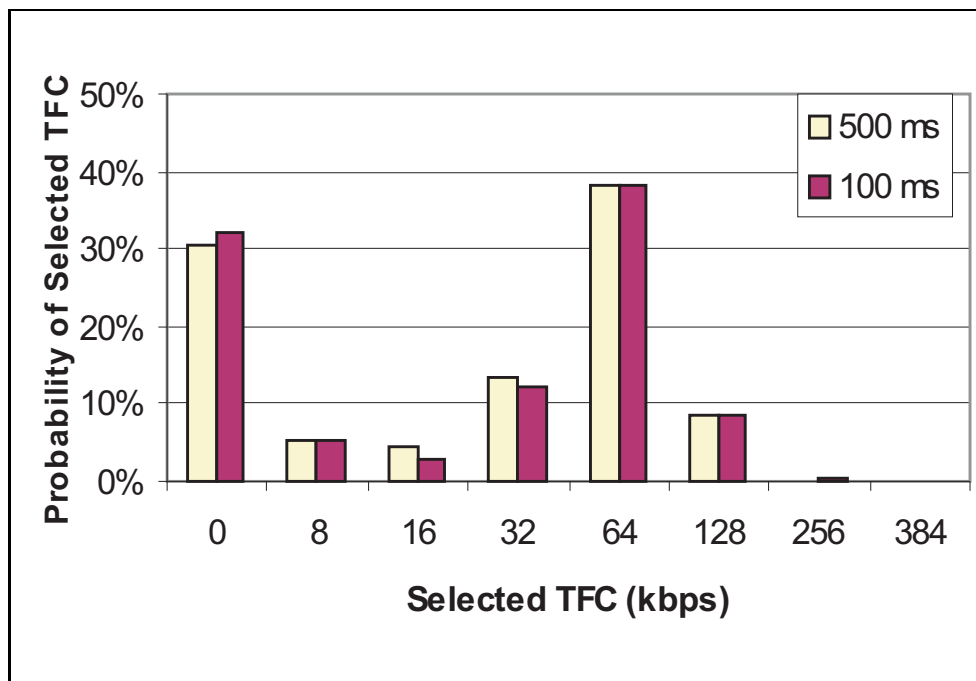


Figure 4.12: Probability of selected TFC for all of the users in the system (TFC Elimination “On and “Off”, 8 users per cell, cell radius 933 m).

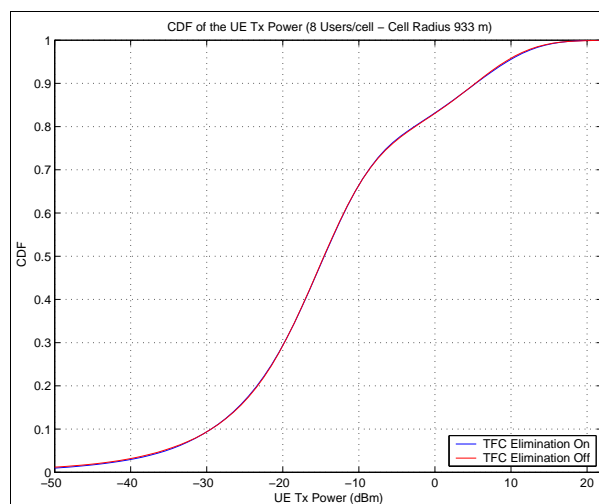


Figure 4.13: CDF of the UE transmission power (TFC Elimination “On and “Off”, 8 UEs per cell, cell radius 933 m).

In absence of the TFC elimination mechanism, around 15% of the times the transmission is done with the maximum transmission power (figure 4.16). These cases correspond

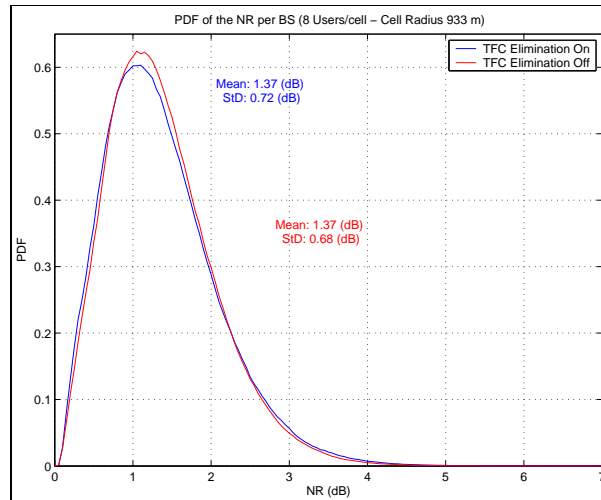


Figure 4.14: PDF of the noise rise (TFC Elimination “On and “Off”, 8 UEs per cell, cell radius 933 m).

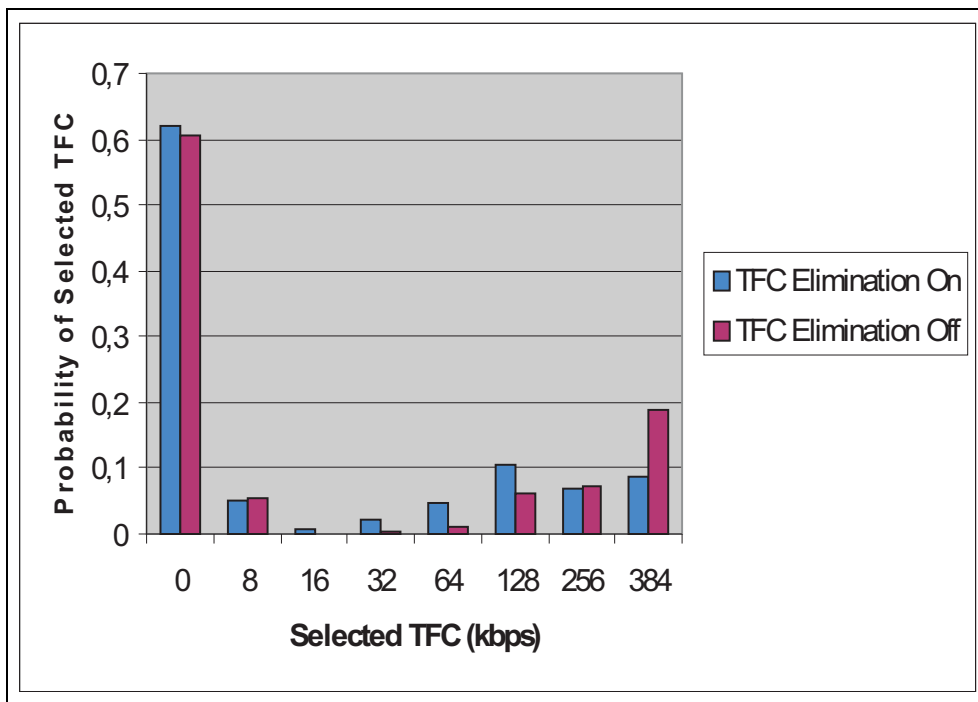


Figure 4.15: Probability of selected TFC for all of the users (TFC Elimination “On and “Off”, 8 users per cell, cell radius 1866 m).

mainly to the transmission of high data rates from UEs that are located far from the serving BS. However, transmission with the maximum power increases the probability of

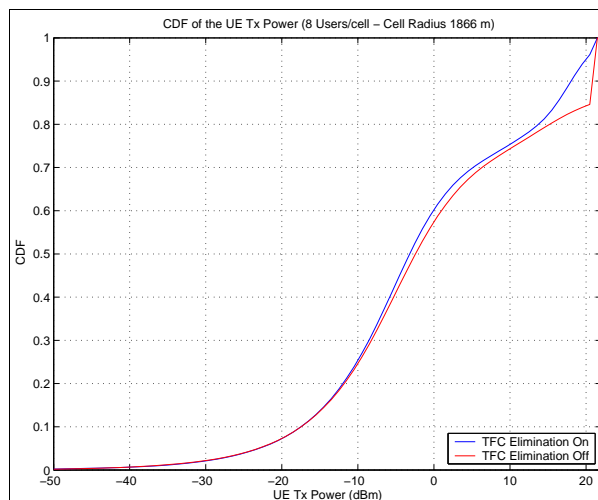


Figure 4.16: PDF of the noise rise (TFC Elimination “On” and “Off”, 8 UEs per cell, cell radius 1866 m).

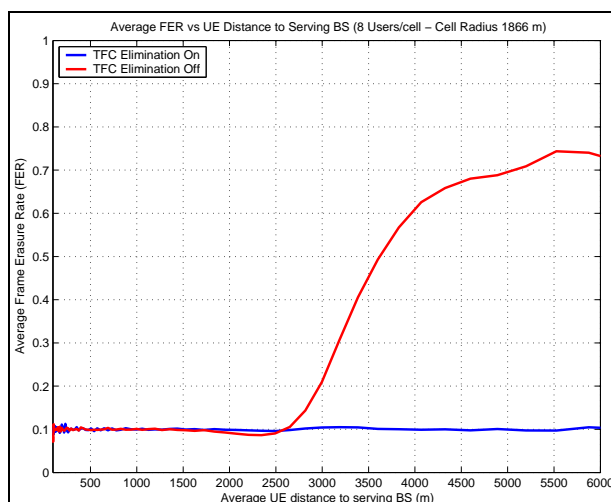


Figure 4.17: FER as a function to the distance from the serving BS (TFC Elimination “On” and “Off”, 8 UEs per cell, cell radius 1866 m).

erroneous reception. Figure 4.17 certifies this statement; it shows the FER as a function of the distance between the UE and its serving BS for the cases that the TFC Elimination mechanism is activated and deactivated respectively. In case the TFC elimination is not applied, the FER increases dramatically for UEs at high distances from their serving BS, principally due to the fact that UEs transmitting at high data rates, transmit at the maximum power and they are not able thus to follow the power control commands. Hence, repeated errors in the transmission of UEs far from their serving Node B set their  $E_b/N_0$

	Cell Throughput	UE Throughput	FER	
TFC Elimination On	477,3 [kbps]	111,7 [kbps]	10%	933 [m]
TFC Elimination Off	479,6 [kbps]	111,9 [kbps]	10%	
TFC Elimination On	460.2 [kbps]	106,5 [kbps]	10%	1866 [m]
TFC Elimination Off	437 [kbps]	103,1 [kbps]	18,32%	

Table 4.5: Cell Throughput, UE throughput FER for the cases TFC Elimination is “On” and “Off”. The cell radius is 933 m and 1866 m.

target to high values. Figure 4.18 shows that the  $E_b/N_0$  target of the users increases considerably when the TFC elimination mechanism is deactivated. This increase results essentially from UEs at the cell borders. Considering the way the outer loop power control operates, the  $E_b/N_0$  target reaches high values for these users and its decrease to lower values is very slow. Hence, these UEs are requested to transmit with very high power even if their radio link conditions improve, resulting in an almost stable situation where these UEs transmit with very high power.

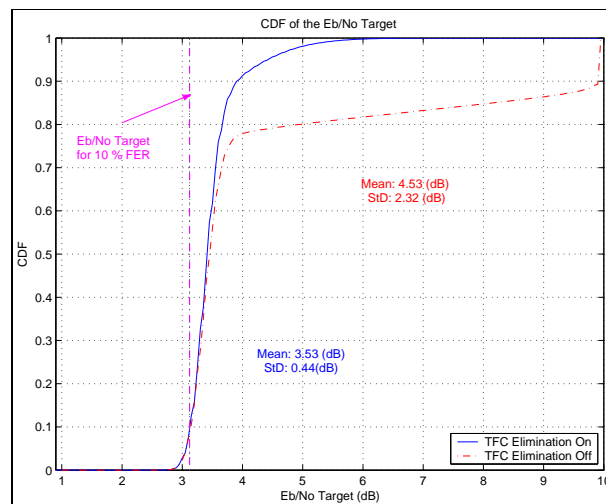


Figure 4.18: CDF of the  $E_b/N_0$  target (TFC Elimination Mechanism “On” and “Off”, 8 UEs per cell, cell radius 1866 m).

In the contrary, the avoidance of transmission with the maximum power in the case of presence of the TFC elimination mechanism assures an invariant to the distance FER.

The erroneous transmission from the UEs that are situated far from their serving BS and attempting to transmit with the maximum power adds interference in the system and increases the measured noise rise in the system, as it can be seen in figure 4.19.

Table 4.5 summarizes the principal results presented in this paragraph. Values of the table are the mean ones.

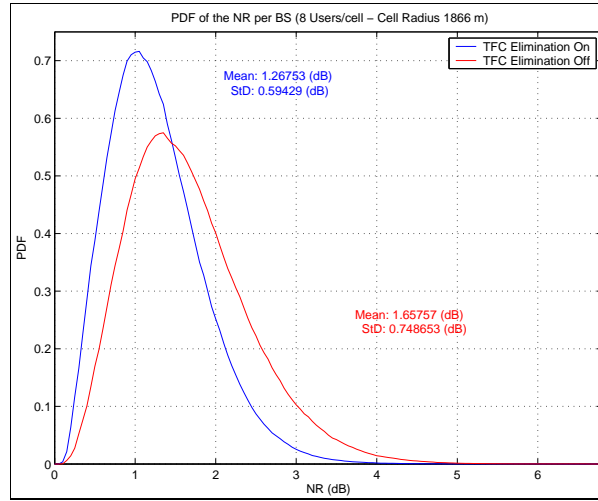


Figure 4.19: PDF of the noise rise (TFC Elimination “On” and “Off”, 8 UEs per cell, cell radius 1866 m).

### 4.8.2 Uplink Packet Data Access Performance

In this section the impact of the PS functioning in the overall system performance is assessed. The emphasis is placed on the air interface load (or equivalently noise rise), cell throughput and the allocated and transmitted data rates by the UEs with various numbers of UEs in the system. At the beginning, the chosen policy with regard to previously inactive users is described.

#### Choice of the Weighting Factor Due to Inactive Users

As discussed in section 4.4.4, at each scheduling period an amount of power is reserved for the users that have been previously inactive and are still in the system. The estimated power due to inactive users ( $P_{inact}$  in equation ) is multiplied with the weighting factor for inactive users (WFIU). Its value ranges from 0 to 1 and it is directly dependent on the probability of inactive users starting transmission at the next packet scheduling period. The value 1 corresponds to the most “conservative” policy; it is assumed that all of the users which have been previously inactive, start transmission at their maximum allocated data rate and as such a considerable margin due to inactive users is taken. On the contrary, the value 0 applies for the case that no power margin is preserved for the users who have been inactive, considering that they will remain inactive in the coming scheduling period. As a result, more power is available for data rate allocations to other users.

Simulations were conducted with the WFIU value set to 0, 0,5 and 1. Figure 4.20 illustrates the impact of the WFIU value on the NR distribution. The lower the power margin reserved for the inactive users, the more space for new data rate allocations and thereby the increase in the obtained NR statistics.

From the results in table 4.6, it can be noticed however that the increase in the NR statistics is higher than the increase in the cell throughput, when the power margin re-

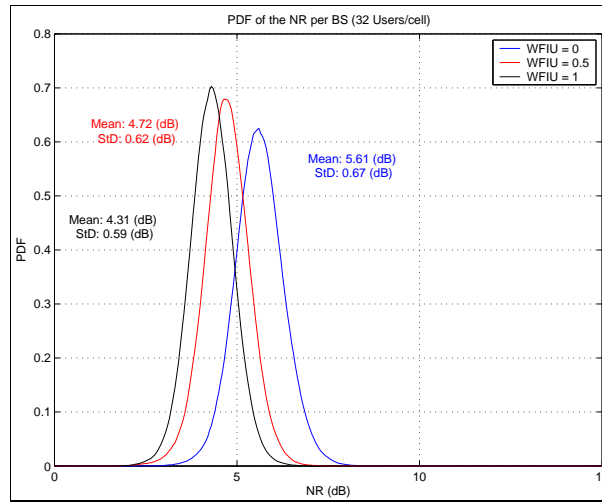


Figure 4.20: PDF of the noise rise (32 UE per cell, weighting factor for inactive users (WFIU) is set 0, 0,5 and 1 respectively).

WFIU	Cell Throughput	UE Throughput	Mean NR	5% NR Outage
0	1384,7 [kbps]	66,27 [kbps]	5,61 [dB]	6,7 [dB]
0.5	1265,7 [kbps]	59,59 [kbps]	4,72 [dB]	5,7 [dB]
1	1199,3 [kbps]	55,14 [kbps]	4,31 [dB]	5,25 [dB]

Table 4.6: Cell Throughput, UE throughput and FER (32 UEs per cell, WFIU is set to 0, 0,5 and 1).

served for inactive users is reduced; e.g. the reduction of the WFIU from 1 to 0 results in an 15,45% increase in the mean cell throughput and in a corresponding increase of 27,62% in the NR value that corresponds to 5% outage.

Hence, the introduction of additional interference is more significant than the gain in the cell throughput. Although the outcome of this study has been obtained for a specific scenario, the resulting trend is expected to be general. Therefore, in the simulations described below the WFIU is set to 1.

### System Performance for Different Load Scenarios

Simulations with different number of users in the system and hence different number of UEs per cell have been conducted. The parameters listed above are used. The resulting mean cell throughput for different number of UEs per cell is displayed in figure 4.21. It can be observed that the cell throughput is increasing with the number of UEs per cell, until a certain point and then a “saturation” in the cell throughput is noticed around the value of 1.25 Mbps. This comes mainly as a result of the setting of a noise rise target in the system. The planned NR target sets the limit for the total uplink load,  $\eta_{UL}$  in the cell and consequently the total cell throughput (equation 4.7).

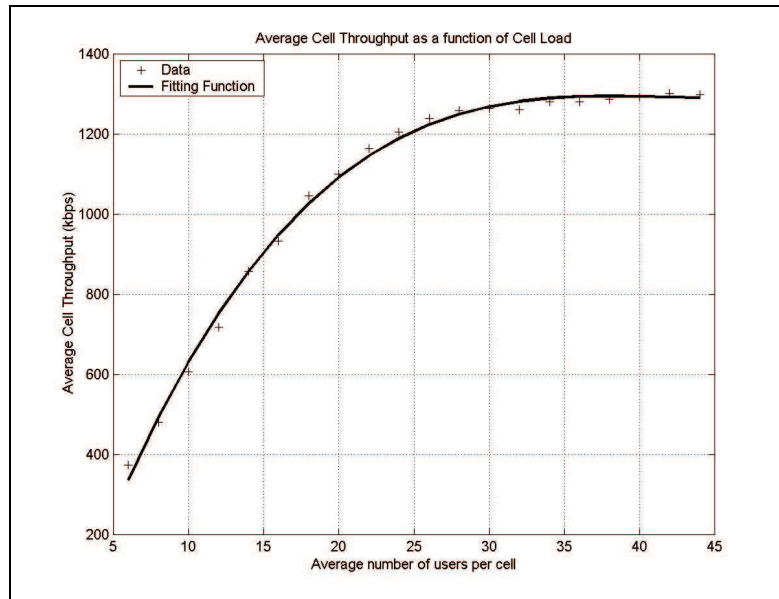


Figure 4.21: Mean Cell Throughput for different number of UEs in the cell.

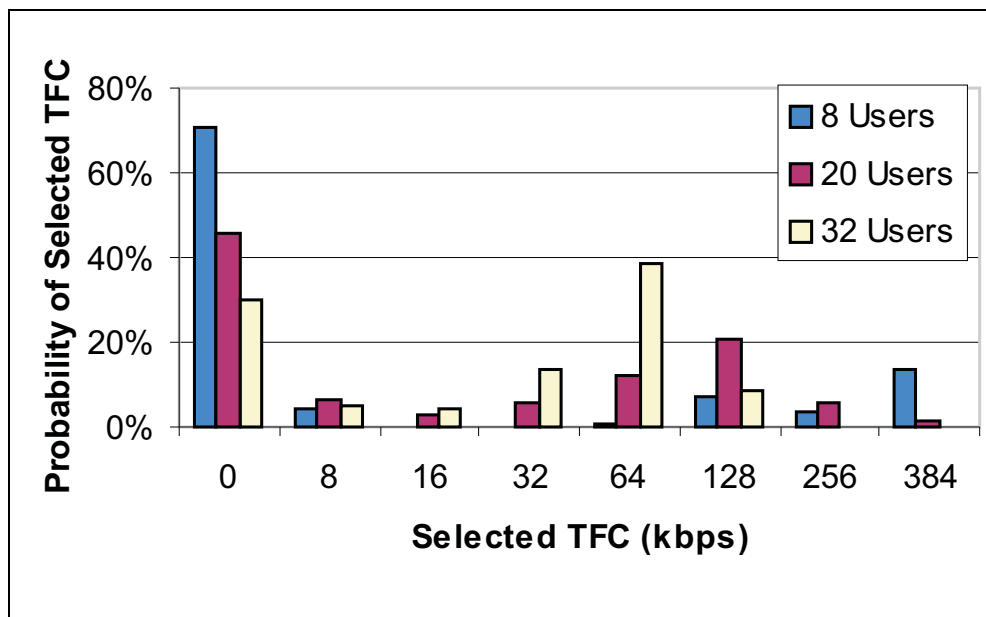


Figure 4.22: Probability of selected TFC for the cases of 8, 20 and 32 users per cell.

Three scenarios standing for the cases of low, medium and high offered load in the system are presented below. The average number of UEs per cell is 8, 20 and 32 respectively. Figure 4.22 shows the probability of selected TFC (and thereby of selected data rate)

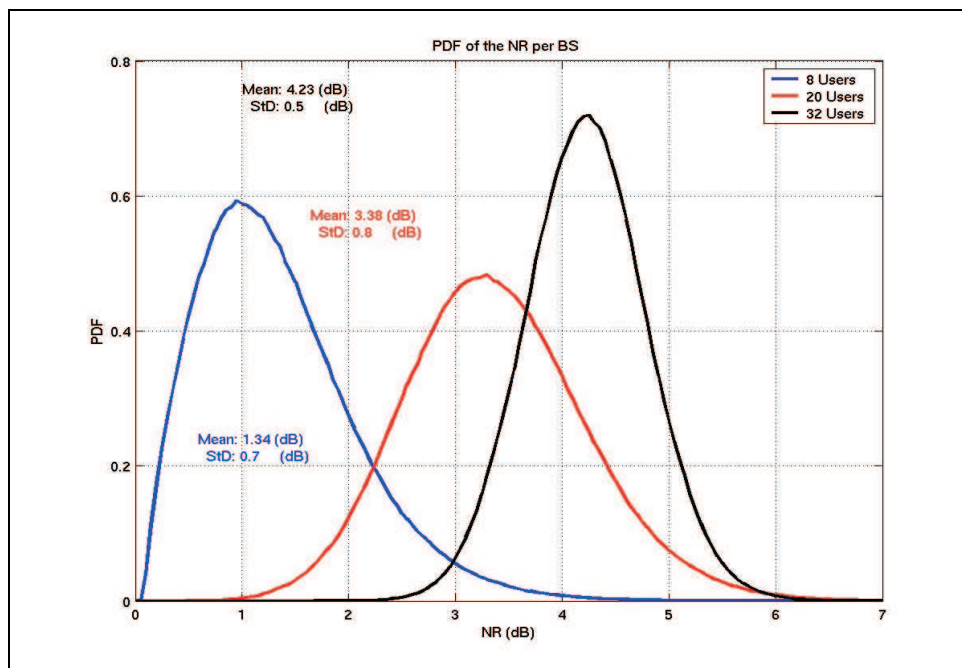


Figure 4.23: PDF of the noise rise for the cases of 8, 20 and 32 UEs per cell.

by the UEs in the examined scenarios. In the case of few users in the system, UEs attempt to transmit with the maximum possible data rate (384 kbps), implying that this data rate has been allocated to the users. With an increased number of users in the system, UEs are mainly attempting to transmit with lower data rates, since high data rate allocation is less probable in that case. This is a direct consequence of the fair scheduling policy. Another effect of the absence of high data rates in the case of medium to high load in the system is that the activity factor of UEs is increasing. This leads to a situation of constant-like transmission at medium to low data rates from the biggest part of the UEs in the system. This results in a low-varying air-interface load in the system, as it can be derived from the NR distributions in figure 4.23

users/cell	NR [dB]		Cell Throughput [kbps]	UE Throughput [kbps]	Delay [sec]
	Mean	Std			
8	1.34	0.72	480,13	116,43	4,97
20	3.38	0.85	1102,6	92,27	5,94
32	4.23	0.56	1268,5	55,5	10,21

Table 4.7: Mean and standard deviation of the NR, Cell Throughput, UE throughput and delay per packet call for the cases of 8, 20 and 32 UEs per cell.

Table 4.7 contains the principal system performance metrics for the examined cases. The dramatic decrease of the user throughput during the packet call and the increase per packet call delay in the case of high number of users can be observed.

## 4.9 Conclusions and Discussion

The uplink packet data access in UMTS has been studied in this chapter. Its principal mechanisms are also described with a focus on the packet scheduler. A network simulator containing a packet scheduler operating according to the principle of fair throughput sharing is therefore implemented. In this part of the work, we tested the performance of an interactive service. In addition, simulations performed helped us to validate our models.

The importance of TFC elimination mechanism in the overall system performance has been quantified. It is shown that when the TFC elimination mechanism is activated, UEs can preserve the same radio link quality in terms of FER with maybe reduced data rates, independently of their location within the cell. This is achieved when the data rates transmitted by UEs depend on their radio path loss, even if UEs in the cell are granted similar data rates. This effect however does not imply that resources allocated by the PS are wasted. The reason for this is that the PS performs allocations on the basis of measurements of the total received power, which is a result of the currently transmitted data rates from the different users.

Simulations have also been performed for various offered loads in the system. A “saturation point” in the cell throughput is detected as a result of the NR target imposed by the network planning; in the simulations, this point is around 1.25 Mbps.

For the cases of high load in the system, UEs are granted data rates much lower than the requested ones, as a consequence of the fair throughput scheduling. This leads to a situation, where UEs remain active for the biggest percentage of the time transmitting at relative low data rates. The average received power is then high and it exhibits small variance.

## Chapter 5

# Enhancements of the Uplink Packet Data Access in WCDMA

In this chapter, the possible enhancements of the uplink packet data access are discussed. The proposed enhancements aim at (i) increasing cell capacity and (ii) improving the offered QoS to users. The potential of three features to meet the above mentioned goals is studied here. We call the first one “Fast Variable Spreading Factor” (VSF). The UEs apply dynamic changes of the spreading factor (SF) according to the physical channel variations in order to maintain an as constant as possible transmission power. The second feature is an uplink packet data access mode with a partly distributed control of the uplink resources. Hence, the packet scheduler controls to smaller extent the uplink packet data access, in comparison to the one currently standardized in 3 GPP. Users can initiate packet data transmission on the basis of the interference level in the cell. Even though this mode is not entirely decentralized, we call it here “decentralized”. The third proposed feature is the faster operation of the packet scheduler.

The chapter is organized as follows: in section 5.1 the motivation for improving the uplink packet data access is given. In addition, the targeted metrics per each proposed feature are listed. Then, the proposed features are presented; the fast variable spreading factor (fast VSF) concept is described in section 5.2. The discussion of the so-called decentralized uplink packet data scheme follows in section 5.3 and then the presentation of the fast packet scheduling feature (section 5.4). The chapter ends with the section 5.5, which contains the conclusions and related discussion.

### 5.1 Motivation for Enhanced Uplink Packet Data Access and Goals

The primary goal of enhancing the uplink packet data access is to increase system capacity. As it is mentioned in chapter 1, the aim of this work is “to optimize the utilization factor of resources allocated to packet data services”. The cell capacity is an implicit measurement of the utilization factor of the total power budget in the system.

Higher cell capacity leads to improved QoS attributes of the users in the system, i.e., higher user throughput, which in most of the cases is translated into reduced experienced

delay per packet call.

### 5.1.1 On the System Capacity Increase

We try to identify the parameters of the formula having an impact on the system capacity. Once the parameters detected, it is discussed whether they can be optimized so as to bring capacity gains.

As it is discussed in 4.7, in our studies the system capacity is the maximum cell throughput for a certain load target. Therefore, in the following we base our investigation on the formula of the cell throughput as a function of the fractional load, which is already discussed in the previous chapter. For the easiness of the reader, we redefine here some parameters already presented in chapter 4.

The fractional load  $L_j$  of a user  $j$  has been defined in [22] as the ratio between the received power from the designated user,  $P_j$  and the total received power,  $P_{Total}$ :

$$L_j = \frac{P_j}{P_{Total}} = \frac{1}{1 + \frac{w}{(E_b/N_0) \cdot R_j v_j}} \quad (5.1)$$

where  $w$  is the UTRAN chip rate,  $E_b/N_0$  is the received energy per bit to noise density of the user and  $R_j$  is the bit rate of the user during activity and  $v_j$  is the activity factor of the user  $j$ .

In the same book, [22], the i-factor of a cell,  $i_f$ , has been defined as the ratio between the received power from users from other cells,  $P_{other}$  and the received power from users in the designated cell,  $P_{own}$ :

$$i_f = \frac{P_{other}}{P_{own}} \quad (5.2)$$

Considering the definition of the fractional load,  $L_j$  of an user  $j$  and that of the i-factor, the total uplink load in a cell,  $\eta$  is written in chapter 4 as:

$$\eta = (1 + i_f) \cdot \sum_{j=1}^M L_j. \quad (5.3)$$

where  $M$  is the number of users per cell. Considering equation 5.1, formula 5.3 becomes:

$$\eta = (1 + i_f) \sum_{j=1}^M \frac{1}{1 + \frac{w}{(E_b/N_0)_j R_j v_j}} \quad (5.4)$$

Let us assume that all the users in the cell have the same mean data rate,  $R$ , the same activity factor,  $v$  and that they exhibit the same received energy per bit to noise density ratio,  $E_b/N_0$ . This is not a so irrelevant assumption for the fair packet scheduler under study, especially in the cases of high offered load in the cell (simulation results in chapter 4 certify this argument). Hence, equation 5.4 can be written as:

$$\eta = (1 + i_f) M \frac{1}{1 + \frac{w}{(E_b/N_0) R v}} \quad (5.5)$$

where

$$R' = Rv \quad (5.6)$$

is the mean data rate per user accounting for both the activity and inactivity periods.

Let us assume that  $\frac{w}{(\frac{E_b}{N_0})R'} \gg 1$ . It is the case, if the number of users per cell,  $M$ , is sufficiently high. In this case, it is unlikely that there are users with high data rates. Formula 5.5 can then be written as:

$$\eta = (1 + i_f) \frac{MR'(\frac{E_b}{N_0})}{w} \quad (5.7)$$

The average throughput per cell,  $C_{ave}$  is equal to:

$$C_{ave} = MR' \quad (5.8)$$

From 5.8 and 5.7, the average cell throughput can also be written as:

$$C_{ave} = \frac{\eta w}{(1 + i_f)(\frac{E_b}{N_0})} \quad (5.9)$$

Hence, according to formula 5.9, for a designated noise rise target in the system and equivalently a certain load target,  $\eta_{target}$ , an increase in the average cell throughput can be obtained through a reduction of the received Eb/No per user, or through a reduction of the i-factor in the system. Similar findings related to cell capacity are presented in [7].

However, reducing the received Eb/No per user results in higher block error rate (BLER). In order to preserve the same link quality in terms of BLER with a reduced Eb/No, additional mechanisms are applied; the most common ones being Hybrid Automatic Repeat Request (HARQ), adaptive modulation and coding (AMC) or shorter transmission time intervals (TTIs) ([31]). These changes however require significant modifications in the physical layer architecture and necessitate additional feasibility studies. These kind of studies are out of the scope here and therefore these techniques are not discussed.

### **i-factor Reduction**

From the discussion in the previous paragraph, it derives that only the reduction of the i-factor can bring a capacity gain, without significantly modifying the existent physical layer architecture. A policy to reduce i-factor is to avoid transmissions that require high power from UEs at the cell borders. This can be achieved if high data rates are not allocated to UEs far from their serving Node B. However, such a scheduling algorithm would “shrink” the cell size, i.e. it will reduce coverage. Moreover, it will not be fair. The fast VSF scheme aims at controlling i-factor by minimizing the variance in the transmission power of UEs close at the cell borders. However, its efficiency in reducing the i-factor is disputable since it inherently increases the variance of the inner cell interference, as it is going to be discussed in section 5.2.

### Efficient Packet Scheduling

Another means to increase system capacity is to improve the efficiency of the packet scheduling. A packet scheduler that dynamically allocates data rates in order to adapt to UEs requests is expected to make a more efficient use of resources and hence increase system capacity. This is the concept of the fast packet scheduling. Results in chapter 4 justify this expectation. In this chapter, it was noticed that even at scenarios with high load in the systems, the observed mean noise rise has a considerable distance from the planned target. A more accurate scheduling is going to reduce the standard deviation of the noise rise in the system, which may result in a mean noise rise closer to the target. Higher mean noise rise in the system is translated into higher cell throughput.

#### 5.1.2 Delay Reduction

As mentioned before, one of the targeted QoS metrics to be improved through this work is the experienced delay per packet call. In our work a decrease in the delay can be obtained either (i) by increasing the data rate of the user during activity period (see section 4.7) or (ii) by reducing the delays imposed by the procedures involved in the uplink packet data access mechanism.

The procedures of the uplink packet data access (described in chapter 4) add delay to the packet transmission. Namely, the capacity requests transmission and the radio bearer establishment are procedures that increase considerably the experienced delay per packet call. The so-called decentralized mode attempts to reduce delays introduced by these procedures due to the reduction of the number of transmitted traffic volume measurements and of allocations and releases of radio bearers. This is achieved when UEs preserve their already activated radio bearers and initiate packet data transmission without previously sending traffic volume measurements to the network (detailed description of the “decentralized” access mode is given in section 5.3).

## 5.2 Fast Variable Spreading Factor

### 5.2.1 Concept

The goal of the fast VSF scheme is to minimize the  $i$ -factor, as mentioned in the previous section. A reduced  $i$ -factor is expected to increase cell capacity (according to 5.9) and to add robustness in the system.

Considering that the  $i$ -factor is essentially influenced by UEs at the cell borders (with the last ones tending to transmit with high power), the  $i$ -factor can be minimized, if UEs far from their serving base station (BS) avoid high peaks in their transmission power. The aim of the discussed here fast VSF scheme is to eliminate the high peaks in the transmission power of UEs at the cell borders. This is achieved by setting a transmission power target for UEs at the cell border. This target is essentially defined by radio propagation conditions and by the UE's data rate. Its value is usually fairly low. The fast VSF changes are applied with the aim to maintain the UE transmission power as close as possible to the transmission power target. Figure 5.1 illustrates the basic concept of the fast VSF scheme.

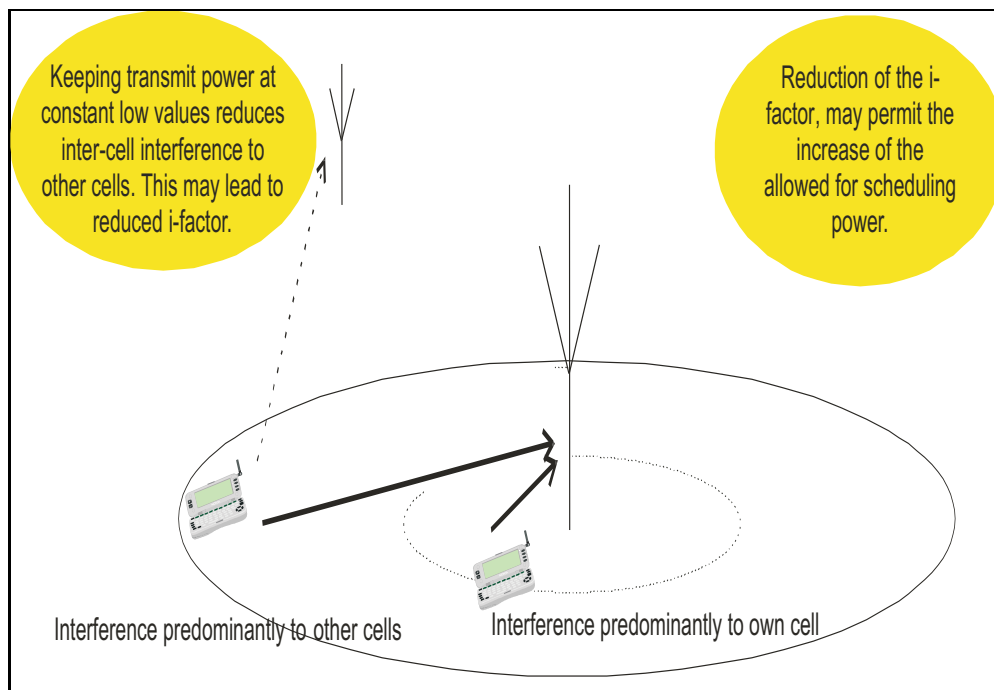


Figure 5.1: Basic concept of the fast VSF scheme.

The stabilization at low values of the transmission power of users close to cell borders is expected to reduce the high peaks in the neighboring cell interference.

In addition, the fast VSF is expected to enhance the per user link, since it prevents UEs from transmitting with highly peaked power. This improvement may lead to better performance in terms of user throughput for UEs far from their serving BS.

UEs transmit with an almost invariant power if they make use of the possibility offered by 3GPP standards to modify their spreading factor according to the physical channel variations. In uplink transmission, a SF change can be performed within the UE, without prior signalling between the UE and the network, [22], [72]). A modification of the SF however implies a change in the transmitted data rate. Considering that a designated UE is allocated a certain data rate, there are restrictions in the SF that can be applied. This issue is going to be described further in the following section.

### 5.2.2 Preliminary Study on the Capability of the Fast VSF to Stabilize i-factor

In this section, the impact of the fast VSF scheme on the noise rise at the serving cell and at adjacent cells is assessed. In related literature, the power received in a Node B from UEs that are outside the own cell, is called “other cell interference. The power received from UEs in the own cell is called “own cell interference. These terms are used here. Results are compared with the ones in the case no VSF is applied. In order to assess the potential of the fast VSF scheme, the two “extreme” cases are considered in

this preliminary study. The first case refers to the absence of fast VSF; no SF changes are performed. In the second “extreme case, the SF changes continually so that the UE transmission power remains constant. It is assumed then that the UE is transmitting with a constant power. For this study, it is also considered that the total received power in the cell is constant and that the user is not moving.

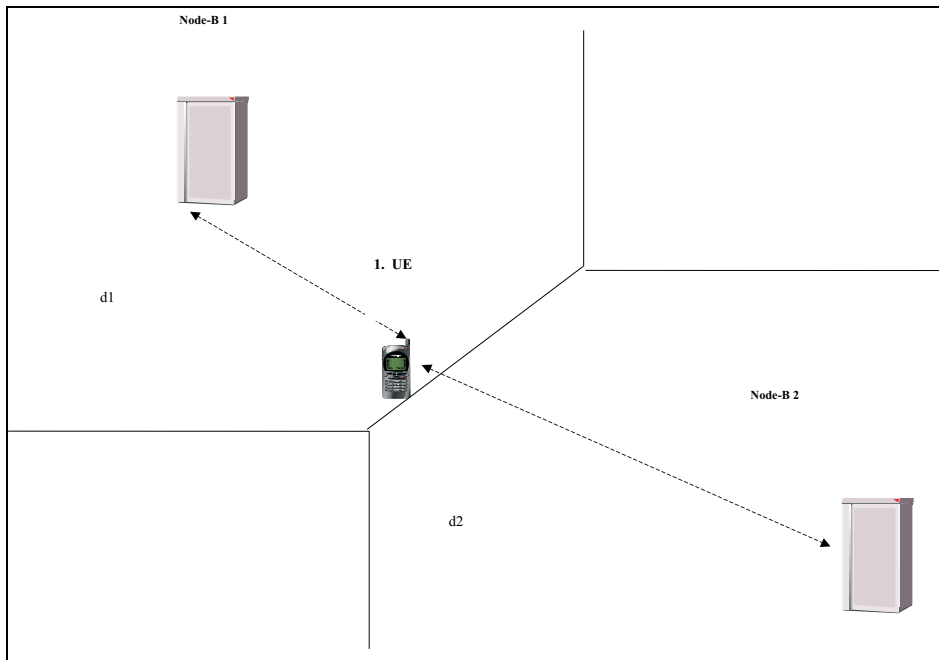


Figure 5.2: UE at the cell border.

As an example imagine an UE at the cell border, as it can be seen in figure 5.2. The  $E_b/N_0$  of a certain UE is given by formula 4.2. In this formula, the useful received power of the UE is not counted in the total interference. For simplicity reasons and without introducing a significant error, we assume that the received power from the designated UE is included in the total cell interference. Formula 4.2 becomes then:

$$\frac{E_b}{N_0} = \frac{w}{r_j} \frac{P_j}{P_{Total}} \quad (5.10)$$

If the formula 5.10 is transformed into logarithmic scale, it becomes then:

$$\frac{E_b}{N_0} = G + P_j - P_{Total} \quad (5.11)$$

where  $G$  is the processing gain. It is defined as the ratio of the chip rate  $w$  to the UE data rate,  $r$ :

$$G = \frac{w}{r} \quad (5.12)$$

The received power,  $P_j^1$ , due to the designated UE (in dB) in the serving Node B 1 is:

$$P_j^1 = P_{Tx} + PathLoss_{d1} + ff_1 \quad (5.13)$$

where  $P_{Tx}$  denotes the mobile transmission power,  $PathLoss_{d1}$  stands for the path loss due to distance  $d1$  (see figure 5.2) and  $ff_1$  the fast fading coefficient of the propagation channel.

From 5.11 and 5.13 the received  $E_b/N_0$  of the designated UE is given by:

$$\frac{E_b}{N_0} = G + P_{Tx} + PathLoss_{d1} + ff_1 - P_{Total} \quad (5.14)$$

In case the fast VSF scheme is not applied, the processing gain,  $G$ , remains constant. In addition, in an ideal case, the fast PC is able to “follow” the fast fading variations. Thus, the transmission power of the designated UE is the inverse fast fading coefficient plus a constant,  $c_1$ :

$$P_{Tx} = -ff_1 + c_1 \quad (5.15)$$

In this case, the statistics of the UE transmission power are similar to ones of the fast fading coefficient. From 5.13 and 5.15, it derives that the received power,  $P_j$ , of this designated UE at Node B 1 (5.2), is equal to:

$$P_j^1 = PathLoss_{d1} + c_1 \quad (5.16)$$

Hence, for a non-moving user, the received power at the serving Node B due to an ideally power controlled user, is not changing.

The received power,  $P_j^2$ , due to this designated UE in the adjacent Node B 2 is equal to:

$$P_j^2 = P_{Tx} + PathLoss_{d2} + ff_2 \quad (5.17)$$

where  $PathLoss_{d2}$  is the radio path loss due to the distance  $d2$  (figure 5.2) and  $ff_2$  is the fast fading coefficient of the propagation channel between the UE and Node B 2.

Considering 5.15, 5.17 becomes:

$$P_j^2 = PathLoss_{d2} - ff_1 + ff_2 + c \quad (5.18)$$

The received power at the adjacent Node B in case the fast VSF scheme is not used, is thus the sum of two uncorrelated Rayleigh distributed variables. The PDF of the sum of  $n$  number of uncorrelated Rayleigh fading procedures is given by ([45]):

$$PDF(ff)_{dB} = \frac{[exp \cdot (\frac{ff}{M})]^n}{M \cdot (n-1)!} \cdot exp[-exp(\frac{ff}{M})] \quad (5.19)$$

where

$$M = \frac{10}{ln10} \quad (5.20)$$

In case the fast VSF mechanism is applied, ideally, the UE transmission power remains constant. The SF is persistently adjusted that:

$$P_{Tx} = c_2 \quad (5.21)$$

In this case, the received power in the serving Node B1 due to the designated UE is:

$$P_j^1 = c_2 + PathLoss_{d1} + f f_1 \quad (5.22)$$

The variance of the received power, in this case, is expected to be the same as the one of the fast fading coefficient.

In the same case, the power received in the adjacent Node B 2 is equal to:

$$P_j^2 = c_2 + PathLoss_{d2} + f f_2 \quad (5.23)$$

The received power at the adjacent Node B 2 exhibits similar statistics as the ones of the fast fading coefficient.

Without lack of generality, a numerical example of the formulas presented above is given. The case of an UE situated at a distance of 800 m ( $d1$ ) far from its serving Node B 1 and at a distance  $d2$  of 1200 m far from its adjacent Node B 2. The path loss due to radio propagation through distance  $d1$  is -125 dB and due to distance  $d2$  is -145 dB. The UE is transmitting at a data rate of 12.2 kbps, hence the processing gain,  $G$ , is 25 dB. The total received power in the serving Node B 1 is constant and it is equal to -100 dBm. The mean of a Rayleigh fading distribution is 0. Its standard deviation and hence the one of the fast fading radio propagation channel is theoretically equal to 5.5 dBs ([45]). Table summarizes the results of the numerical example in terms of mean and standard deviation of the received power due to a certain UE in the serving Node B 1 and in an adjacent Node B 2. The cases where the VSF is “on” and “off” are presented.

	Received Power in Node B 1		Received Power in Node B 2	
	Mean [dBm]	StD [dB]	Mean [dBm]	StD [dB]
Fast VSF off	-121	-	-141	7.877
Fast VSF on	-121	5.57	-143.5	5.57

Table 5.1: Mean and standard deviation of the received power in the serving Node B 1 and in an adjacent Node B, due to an UE at the borders of the cell.

The findings of this preliminary study show that the use of the VSF leads to an increase in the variance of the received power in the serving Node B. To the contrary, it exhibits the tendency to reduce the mean and standard deviation of the received power in adjacent Node Bs, comparing to the case no fast VSF is applied.

The fact that the fast VSF scheme increases the variance in the received power in the serving Node B can potentially lead the system to instability. The probability of instability in cases of high concentration of UEs close to their serving Node B. Moreover, the indicated reduction in the variance of the other cell interference is more evident when the fast VSF is applied to UEs at cell borders. For these reasons, there is an interest in investigating the fast VSF scheme in cases the latter one is applied to UEs at cell borders.

In these cases, the evaluation of the trade off between increased variance of the own cell interference and reduced variance of other cell interference is of high interest.

### 5.2.3 Implementation

The fast VSF scheme aims at minimizing the variance of the UE transmission power. The algorithm materializing the fast VSF is implemented inside the UE. It does not require significant modifications of the 3GPP standards. It works in collaboration with the other radio link mechanisms, that have been already implemented inside the UE, e.g. the “TFC elimination”.

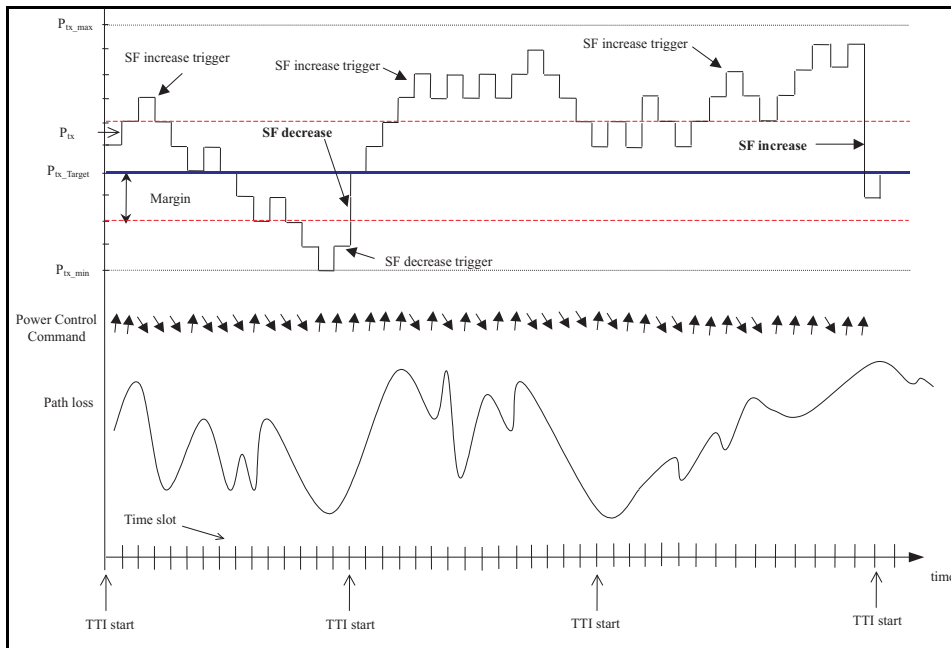


Figure 5.3: Implementation of the fast VSF scheme.

The principle of the fast VSF algorithm can be seen in figure 5.3. In order to maintain the UE transmission power constant, a transmission power target per UE is defined. In addition, a desired area of operation are determined ( $P_{tx\_Target}$  and  $[P_{tx\_Target} - \text{Margin}, P_{tx\_Target} + \text{Margin}]$  respectively in figure 5.3). At the beginning of each transmission time interval, it is checked whether the current transmission power of the user ( $P_{tx}$  in figure 5.3) is within the desired area of operation. In case the current transmission power is outside the desired area of operation, the UE is changing its SF in order to bring its transmission power inside the area of  $[P_{tx\_Target} - \text{Margin}, P_{tx\_Target} + \text{Margin}]$ . The ideal operation of the algorithm requires that all the SFs are possible and that the UE is choosing the one that brings its transmission power as close as possible to the target. However, certain limitations in the use of SFs have to be considered. The first one is imposed by the “TFC Elimination” mechanism; SFs corresponding to data rates and hence to TFCs that are in the “blocked” state, cannot be applied. The second limitation is imposed by the maximum

data rate that is allocated to the UE. In case a significant number of UEs decides to apply SFs that correspond to much higher data rates than the ones they are allocated, it is very likely that the noise rise reaches values much higher than the target, leading thus the system to instability. Therefore, a limit in the maximum data rate and hence in the minimum SF that can be applied by each UE has to be determined. This limit is set in function of the allocated data rate; e.g. the maximum data rate of an UE can be equal to its allocated data rate, or it can be one step higher than the allocated data rate.

The target for the transmission power of each UE is set by the UE itself. It is defined by solving the following equation:

$$\left(\frac{E_b}{N_0}\right)_{target} = \frac{w}{r} \frac{P_{rx}}{P_{Total} - P_{rx}} = \frac{w}{r} \frac{P_{tx} \cdot G}{P_{Total} - P_{tx} \cdot G} \quad (5.24)$$

where  $P_{rx}$  is the received power of the user,  $P_{tx}$  is its transmission power and  $G$  is the average path gain, including the radio attenuation and the shadow fading. Hence, the transmission power of a user is:

$$P_{tx\_target} = \frac{\left(\frac{E_b}{N_0}\right)_{target} \cdot r \cdot P_{Total}}{G(w + \left(\frac{E_b}{N_0}\right)_{target} \cdot r)} \quad (5.25)$$

The setting of the transmission power target by the UE is feasible, since the  $\left(\frac{E_b}{N_0}\right)_{target}$  can be transmitted to the UE by the network and the value of the total received power is diffused in the entire cell periodically ([77]). In addition, the UE can estimate the average radio path gain,  $G$ , by measuring the pilot channel, [62]. The data rate,  $r$ , that is used for the estimation of the target is the data rate allocated by the PS to the UE.

However, a number of the parameters defining the transmission power target are subject to change. Therefore, the transmission power target is computed periodically. The power target update period is chosen to be equal to a dozen of TTIs.

In order to obtain the expected gains from the fast VSF scheme, the transmission power target has to be set to relative values. Therefore, an upper limit for the power target has been defined.

#### 5.2.4 Simulation Parameters

The fast VSF has been tested with the simulator presented in chapter 4. Hence, the biggest part of the assumptions and parameters listed in this chapter apply for the simulations here as well. A number of parameters that are related to the fast VSF scheme have been introduced to this version of the simulator and their description follows.

As in the simulations presented in chapter 4, the system is consisted of only packet data users. The traffic model scenario B is used in this case. It results in a high offered load in the cell deriving from few users carrying high data rates each. Consequently, the almost “stable” situation that occurs when the offered load in the system is high, as it is described in chapter 4, is avoided.

Users are moving at a speed of 3 km/h. Higher speeds have also been tested and tests have shown that the fast VSF scheme is able to reduce the variance of the UE transmission power only at low speeds. (More details of this study can be found in appendix B).

Parameter	Value
UE Speed	3 [km/h]
Traffic Model	Scenario B
Minimum UE-Node B Distance for the application of fast VSF	1.5 [km]
Data rate steps above the allocated Margin	2
Margin	2.5 [dB]
Max UE Tx Power	21 [dBm]
Max Tx Power Target	18.5 [dBm]
Tx Power Target Update	100 [ms]

Table 5.2: Simulation parameters for the fast VSF scheme.

The fast VSF is applied to users whose path loss corresponds to a distance of 1500 m and more. Upon application of the fast VSF, users are allowed to use data rates from 0 kbps up to the maximum allocated one plus 2 steps more. The margin that defines the desired area of operation is equal to 2.5 dB (figure 5.3). The transmission power target is updated every 100 ms and its maximum value is set to the value that corresponds to the maximum UE transmission power minus the margin, hence to 18.5 dBm.

### 5.2.5 Simulation Results

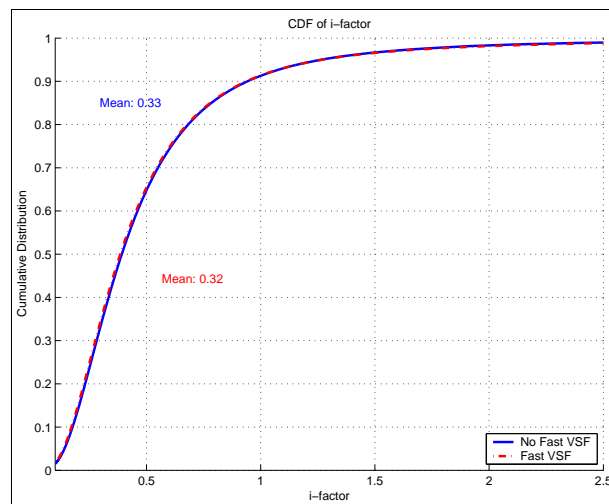


Figure 5.4: CDF of i-factor (fast VSF “On” and “Off”, 12 UEs per cell, traffic model scenario B).

The fast VSF has been simulated for different numbers of users in the system. The results that are shown here are obtained in the case of 12 UEs per cell in average. They are representative however of the tendencies observed in most of the simulated cases. Moreover, the observed value of the cell throughput for this number of UEs is close to

the maximum cell throughput for this NR target; hence, it can be easily argued that it corresponds to the system capacity. Consequently, an increase in the observed cell throughput can be considered as a capacity gain. The same applies for the cell throughput comparisons of the other proposed schemes.

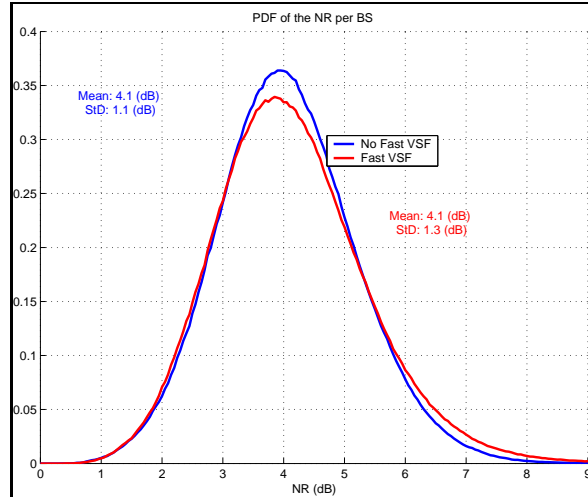


Figure 5.5: PDF of the noise rise (fast VSF “On” and “Off” , 12 UEs per cell, traffic model scenario B).

Figure 5.4 shows the i-factor CDF for the cases the fast VSF is activated and deactivated respectively. The use of fast VSF is not reducing the i-factor. The main reason being that the SF changes increase the variance of the own cell interference. This results in highly variant total received power in the cell. Especially, in the cases of sudden increase of the received power in the cell, UEs in the cell are obliged to increase their transmission power in order to meet the received  $E_b/N_0$  requirements. Figure 5.5 certifies this assumption. Figure 5.5 depicts the noise rise PDF in the system. Therein, it can also be seen that the NR presents higher “long tails” in its PDF.

Figure 5.6 displays the cumulative distribution function of the delay per packet call, when the Fast VSF is deactivated and activated respectively. The experienced delay is reducing when the fast VSF is activated. The main reason for this reduction is that users far from their serving BS are transmitting at higher data rates, as it can be seen in figure 5.7.

Users far from their serving BS are transmitting with higher data rates when the fast VSF is applied. This is a direct sequence of the setting of the transmission power target. There is no penalty in the average UE transmission power due to the transmission of higher data rates of UEs at cell borders, since these UE in question are transmitting with a power close to the target.

Table 5.3 lists the performance metrics for the cases the fast VSF is activated and deactivated respectively. Displayed values are the mean ones. There is an increase of about 1.2% in both cell throughput and user throughput. The observed increase in these metrics is insignificant and it can easily argued that it is simulation “noise”. In any case,

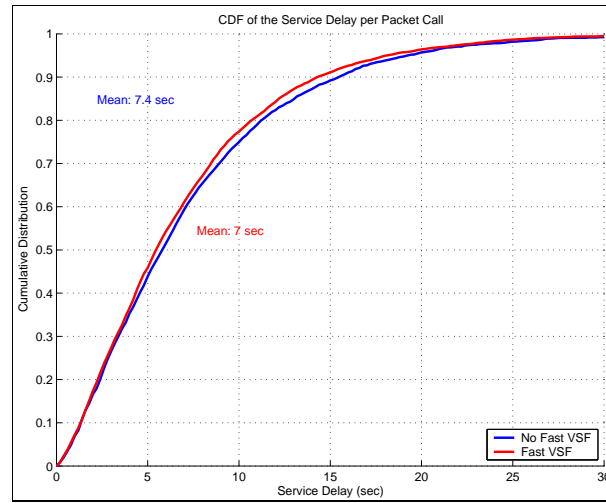


Figure 5.6: CDF of the experienced delay per packet call (fast VSF “On” and “Off”, 12 UEs per cell, traffic model scenario B).

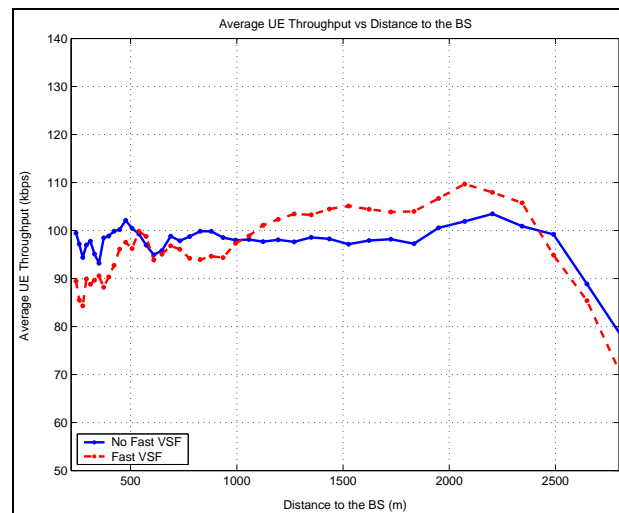


Figure 5.7: Average UE throughput during activity period (fast VSF “On” and “Off”, 12 UEs per cell, traffic model scenario B).

	Cell Throughput	UE Throughput	Delay
Fast VSF On	1198 [kbps]	170.4 [kbps]	7.1 [sec]
Fast VSF Off	1184.2 [kbps]	169.4 [kbps]	7.4 [sec]

Table 5.3: Cell Throughput, UE throughput and delay per packet call (fast VSF “On” and “Off”, 12 UEs per cell, traffic model scenario B).

the gain observed in these simulations in conjunction with the difficulties related to the implementation of the fast VSF scheme make the fast VSF scheme a not so appealing proposal for operators.

### 5.3 Decentralized Uplink Packet Data Access

In this section an alternative uplink packet data access scheme is presented ([13], [14]). In this mode, UEs participate more in the control of the uplink packet data transmission. Therefrom, this access mode is called “decentralized” in this chapter.

In the following paragraph, the motivation for introducing an uplink transmission mode with more distributed control is stated. Then, the concept of the decentralized packet data transmission is explained. At the end of this section, the cases where the decentralized scheme is expected to improve the performance of the system are discussed.

#### 5.3.1 Motivation For Decentralized Uplink Packet Data Access

In a typical procedure of the uplink packet data access, UEs report their RLC buffer size to the packet scheduler. The packet scheduler allocates data rate based on these reports, as it is described in chapter 4. Following the data rate allocation, a radio bearer is established. At the end of the packet call transmission, usually the radio bearer is released. At the arrival of a new packet call a new measurement report is sent. If data rates are granted, a new radio bearer allocation takes place. This mechanism can be seen in figure 5.8. Therein the typical uplink packet data transmission, involving recursive radio bearer establishments and releases is illustrated.

In a designated user’s packet session, this procedure can be repeated several times, introducing thus significant delays to the packet data transmission. In addition, it creates a signalling overhead in the system ([77], [79]). Moreover, the arrival of the new packet call may happen shortly after the release of the radio bearer.

In order to avoid the recursive radio bearer establishments and releases, the decentralized scheme proposes that the radio bearer that is dedicated for the uplink packet data remains open till the end of the packet session.

The changes that the decentralized mechanism introduce are presented in the following paragraphs. The limited cases in which the decentralized scheme is expected to exhibit gain in comparison to the centralized scheme are also presented.

#### 5.3.2 Decentralized Uplink Packet Data Access Concept

In the following paragraphs the concept of the decentralized uplink packet data access is presented. In addition, the changes in the nominal uplink packet data access required by the decentralized mode are listed. At the end of this section, the scenarios, where the decentralized scheme is expected to exhibit gain in comparison to the centralized mode are discussed and explained. Therefrom, the cases that worth to be simulated are presented.

The decentralized scheme proposes that a radio bearer carrying packet data is not released and re-established during the transmission of a single packet session. This can be achieved by setting the inactivity timer to values in a way that the timer is more likely

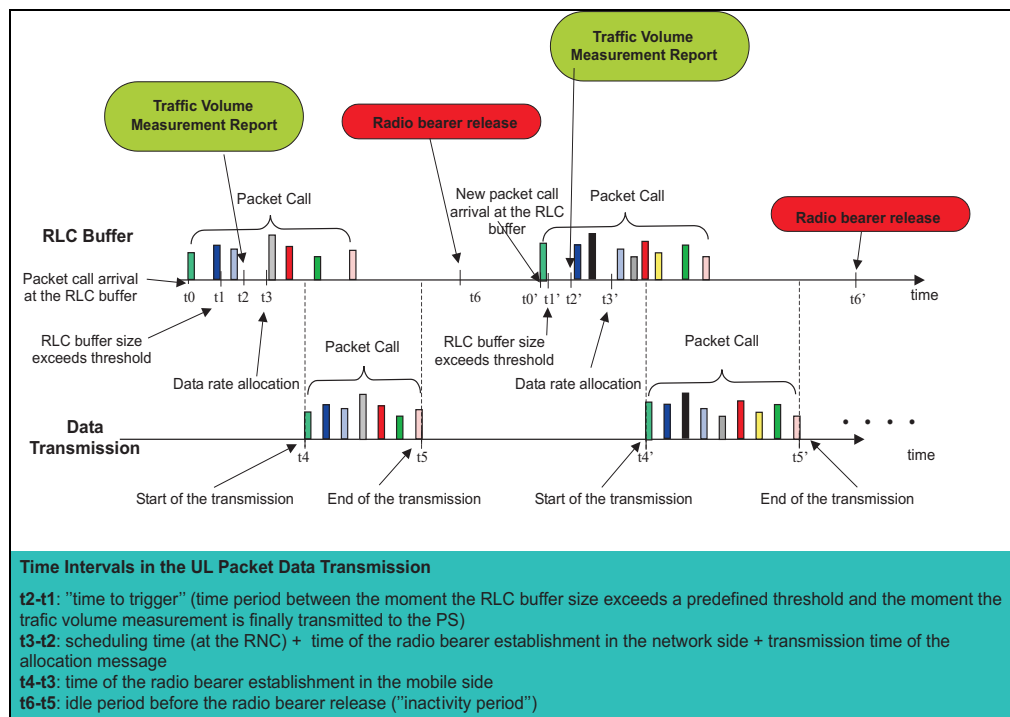


Figure 5.8: Motivation for the proposal of the decentralized scheme.

triggered at the end of the packet session. This mechanism results in a higher number of packet data radio bearers per cell than in the centralized scheme. Therefrom, a number of changes in the uplink packet data access is introduced. They are discussed in the following paragraphs.

### Traffic Volume Measurement Reports

No modification is introduced in the way traffic volume measurements are reported by the UEs to the network, in comparison to the centralized scheme.

### Packet Scheduling

The operation of the packet scheduler in the decentralized scheme is similar to the operation in the centralized one; the functions, timers and assumptions described in chapter 4 apply also for the case of the decentralized mode. The increase in the number of packet data radio bearers in the system leads consequently to an increase of the inactive packet data users.

It was shown in chapter 4, that a power margin is considered for packet data users, which have open radio bearers and which have been detected inactive previously. In case the inactive users are considered in the same way in the decentralized scheme, the margin due to inactive users is going to have very high values. This would result in a small amount

of available power for new data rate allocations. Therefore, a change in the consideration of the inactive packet data users in the decentralized scheme is required. These users are not considered in the estimation of the available for scheduling power and hence the weighting factor for inactive users (WFIU) is set to 0.

### Packet Data Access

The principle of the uplink packet data access, as it is described in chapter 5 for the centralized case, remains the same for the decentralized mode.

The number of users which have been granted data rates and which are inactive is increasing in the decentralized mode, as it is discussed in the previous paragraph. Moreover, no margin is considered for these users. Consequently, if an important number of inactive users restarts packet data transmission, it is very likely that the noise rise per cell exceeds the planned target.

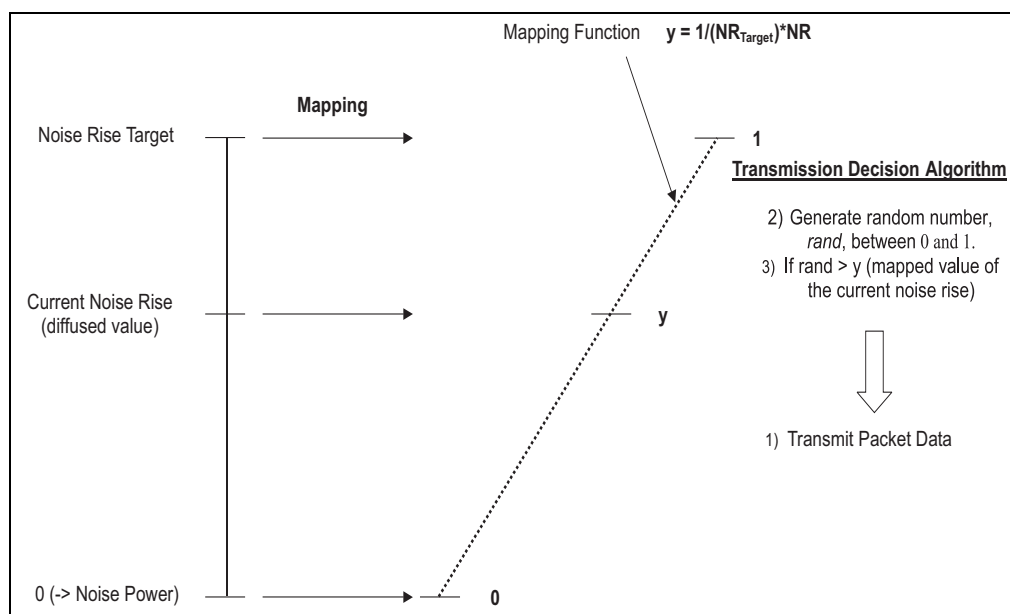


Figure 5.9: Packet data transmission mechanism in the decentralized scheme.

Therefore, an additional mechanism controlling the uplink packet data access is required. This mechanism is located in the UEs and therefrom the name of the discussed transmission mode is “decentralized”. Users that are allocated data rates decide whether to transmit or not based on the interference level in the cell. The cell interference is diffused periodically in the cell ([77]). The diffused value of the interference is mapped to a number,  $y$ , between 0 and 1, with the aid of a specific mapping function. Each UE bearing packet data, before starting the packet data transmission, is generating a random number,  $rand$ , between 0 and 1. This number is compared to the mapped interference value,  $y$  and the UE is transmitting if the random number is higher than  $y$ . The principle of this decision mechanism is displayed in figure 5.9. The function that is mapping the

diffused value of the interference to a value  $y$  between 0 and 1 is:

$$y = \frac{1}{NR_{target}} \cdot NR_{bch} \quad (5.26)$$

where  $NR_{target}$  is the planned noise rise target and  $NR_{bch}$  is the noise rise that corresponds to the currently broadcasted interference level in the cell. Noise rise values are in dB.

Formula 5.26 is applied for noise rise values between 0 and  $NR_{target}$ . When the broadcasted level of interference results in a noise rise, higher than the  $NR_{target}$ , then  $y$  is equal to 1.

### 5.3.3 Simulated Cases

The increase of the open uplink radio bearers per cell in the decentralized mode results in a respective increase of the downlink radio bearers, since a radio access bearer is bidirectional ([61]). However, an open downlink radio bearer requires a downlink orthogonal variable spreading factor (OVSF) channelization code, which is a scarce radio resource ([68]). Hence, the decentralized mode may lead to a waste of downlink channelization codes. This waste of OVSF channelization codes is avoided in the case packet data users support a real time service simultaneously and hence downlink radio bearers are already open for the real time service. These cases consisted the simulation scenarios for this work.

### 5.3.4 Simulation Parameters

A network level simulator is used in order to assess the performance of the decentralized scheme. The network is consisted of three-cell sectors and directional antennas. The same assumptions for the radio propagation models and for the procedures involved in UTRAN, as they are described in chapter 4, are applied in this simulator. In addition, the same simulation techniques are used ([24]).

In order to be able to assess the benefit from the decentralized mode, the signalling between UEs and the RNC is considered in this simulator. Mainly, the transmission of capacity requests from UEs to the RNC and its associated delay are implemented. Considering the delay budgets in UTRAN ([77], [22]), the delay is set to 100 ms. Moreover, this simulator presents a number of other differences, in comparison to the one presented in chapter 4. The most important of them being the lack of SHO and load control mechanisms in this simulator.

In regards to the parameters that are related to the decentralized scheme, the “inactivity period” timer is set to a significantly high value, so as to make sure that the radio access bearer is released at the end of the packet session. In these simulations, it is set to 20 seconds. The cell interference level is broadcasted every 40 ms in the cell.

The traffic models that are used are similar to the ones described in the previous chapters; the model used for the speech is similar to the one described in chapter 3. The typical “On-Off” model is used with the “On” and “Off” periods being exponentially distributed and with mean values equal to 1 second for both cases. For the packet data traffic, the model used is similar to the one in chapter 3.

### 5.3.5 Simulation Results

The decentralized uplink packet data access has been tested for various numbers of users per cell. The displayed here results focus on cases of 10 users per cell. In the scenarios presented here, all of them bearing a speech service and either half of them (5) or all of them bear a packet data service in parallel with the speech.

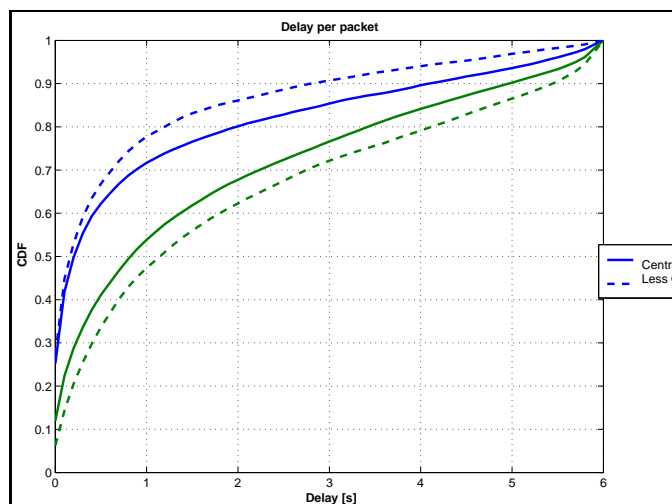


Figure 5.10: CDF of the experienced delay per IP packet, for the cases of the centralized and decentralized schemes (10 UEs per cell).

Figure 5.10 depicts the CDF of the delay per IP datagram for both the centralized and the decentralized schemes. Blue lines correspond to the cases where half of the UEs have a packet data service simultaneously with speech. Green lines correspond to the cases where all of the users have both speech and packet data service in parallel. It can be seen that in the decentralized scheme, the delay per IP datagram is reducing, at cases of medium load in the system; namely for the case where 5 users bear also packet data, the mean delay is decreasing approximately 25% for the 90% of the delay CDF. For the case of high load in the system (10 UEs per cell, all of them bearing both speech and packet data), the delay per packet is increasing when the decentralized mode is applied. The reason for this is that the high offered load leads to high noise rise in the system and consequently to a high mapped value  $\gamma$  of the noise rise. Hence, the probability that a packet data user generates a random number higher than  $\gamma$  is reducing, resulting thus in longer delays in the transmission of packets.

Figure 5.11 displays the CDF of the UE transmission power for the case of 10 UEs per cell under discussion here. As before, blue lines correspond to the case where half of the UEs have a packet data service along with the voice. Green lines correspond to the case all of the UEs have both speech and a packet data service in parallel. It can be seen that UEs transmit at lower power levels in the decentralized mode. The reason for this being that UEs statistically do not tend to transmit when the NR in the system is high, avoiding thus transmission with high power.

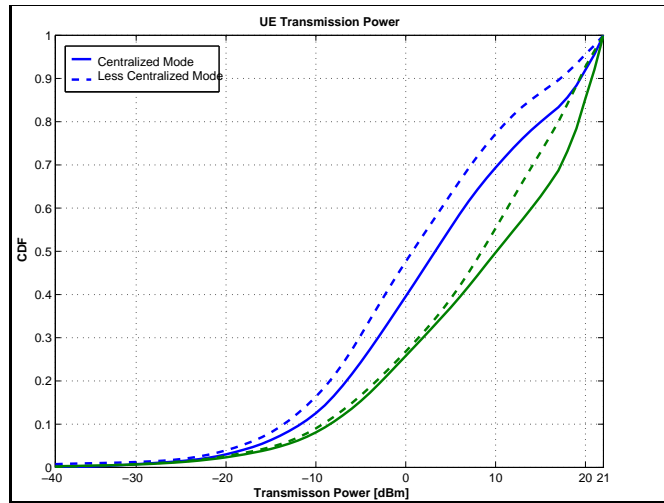


Figure 5.11: CDF of the UE transmission power, for the cases of the centralized and decentralized schemes.

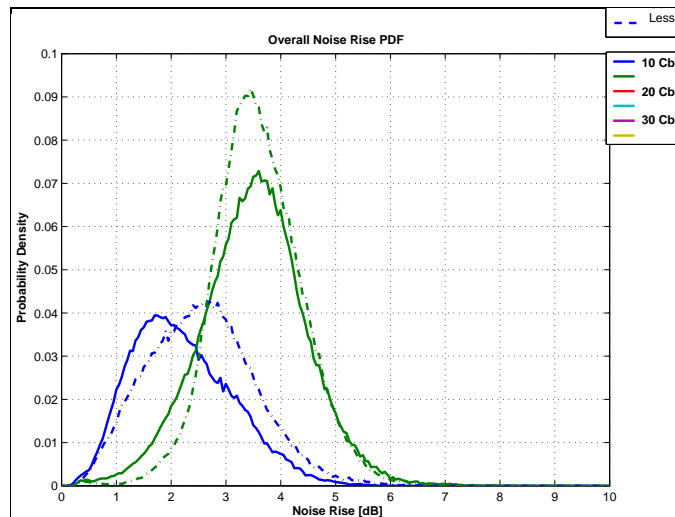


Figure 5.12: PDF of the noise rise, for the cases of the centralized and decentralized schemes.

Figure 5.12 depicts the noise rise PDF for the tested cases. It can be seen that the StD of the noise rise is reducing in the decentralized mode.

## 5.4 Fast Packet Scheduling

### 5.4.1 Concept

Faster packet scheduling is expected to increase cell capacity and the UE throughput by improving the utilization of the available resources. This is anticipated to lead to more frequent high data rate allocations, than in the cases presented in chapter 4. The main idea involves very dynamic modifications of the allocated data rates to UEs so as to adapt to the typically bursty nature of their source traffic ([15]).

The packet scheduling becomes faster by shortening its related time periods and timers; hence by reducing (i) the packet scheduling and modification periods, (ii) the lifetime of a request in the PS buffer and (iii) the value of the inactivity timer.

### 5.4.2 Simulation Parameters

For the case of fast packet scheduling, the PS period is equal to the modification period, as in chapter 4. Both of the PS period and the modification period are equal to 100 ms. This value corresponds to the fastest possible scheduling period when the PS functionality is located in the RNC, due to delays in UTRAN ([22]). The value of the inactivity timer and the lifetime of a traffic volume measurement in the PS are scaled accordingly and therefore they are set to 400 ms. Table 5.4 summarizes the timing related parameters of the fast PS. The table contains also the parameters for the case of scheduling period equal to 500 ms. The latter one is called “reference case” in the table and in the following.

	Reference Case	Fast Packet Scheduling
Packet Scheduling Period	500 [ms]	100 [ms]
Modification Period	500 [ms]	100 [ms]
Inactivity Timer Value	2 [sec]	400 [ms]
Maximum Lifetime of a Traffic Volume Measurement in the PS queue	2 [sec]	400 [ms]

Table 5.4: Timing related parameters for the reference case and for the fast packet scheduling case.

The comparison between the reference case and the fast scheduling proposal is performed in terms of NR outage probability; both of the schemes exhibit the same 2% NR outage probability.

It is anticipated that the expected increase in the allocations of high data rates in the fast scheduling case is going to enlarge the long tails of the NR distribution and hence shift upwards the NR value that corresponds to the 2% of NR outage. In order to prevent this effect and make the comparison between the two schemes feasible, the NR target is equal to 5 dB for the fast scheduling case.

Both of the traffic model scenarios that are presented in chapter 4 are simulated. When the traffic model scenario A is simulated, there are 32 UEs per cell, each one generating a data rate of 115 kbps approximately during packet call period. The same level of mean generated load in the cell is obtained with the traffic scenario B, when there are 12 UEs

per cell, each UE having a source data rate equal to 230 kbps approximately during packet call.

### 5.4.3 Simulation Results

The fast packet scheduling is simulated and compared to the reference case for different number of users in the system.

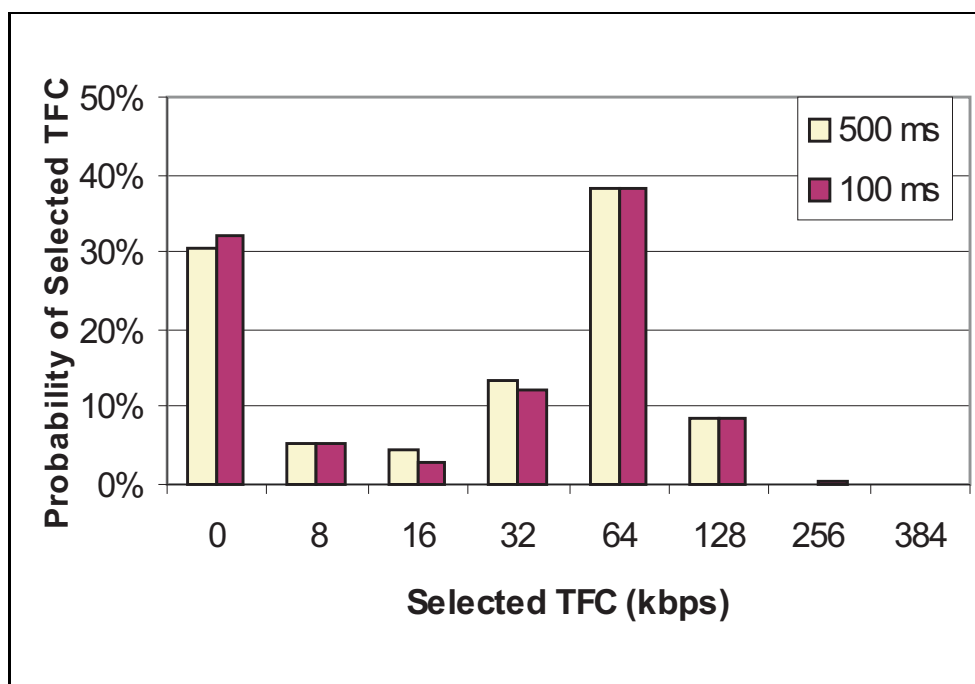


Figure 5.13: Probability of selected TFC for all of the users in the system, for the cases the packet scheduling period is 500 and 100 ms, (columns 1 and 2 respectively, 32 UEs per cell, traffic model scenario A).

For the traffic scenario A and for 32 UEs per cell, the gain obtained from fast packet scheduling is insignificant; the cell capacity gain is 1.7% when the PS period is shorter (see table 5.5), while the noise rise distributions are similar in both cases.

The reason for such a small improvement due to faster scheduling is that in this case the air interface load in the cell is almost constant and consequently no much gain can be expected by the faster scheduling ([15]). It can be seen in figure 5.13, that UEs are most of the times attempting to transmit with 64 kbps, a data rate that is approximately the half of the generated data rate per user and consequently, the percentage of the time UEs are active is increasing (approximately 70%, figure 5.13). As a result, there is a high number of active UEs in the cell, each UE transmitting at a low data rate, which leads to an almost invariant and high NR in the cell. Under such conditions, the fast packet scheduling cannot bring any gain compared to the reference case.

In case of traffic scenario B and of 12 UEs per cell, the mean offered load in the cell is

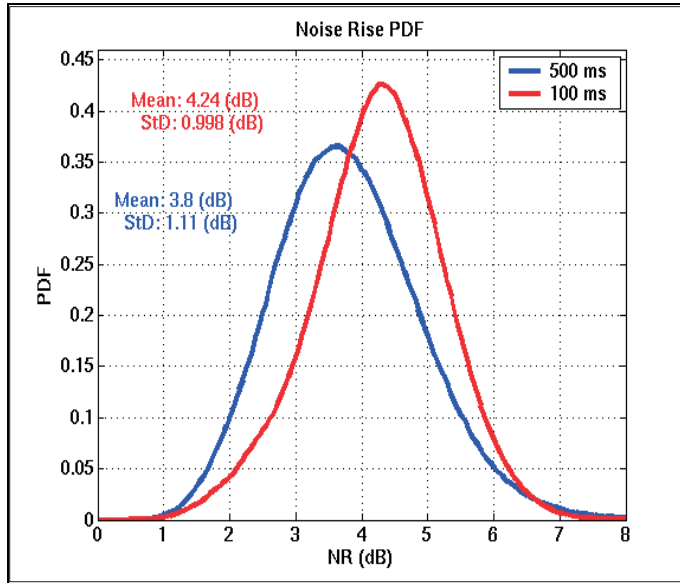


Figure 5.14: PDF of the noise rise, for the cases the packet scheduling period is 500 and 100 ms (12 UEs per cell, traffic model scenario B).

almost equal to the one in the previous case, but it exhibits higher variance. Under these conditions, a capacity gain of 8.1% is obtained when the PS period is reduced from 500 ms to 100 ms (5.5), while preserving the same noise rise value at 2% outage. Figure 5.14 displays the PDF of the noise rise in the system. With more frequent packet scheduling, the mean noise rise slightly increases, as a consequence of the increased cell throughput. The standard deviation of the noise rise however reduces, allowing thus the maintenance of the same 2% outage probability.

In addition, the mean UE throughput is slightly increasing with faster packet scheduling (see table 5.5). This effect in conjunction with the shorter PS period leads to a considerable reduction of the delay per packet call; figure 5.15 displays the CDF of the delay per packet call. The mean delay is reducing by approximately 11% when the PS period is reduced from 500 ms to 100 ms.

These improvements are mainly due to the increased probability of allocating high data rates, when the packet scheduling is done faster, as it is shown in figure 5.16.

Table 5.5 summarizes the obtained results for PS periods equal to 500 and 100 ms respectively, for both of the traffic model scenarios. In order to have the same average offered load in the system, there are 32 UEs per cell when the traffic model scenario A is applied and 12 UEs per cell when the traffic model scenario B is applied respectively.

It can be seen in table 5.5 that the cell throughput is equal to 1.224 Mbps in case of fast packet scheduling, when there are 12 UEs per cell. In ideal conditions, i.e. when the load in the system corresponds to the planned noise rise target, the received  $\frac{E_b}{N_0}$  is equal to the  $(\frac{E_b}{N_0})_{target}$  for 10% FER from the AVI curves and the cell is perfectly isolated (i-factor equal to 0), the maximum cell capacity is derived. For 12 UEs and for a NR

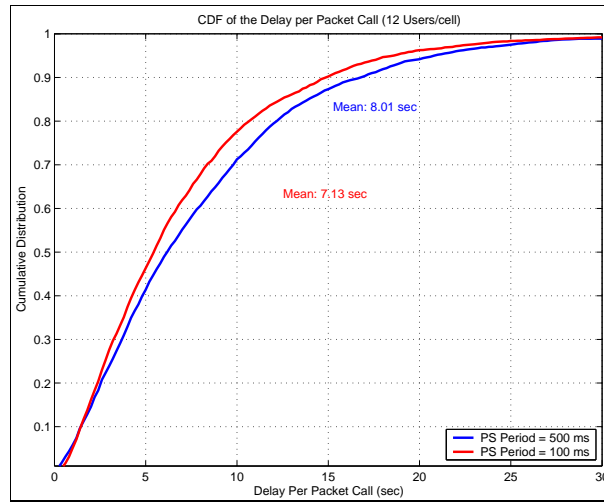


Figure 5.15: CDF of the delay per packet call, for the cases the packet scheduling period is 500 and 100 ms (12 UEs per cell, traffic model scenario B).

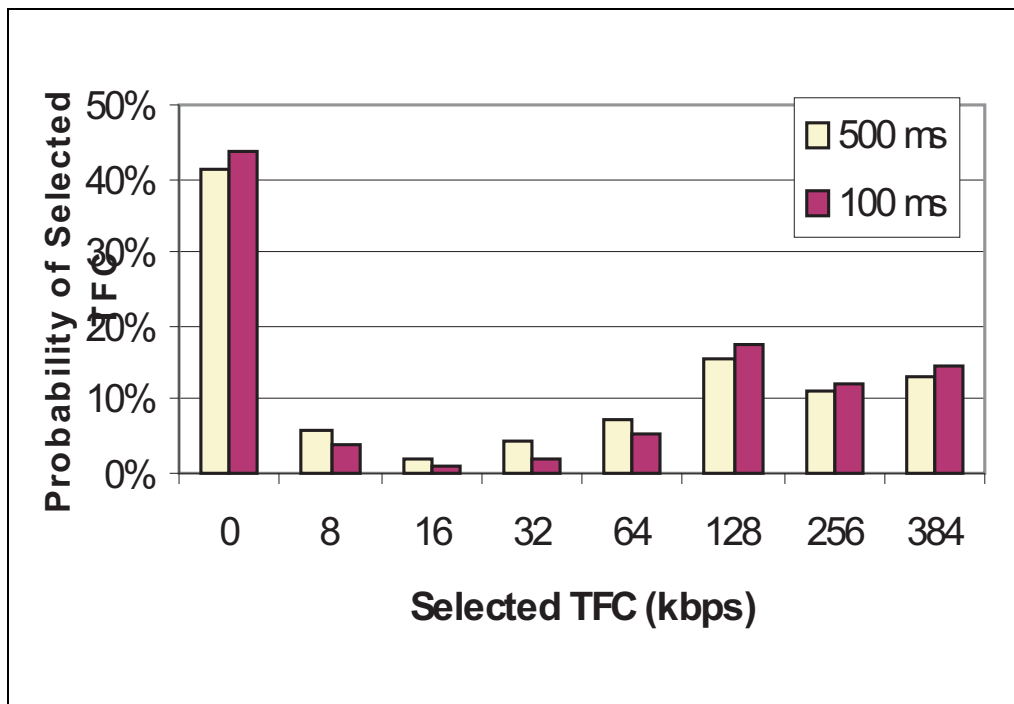


Figure 5.16: Probability of selected TFC for all of the users, for the cases the packet scheduling period is 500 and 100 ms, (columns 1 and 2 respectively, 12 UEs per cell, traffic model scenario B).

Users/cell	Scheduling Period	Cell Throughput	UE Throughput	Packet Call Delay
32 (Traffic Model A)	500 [ms]	1182 [kbps]	73 [kbps]	11.2 [sec]
	100 [ms]	1202 [kbps]	73 [kbps]	8.6 [sec]
12 (Traffic Model B)	500 [ms]	1132 [kbps]	157 [kbps]	8.01 [sec]
	100 [ms]	1224 [kbps]	165 [kbps]	7.13 [sec]

Table 5.5: Cell Throughput, UE throughput and delay per packet call for the cases of packet scheduling period equal to 500 ms and 100 ms, for both of the traffic model scenarios.

target equal to 5 dB and from formulas 5.3, 5.5 and 5.8, an approximation of the cell capacity can be obtained. The maximum cell throughput is equal to 1.313 Mbps. Hence the cell capacity that is obtained in the case of fast scheduling is close to the approximation of the theoretical maximum capacity (it is 93% of the approximation of the theoretical maximum). Considering the imperfections in the radio interface, it seems that the cell capacity in the fast scheduling case is very close to the maximum value of cell capacity that can be obtained from system level simulations for the above listed assumptions.

## 5.5 Conclusion and Discussion

In this chapter, the possibility to increase the uplink cell capacity and to improve the user QoS metrics, such as the user throughput and the experienced delay per packet call, is investigated. Therefore, three mechanisms are proposed: i) the fast variable spreading factor, ii) the decentralized uplink packet data access and iii) the fast packet scheduling.

The fast VSF scheme is attempting to increase the system capacity by stabilizing the other cell interference. Results show that the other cell interference is stabilizing upon application of the fast VSF scheme, but the variance of the intra cell interference is increasing due to the sudden changes of the transmitted data rates from many UEs in the cell. As a result, the increase in cell capacity is marginal. Consequently, the proposed here fast VSF scheme is not recommended for use.

The decentralized scheme attempts to improve mainly the delays in the packet transmission, by reducing the signalling. Results have shown, that in the cases of medium load in the system, the delay per transmitted IP packet can be reduced up to 25%. Hence, the implementation of the decentralized scheme is of high interest, in systems where the expected load is not very high.

The fast scheduling is expected to increase cell capacity essentially by allocating more frequently higher data rates to UEs. Results have shown that a capacity gain of 8.1% can be obtained when the generated traffic in the system exhibits a considerable variance. The obtained value of the cell capacity is very near to the maximum theoretical value that can be obtained with the applied here assumptions. Consequently, the implementation of the fast packet scheduling scheme worths an effort. In addition, further investigations on the potential of even faster packet scheduling are of high interest.

## Chapter 6

# Conclusions and Further Work

### 6.1 Conclusions

This thesis has evaluated the performance of the uplink packet data access in UMTS. Performance evaluation criteria are the cell capacity and the QoS experienced by the users in the system. In addition, potential improvements of the uplink packet data access are investigated.

The first mechanism of the uplink packet data access under study is the TFC selection. An algorithm for the TFC selection has been proposed in 3GPP. The selection is based on traffic priorities; the algorithm always attempt to maximize the data rate of the traffic with the highest priority. Its performance has been tested for a scenario with mixed traffic: speech and high data rate interactive traffic. Results have shown that the introduction of an additional packet data service to the speech shrinks the coverage area for both services.

In order to mitigate this effect, a modified TFC selection algorithm is discussed. The algorithm aims at preserving the required QoS of speech for even higher distances than in the case of the 3GPP compliant algorithm. This is achieved by introducing an additional TFC elimination margin that is applied only whenever speech is transmitted. A by-product of this additional margin is that simultaneous transmissions of speech and packet data, which require high transmission power, are avoided. Results have shown that the coverage area increases in comparison to the 3GPP compliant algorithm. In addition, the UE throughput increases without a corresponding increase in the UE transmission power, mainly due to reduction of losses and consequently of retransmissions.

The modified TFC selection algorithm has been tested for a scenario with a mix of voice and interactive traffic. The algorithm can be applied for other scenarios, with two traffic types of different priorities, e.g. streaming and interactive.

The lesson we learned from these studies is that the TFC selection is a mechanism with significant impact on the performance of the uplink packet data access. The TFC selection algorithm can be shaped and modified in order to provide the QoS and the coverage we target at. For this reason, appositely conceived admission control policies are required.

The impact of the TFC elimination mechanism has then been assessed by means of network level simulations. Results show that the TFC elimination has an impact on UEs

that are located at distances higher than 2 km far from the serving Node B. In the case of absence of the TFC elimination, the FER experienced by these UEs rises to undesirably high levels. Hence, these users create a significant amount of unwanted interference in the system. In this case, capacity losses of about 5% can be observed.

The overall system performance of the uplink packet data access is then assessed. Principal performance evaluators are the cell capacity and the experienced QoS by the users, i.e. the user throughput during activity and the experienced delay. A packet scheduler that functions according to the principle of fair throughput sharing among UEs is therefore implemented. The tested service is an interactive service, with a mean data rate equal to 115 kbps during activity. Results show that cell capacity is approximately 1.25 Mbps. For the simulated service, this capacity is sufficiently high in order to offer an acceptably good QoS to approximately 20 UEs per cell.

Mechanisms that improve the uplink packet data access are then studied. They are the fast VSF, the decentralized uplink transmission and the faster scheduling. Their characteristic is that they don't require significant changes in the existing 3GPP standards.

The fast VSF aims at increasing system capacity by stabilizing the i-factor. Results have shown that the fast VSF is not bringing any significant gain, due to the fact that it does not succeed in stabilizing the i-factor. The reason for this is that while it stabilizes (reduces the variance of) the other cell interference, in the same time it increases the variance of the own cell interference.

We have learned that stabilizing the transmission power of UEs by applying the fast VSF scheme is not stabilizing the i-factor of the system.

We have also learned that if the fast VSF is applied without any limitation in the maximum data rate transmitted per UE, it may lead the system to instability. Therefore, a limitation on the number of data rate steps above the allocated data rate of each UE has to be defined.

The performance of an alternative uplink transmission mode, with a more distributed control of resources is then investigated. The main aim is to reduce the delay per packet. This is achieved by minimizing the amount of exchanged signaling between the UE and the network. Results show that under certain assumptions a gain of approximately 25% per packet delay can be obtained. In addition, the decentralized mode is a reliable system despite the loosening of the centralized control.

The potential of the fast packet scheduling is then investigated. Without applying any change in the packet scheduling and by simply upgrading and downgrading users faster, a capacity gain of approximately 10% is observed. The main reason being that the faster functioning of the PS makes more accurate allocation of resources, minimizing thus the margins considered in the packet scheduling.

## 6.2 Future Work

The contributions in this manuscript have tried to set the stage for future in depth studies and developments in the uplink packet data access in WCDMA-based systems. The potential of a number of mechanisms related to the packet scheduling to increase system capacity has been put in evidence throughout the thesis. The capacity benefits provided

by more elaborate than the current one packet scheduling have been demonstrated.

To that respect, studies on advanced scheduling algorithms would be of high interest. Moreover, their combination with advanced physical layer mechanisms such as Hybrid Automatic Repeat Request (HARQ) or Adaptive Modulation and Coding (AMC) or shorter TTIs is expected to bring even higher capacity gain. The implementation of such algorithms though, involves significant changes in the existing 3GPP standards. In addition, their implementation requires the transfer of the packet scheduler from the RNC to the Node B. Hence, additional investigations on protocol architecture aspects might be needed. It is hoped, that the lessons learned here, will provide a part of the required knowledge for these and for other related future studies.

# Appendix A

## Simulators Description

Results presented in this manuscript are obtained by three different simulators. The first one is used for the TFC selection studies. The second is used for the assessment of the uplink packet data access performance (i.e. results presented in chapter 4) and for investigations on the potential of the fast VSF and of fast packet scheduling. The third one is used in studies about the decentralized uplink packet data access.

The first simulator is a single-link simulator, i.e. it models the transmission from a single UE to the network, whilst the other ones are system level simulators.

All of them simulate the functioning of layers 1-2 of the UE. The second and third simulators include also a simplified modeling of few RRM functions and of few RRC elements, e.g. . The implementation of layer 3 procedures in the simulators has been discussed in chapters 4 and 5.

Layer 1-2 modeling involves the functions of RLC layer buffering, TFC selection in MAC layer, access to transport and physical channels. A significant part of the simulators consists of models related to the transmission in the physical layer and its control. Hence, mechanisms such as radio propagation modeling, fast fading, fast and outer loop power control, reception in the physical layer are also implemented.

Users mobility is considered in our simulator apart from the first one. This is the essential reason for not implementing a slow-fading (also known as shadow fading) functionality in the single-link simulator.

Simulators 2 and 3 present many similarities. The motivation for implementing these simulators being slightly different, explains the few differences. As mentioned above, simulator 3 is implemented in order to study the decentralized scheme. The main aim therein is to reduce delays per packet by avoiding recurrent signalling as discussed in chapter 5. Therefore, simulator 3 is more elaborated than simulator 2 in the modeling of RLC buffers; in simulator 3 a timestamp is attached to every packet in the buffer, making thus possible the measurement of delay per packet in the buffer. This is also the reason for modeling the RRC signalling that is related to capacity requests and allocations in simulator 3.

Other differences between simulator 2 and 3 are related to SHO and antenna diversity. In simulator 3, no SHO and no dual antenna receiver have been implemented. In addition, there is a difference in the fast fading modeling. In simulator 1 and 2, fast fading has been implemented as a Rayleigh procedure [26] and the power delay profile Veh A is used [78].

In simulator 3, the fast fading after RAKE combining has been modeled. Therefore, no power delay profile has been implemented. The fast fading coefficient received after RAKE combining has been modeled as a correlated procedure which follows a normal distribution ([45]). According to this modeling, the fast fading coefficient at an instant  $n$  is given (in dB) as:

$$X_n = \lambda X_{n-1} + \mu \epsilon_n \quad (\text{A.1})$$

where  $\epsilon_n$  is a normally distributed variable with a mean value equal to 0 and a variance equal to 1. Consequently, the fast fading factor,  $X_n$ , is also a normally distributed variable, with a mean value equal to 0. In that case, its variance,  $Var[X]$ , is given by :

$$Var[X] = E[X^2] = \frac{\mu^2}{1 - \lambda^2}. \quad (\text{A.2})$$

## A.1 Fast Power Control

In order to compensate the fast fading effect, the fast power control mechanism runs 15 times per radio frame (that corresponds to one power control command per slot). The decision of the power control algorithm to increment or decrement the UE transmission power is based on the received energy per bit to noise density ratio  $\frac{E_b}{N_0}$  at Node B ([58]). A target for the received  $\frac{E_b}{N_0}$  is set. The  $\frac{E_b}{N_0}_{target}$  is defined by the desired block error rate (BLER) and it is controlled by the outer loop power control, as it is going to be described in the next paragraph. In case the received  $\frac{E_b}{N_0}$  is below the target, the Node B commands the UE to increase its transmission power. In the opposite case, the UE is requested to decrease its power.

Errors in the reception of the power control command at the UE, are also considered. Errors are simulated according to the model of A.1. This is a binary symmetric channel model for the downlink direction of transmission.

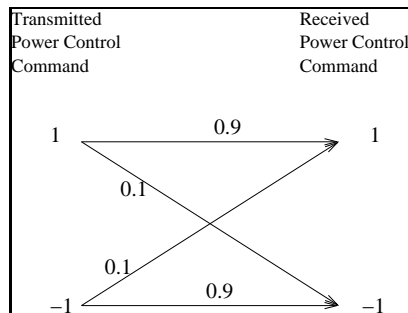


Figure A.1: Model of errors of the power control command

No delays in the fast power control are considered in the simulation. The probability of the UE receiving an erroneous fast power control command is taken into account. Table A.1 summarizes the parameters related to the fast power control.

Fast Power Control Parameters	
Frequency	1.5 [kHz]
Step	1 [dB]
Delay	0
Error	4%

Table A.1: Parameters related to the fast power control function.

## A.2 Outer Loop Power Control

The outer loop power control operates in collaboration with the fast power control in order to preserve the the users radio link quality in the desired level (the radio link quality can be measured in terms of bit error rate (BER), frame error rate (FER) or block error rate (BLER) ([77]). In this work, the measurement of the BLER is used). It is in charge of setting the energy per bit to noise density target,  $(E_b/N_0)_{target}$ , used by the fast power control. It is performed at a frequency of 10-100 Hz. In the uplink direction of transmission, it is located in the RNC, for the reason that it has to be applied in the functional component where the received blocks are decoded ([22]). This happens in the RNC, where a possible soft handover (SHO) combining occurs, as it can also be seen in figure A.2.

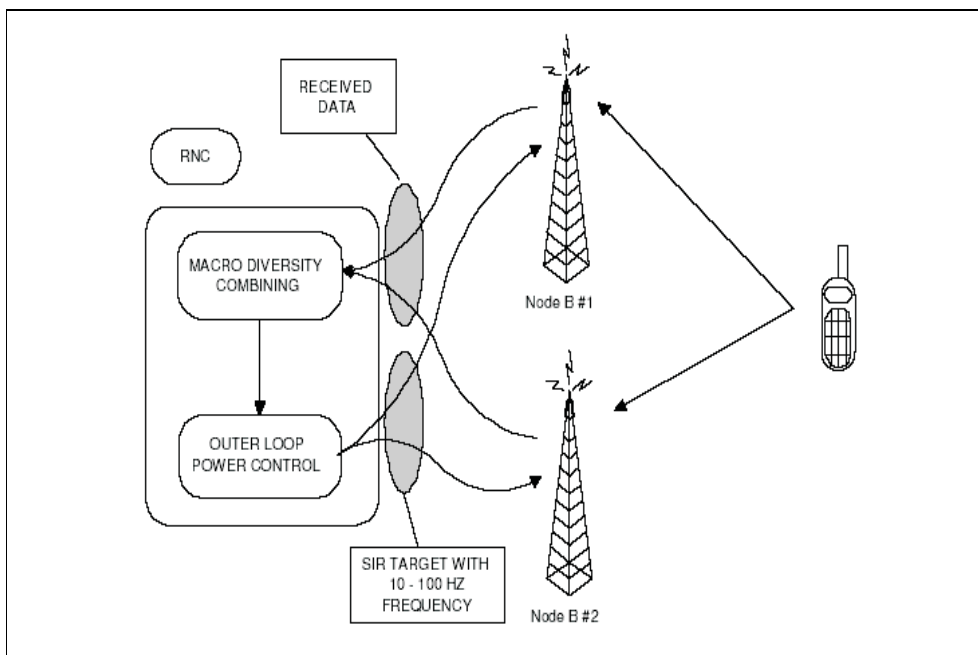


Figure A.2: Model of the outer loop power control in uplink.

There are two options for the  $(E_b/N_0)_{target}$  setting, as it is explained in [33]. The first option consists in setting a constant  $(E_b/N_0)_{target}$  for all the UEs. The second option is to

set a variable  $(E_b/N_0)_{target}$ . The variations of the  $(E_b/N_0)_{target}$  in this case are performed in function of the quality of the received signal.

In the case the  $(E_b/N_0)_{target}$  is set to constant value, this value has to correspond to the worst case in terms of radio link quality. Consequently, it has to be set to a significantly high value resulting thus in a capacity waste. Therefore, the second option is a more suitable solution. The basic concept of the outer loop power control in this case can be seen in figure A.3; at each execution step of the outer loop power control the quality of the received signal is compared to the desired quality. If it is better, then the  $(E_b/N_0)_{target}$  is reduced, otherwise it is increased.

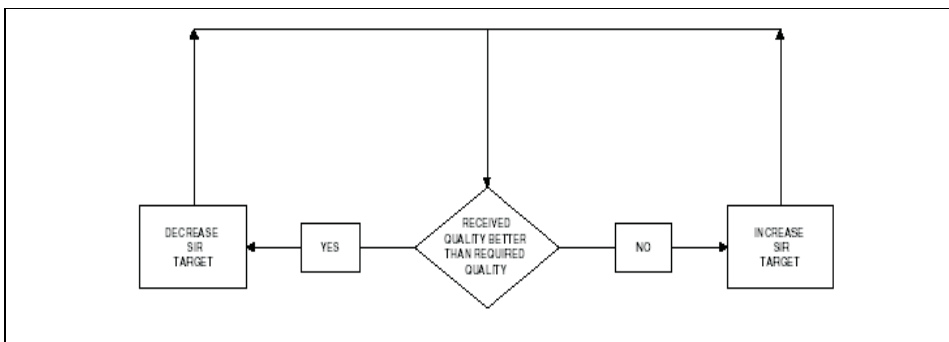


Figure A.3: General Model of the outer loop power control.

From the previous description, it derives that in order to perform the outer loop power control with a variable  $(E_b/N_0)_{target}$ , a measurement of the received signal quality is needed. In our simulations, the signal quality is measured in terms of BLER. In reality the BLER is computed according to the outcome of the cyclic redundancy check (CRC). The latter is a procedure that detects whether there is an error in the received block ([72]). It is performed in every transmission time interval in the RNC (in uplink). Figure A.4 presents the pseudo-code of the outer loop power control algorithm implemented here. The parameters for the outer loop power control are listed in the following section.

In the simulation however, the CRC check is not implemented as it is presented in 3 GPP standards ([72]). Such an implementation would add a lot of complexity in the simulator and it is generally avoided in system level simulators. An interface consisted of lookup tables, where the probability of a correct CRC check is mapped to a value of the received energy per bit to noise density,  $E_b/N_0$  of the user is usually used. The concept of these lookup tables is introduced in [20] and they are named Actual Value Interface (AVI) tables.

```
IF CRC check OK

Step_down = BLER_target * Step_size;
Eb/No_target(n+1) = Eb/No_target(n) - Step_down;

ELSE

Step_up = Step_size - BLER_target * Step_size;
Eb/No_target(n+1) = Eb/No_target(n) - Step_up;

END

where

Eb/No_target(n) is the Eb/No target in frame n,
BLER_target is the BLER target for the call and
Step_size is a parameter, typically 0.3 - 0.5 dB
```

Figure A.4: Pseudo-code of the simulated model of the outer loop power control.

## Appendix B

# On the capability of the fast VSF to reduce the variance of the UE transmission power

The aim of the fast VSF scheme is to reduce the variance of the UE transmission power, which will lead to a minimization of the other cell interference, as it is shown in chapter 5. However, the potential of the proposed fast VSF scheme depends on a number of parameters; among them the TTI size, the UE speed, the fast PC step and delay can be identified. In the following, the impact of the TTI size and the UE speed on the capability of the fast VSF to minimize the UE transmission power is assessed.

In an ideal scenario of uplink transmission, the fast PC is able to “follow” the fast fading variations in order to maintain the received  $E_b/N_0$  in the Node B constant. In this case, the UE transmission power is characterized by similar statistics as the ones of the fast fading. Therefore, the fast fading characteristics needed for our study are presented next. Based on these characteristics, the TTI size and the UE speed values that could minimize the standard deviation of the UE transmission power are computed. Then, simulation results are presented.

### B.1 Considerations on the TTI size and UE speed in relation with the fast fading characteristics

An indisputable advantage is obtained by the fast VSF when the latter one is able to adjust the UE transmission power at the appropriate time instant in order to mitigate deep fades in the propagation path loss. The SF can change only at the beginning of transmission time intervals, the latter ones being equal to multiples of radio frames [62]. In the following, a TTI is equal to one radio frame.

According to Rayleigh statistics the envelope of a signal, that is distorted by fast fading, experiences in average two fades every wavelength (figure B.1). Considering the fast fading dynamics (up to approximately 60 dB) and the number of PC steps per radio frame (15), it can be understood that in case a TTI corresponds to a wavelength period, it is almost impossible for the fast VSF mechanism to adapt the SF applied for transmission.

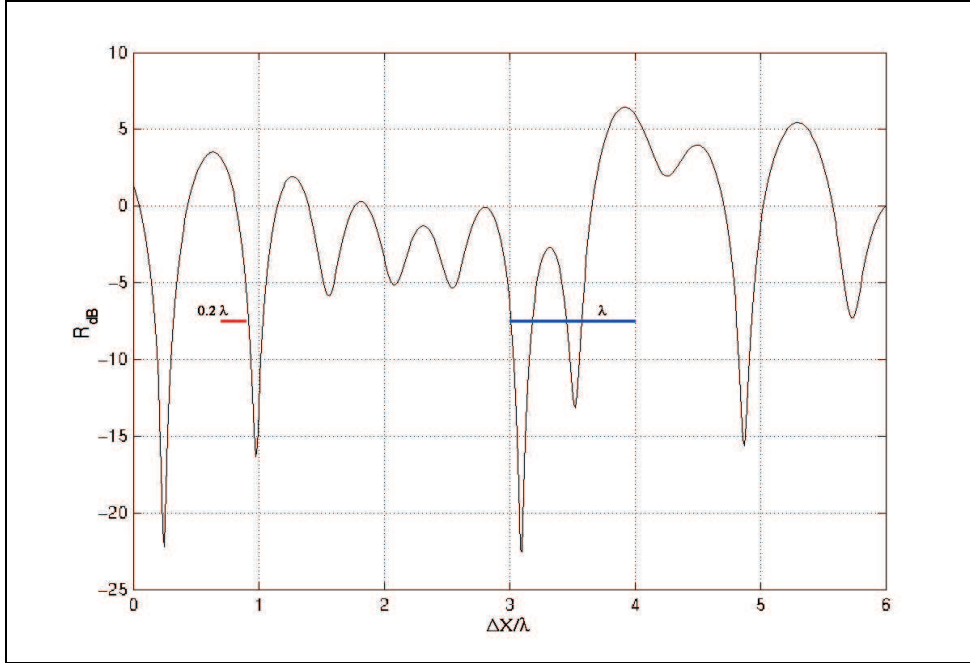


Figure B.1: Fast fading in relation with the TTI size.

Therefore, the fast fading experienced in two consecutive TTIs must be correlated. Hence, the space separation between two consecutive TTIs should be significantly smaller than a wavelength period. The situation is better depicted in figure B.1, where  $\Delta x/\lambda$  is the space separation in terms of number of wavelengths and  $R_{dB}$  is the received varying signal power, normalized so as the mean average received power equals 0 dB. This figure illustrates two cases; in the first one, the TTI is equal to one fifth of the wavelength period and in the second one the TTI is equal to one wavelength period. The SF changes can effectively compensate the deep fade, in case the TTI corresponds to 0.2 wavelength periods.

The fast VSF scheme can be efficient when the fast fading experienced between two consecutive TTIs exhibits a correlation higher than  $1/e$ . We choose to have as reference values the ones that correspond to 0.7 and to 0.5 autocorrelation. Figure B.2 illustrates the Rayleigh envelope autocorrelation of fast fading ([55]). The Clarke's scattering model is used. It can be seen that autocorrelation values of 0.5 and 0.7 correspond to distances equal to  $\lambda/10$  and  $\lambda/5$  respectively. Herein, these distance values are used in order to determine the required TTI at various UE speeds.

Table B.1 reports the time separation needed in order to obtain an autocorrelation of about 0.7 and 0.5 respectively, in case of different UE speeds. According to 3GPP specifications ([65]), in uplink transmission the wavelength is equal to 14 cm. (This wavelength corresponds to a central frequency of 2140 MHz). The time intervals in table B.1 correspond to distances equal to 1.4 cm and 2.8 cm respectively.

Values in table B.1 show that in case of TTI size equal to 10 ms, the fast VSF can successfully “follow” the fast fading only in a low mobility scenario. An efficient fast VSF

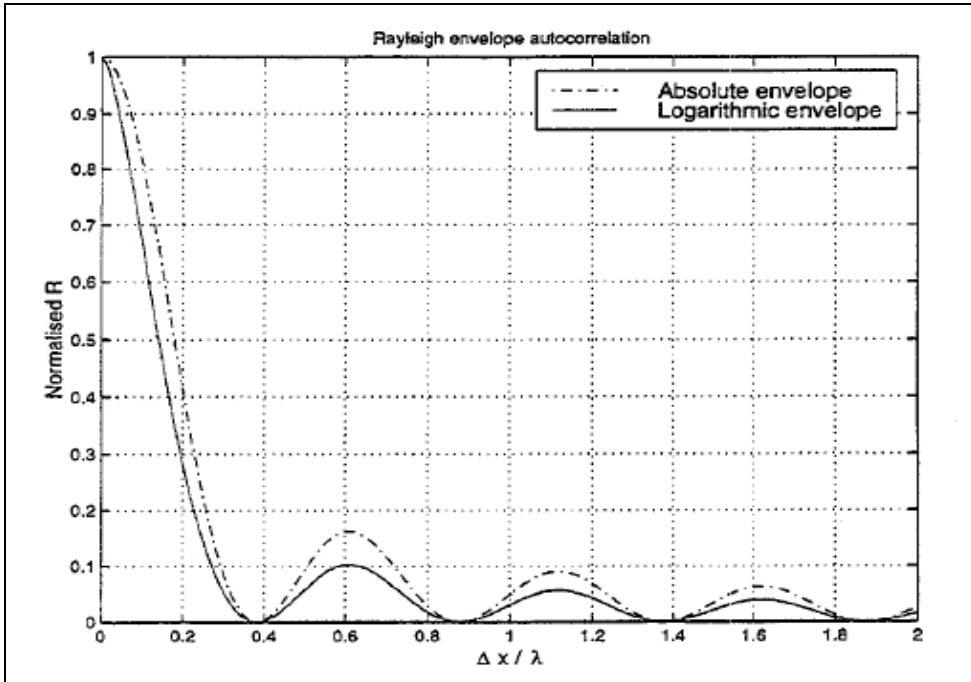


Figure B.2: Envelope autocorrelation of fast fading in Clarke's scattering model ([55]).

UE Speed km/h	Time separation for 0.7 autocorrelation	Time separation for 0.5 autocorrelation
3	16.8 ms	33.6 ms
30	1.7 ms	3.4 ms
50	1.0 ms	2.0 ms
100	0.5 ms	1.0 ms

Table B.1: Time required in order to have an auto-correlation equal to 0.7 and 0.5 for various UE speeds.

scheme, even for users moving at higher speeds requires shorter TTIs.

## B.2 Simulation Studies and Results

The efficiency of the fast VSF scheme to reduce the variance of the UE transmission power is tested by means of simulations. Therein, the performance of a single-link is tested. The fast VSF scheme presented in chapter 5 is applied. Considering that the potential of the fast VSF is assessed with this simulator, no limitations are applied in terms of UE transmission power and in terms of SF applied, i.e. the UE can apply any SF value (even if it is not an integer) in order to maintain its transmission power as constant as possible.

For the simulation, a single UE transmitting initially at 60 kbps is used. It is located at a distance that corresponds to 125 dB radio path loss. The interference is constant

Parameters	Values
Simulation Time	336.448 [sec]
Eb/Notarget	4 [dB]
UE Max Tx Power	$+\infty$ [dBm]
UE Min Tx Power	$-\infty$ [dBm]
UE Tx Power Target	11 [dBm]
Margin	1.5 [dB]
PC step	1 [dB]
PC Delay	1 slot
$I_{total}$	-100 [dBm]
Radio Path Loss	125 [dB]

Table B.2: Main simulation parameters.

in the cell, it is equal to -100 dBm. From these values, the transmission power target is computed to be equal to 11 dBm. The so-called “Margin” in chapter 5 is equal to 1.5 dB. Fast PC is performed 15 per radio frame and the PC step is equal to 1 dB. Table lists the principal simulation parameters.

The transmission power of the UE is traced for various UE speeds and for different TTI sizes. Figure B.3 displays the standard deviation of the UE transmission power in function of UE speed for the cases of TTI size equal to 15, 5 and 3 slots. In the absence of the fast VSF scheme at low speeds, the standard deviation of the UE transmission power is equal to 5.5 dB. related literature ([45]), it is known that this value corresponds to the standard deviation of a fading radio channel. This value is expected since, in absence of fast VSF, the statistics of the transmission power of an ideally power controlled UE are similar to the ones of the fast fading. In the same figure (B.3), it can be seen that when the TTI size is 10 ms (equal to 15 slots) the fast VSF can reduce the variance of the transmitted power by the UE only when the UE speed is below 5 km/h.

Figure B.3 shows also the the variance of the UE transmission power decreases with shorter TTIs. In the same figure, it can be seen that the standard deviation increases till a certain speed. For higher speeds the standard deviation then decreases. This effect is noticed for all the TTI lengths. However, it is more evident in the case the TTI is equal to 15 slots. The reason for this being that the power control PC is able to “follow” fades till certain UE speeds (around 20 km/h). Thus, the UE transmission power reaches often high and low peaks (which are related to the deep and flat fades of the radio propagation channel). In higher UE speeds, the mobile goes through several fades during the duration of a single TTI and the PC is unable to “follow” these changes. This leads to an UE transmission power that fluctuates around the mean and consequently to a lower standard deviation.

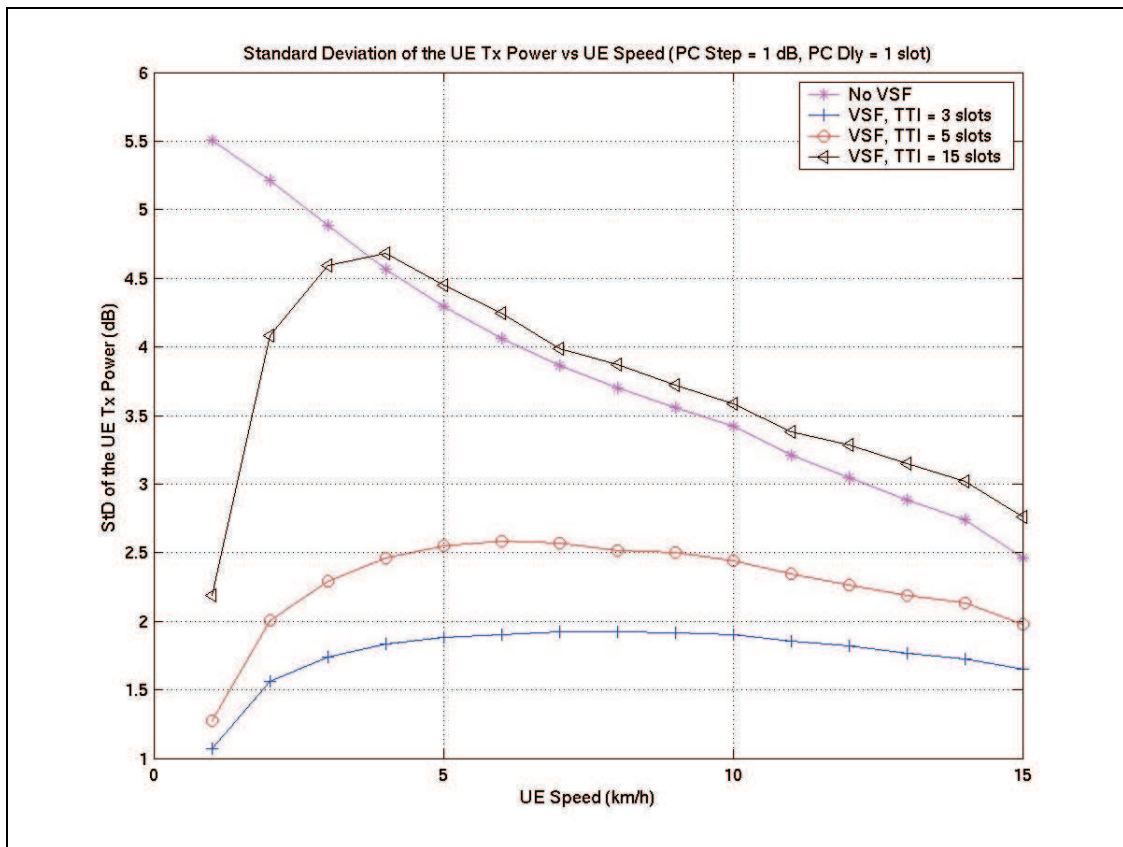


Figure B.3: Standard deviation of the UE transmission power versus UE speed for the cases the fast VSF is deactivated and activated.

# Bibliography

- [1] Ameigeiras, P., J., Lopez, I., Wigard, J., Madsen, N. A. H., Mogensen, P., “Generic Traffic Models for Packet Data Services in 3G Wireless Networks”, *Proceedings of Wireless Personal Multimedia Communications Conference, WPMC 2001*, September 2001.
- [2] Anderlind, E., Zander, J., “A Traffic Model for Non-Real-Time Data Users in a Wireless Radio Network”, *IEEE Communications Letters*, Vol. 1, No. 2, March 1997.
- [3] Andrews, M., Kumaran, K., Ramanan, K., Stolyar, A., Whiting, P., Vijayakumar, R., “Providing quality of service over a shared wireless link”, *IEEE Communications Magazine*, Volume 39, Issue 2, pp. 150-154, Feb. 2001.
- [4] Baey, S., Dumas, M., Dumas, M. C., “QoS Tuning and Resource Sharing for UMTS WCDMA Multiservice Mobile”, *IEEE Transactions on Mobile Computing*, Vol. 1, No. 3, July-September 2002.
- [5] Balachandran, K., Demetrescu, C., Ejzak, R., Nanda, S., Xie, H., “MAC Layer Statistical Design for Statistical Multiplexing of Voice and Data over EGPRS”, *Proceedings of Wireless Communications and Networking Conference 2000, WCNC 2000 IEEE*, Page(s): 913-923, vol. 2.
- [6] Borella, M. S., “Source Models of Network Game Traffic”, *Proceedings of Network+Interop'99 Engineers Conference*, May 1999.
- [7] Boyer, P., Stojanovic, M., Proakis, J., “A simple generalization of the CDMA reverse link pole capacity formula”, *IEEE Transactions on Communications*, Volume 49, Issue 10, pp. 1719-1722, October 2001.
- [8] Brady, P. T., “A Model for Generating On-Off Speech Patterns in Two-Way Conversation”, *The Bell Systems Technical Journal*, Volume 48, No. 7, September 1969.
- [9] Chang, K., Han, Y., “QoS-based adaptive scheduling for a mixed service in HDR system”, *Proceedings of the 13th IEEE International Symposium on Personal, Indoor and Mobile Radio Communications (PIMRC 2002)*, Volume 4, pp. 1914-1918, September 2002.
- [10] Chin-Lin, I., Nanda, S., “Load and Interference Based Demand Assignment (LIDA) for Integrated Services in CDMA Wireless Systems”, *Proceedings of IEEE Global*

- Telecommunications Conference (GLOBECOM '96)*, Volume 1, pp. 235-241, Nov. 1996.
- [11] Dimou, K., Godlewski, P. "MAC Scheduling For Uplink Transmission in UMTS WCDMA", *Proceedings of 53rd IEEE Conference on Vehicular Technology (VTC Spring 2001)*, Volume 4, pp. 2625-2629, May 2001.
- [12] Dimou, K., Godlewski, P., "Transport Format Combination Selection Procedure in Uplink in MAC UMTS: Algorithms and Performance", *Proceedings of International Conference on Third Generation and Beyond, 3G Wireless*, May 2001.
- [13] Dimou, K., Godlewski, P., "Scheduling Issues For Uplink Transmission in WCDMA UMTS", *Proceedings of 4th Symposium on Wireless Personal Multimedia Communications, WPMC'01, Volume 2*, pp. 991-995, September 2001.
- [14] Dimou, K., Godlewski, P., "Decentralized Uplink Packet Data Transmission in WCDMA Based Systems", *Proceedings of IST Mobile and Wireless Telecommunications Summit, Volume 1*, pp. 719-723, May 2002.
- [15] Dimou, K., Rosa, C., Sørensen, T., B., Wigard, J., Mogensen, P., "Performance of Uplink Packet Services in WCDMA", *Proceedings of the 57th IEEE Conference on Vehicular Technology (VTC Spring 2003)*, Volume 3, pp. 2071-2075, April 2003.
- [16] Femenias, G., Carrasco, L., "WCDMA MAC Protocol for Multimedia Traffic Support", *Proceedings of 51st IEEE Conference on Vehicular Technology (VTC Spring 2000)*, May 2000.
- [17] Fiorini, A., "Uplink user bit-rate adaptation for packet data transmissions in WCDMA", *Proceedings of the 11th IEEE International Symposium on Personal, Indoor and Mobile Radio Communications (PIMRC 2000)*, Volume 2, pp. 1510-1514, September 2000.
- [18] Garg, V., Garg, M., "Role of MAC/RLC in Achieving Higher-data Rates and QOS in Third Generation (3G) UMTS System", *Proceedings of IEEE International Conference on Personal Wireless Communications, 2000*, pp. 459 -463.
- [19] Ghosh, A., Cudak, M., Felix, K., "Shared Channels for Packet Data Transmission in W-CDMA", *Proceedings of 50th IEEE Conference on Vehicular Technology (VTC Fall 1999)*, vol. 2, pp. 943-947, October 1999.
- [20] Hartmann, M., Lappetelainen, A., Holma, H., Hamalainen, S., Slanina, P., Salonaho, O., "A Novel Interface Between Link and System Level Simulations", *Proceedings of ACTS Mobile Telecommunications Summit*, Aalborg, Denmark, pages 599-604, October 1997.
- [21] Holma H., Laakso J., "Uplink Admission Control and Soft Capacity with MUD in CDMA", *Proceedings of 50th IEEE Conference on Vehicular Technology (VTC Fall 1999)*, pp. 431-435, October 1999.

- 
- [22] Holma, H., Toskala, A., "WCDMA for UMTS: Radio access for third generation mobile communications", John Wiley and Sons, 2002.
- [23] Hwang, G-H., Cho, D-H, "Dynamic rate control based on interference and transmission power in 3GPP WCDMA system", *Proceedings of 52nd IEEE Conference on Vehicular Technology, (VTC Fall 2000)*, Volume 6, pp. 2926-2931, September 2000.
- [24] Hytönen, T., "Optimal Wrap-around Network Simulation", Helsinki University of Technology, Institute of Mathematics Research Reports, 2001, [www.math.hut.fi/reports/](http://www.math.hut.fi/reports/), Report Number A432.
- [25] Iracheta, M., Poza, M., "On the Quest of a Better World Wide Web Traffic Model for UMTS", *Proceedings of International Conference in 3G Mobile Communication Technologies (3G 2000)*, pp. 456-460, May 2000.
- [26] Jakes, W., "Microwave Mobile Communications", IEEE Press, 1994.
- [27] Jalali, A., Padovani, R., Pankaj, R., "Data Throughput of CDMA-HDR a High Efficiency-High Data Rate Personal Communication Wireless System", *Proceedings of 51st IEEE Conference on Vehicular Technology (VTC Spring 2000)*, vol. 3, pp. 1854-1858, May 2000.
- [28] Kaaranen, H., Ahtiainen, A., Laitinen, L., Naghian, S., Niemi, V., "UMTS Networks: Architecture, Mobility and Services", John Wiley and Sons, 2001.
- [29] Kinnunen, P., "Advanced and Basic RRM Project:ABRRM - Actual Value Interface Tables for Wallu Simulator", *Nokia Internal Report, V0.3.0*.
- [30] Kleinrock, L., "Queuing Systems, Volume II: Computer Applications", John Wiley and Sons, 1976.
- [31] Kolding, T. E., Pedersen, K. I., Wigard, J., Frederiksen, F., Mogensen, P., E., "High Speed Downlink Packet Access: WCDMA Evolution", *IEEE Vehicular Technology Society News*, pp. 4-10, February 2003.
- [32] Kumar, S., Nanda, S., "High Data-Rate Packet Communications for Cellular Networks Using CDMA: Algorithm and Performance", *IEEE Journal in Selected Areas of Communication*, vol. 17, no. 3, pp. 472-492, March 1999.
- [33] Kumar, P., Sampath, A., Holtzman, J., "On setting reverse link target SIR in a CDMA system", *Proceedings of IEEE Conference on Vehicular Technology (VTC 1997)*, May 1997, volume 2, pages 929-933.
- [34] Kumaran, K., Qian, L., "Uplink Scheduling in CDMA Packet-Data Systems", *Proceedings of INFOCOM 2003, 22nd Annual Joint Conference of the IEEE Computer and Communications Societies*, Volume 1, pp. 292-300, March-April 2003.
- [35] Kwok, Y-K., Lau, V.K.N., "System modeling and performance evaluation of rate allocation schemes for packet data services in wideband CDMA systems", *IEEE Transactions on Computers*, Volume 52, Issue 6, pp. 804-814, June 2003.

- 
- [36] Lagrange, X, Godlewski, P., Tabbane, S., “Réseaux GSM-DCS”, Edition Hermès.
- [37] Lee, S., Song, Y. J., Cho, D. H., Lee, H., Park, S. D., Kim, Y., “The Design and Performance Evaluation of High Speed Packet Data MAC Protocol for CDMA Based IMT2000”, *Proceedings of IEEE Global Telecommunications Conference, Globecom’99*, Page(s): 2694-2698.
- [38] Mah, B., “An Empirical Model of HTTP Network Traffic”, *Proceedings of INFOCOM’97*, Volume 2, Kobe, Japan. April 1997.
- [39] Mandyam, G. D., Tseng, Y. C., “Packet Scheduling in CDMA Systems Based on Power Control Feedback”, *Proceedings of IEEE Conference on Communications, ICC’01*, vol. 9, pp. 2877-2881, June 2001.
- [40] Mella, P., “System Feature Specification for Packet Scheduler”, *Nokia Internal Report, V3.0.2*.
- [41] Miltiades, E., et al. “A Multiuser Description Traffic Source Model”, *IEEE Transactions on Communications*, vol. 44, no. 10, October 1996.
- [42] Nieminen, T., “Report on WWW-Traffic Modeling and WaveLAN Measurements”, Helsinki University of Technology, Communications Laboratory, 1988.
- [43] Ojanpera, T., Prasad, R., “An overview of air interface multiple access for IMT-2000/UMTS”, *IEEE Communications Magazine*, vol. 36, Issue: 9, pp. 82-86, September 1998.
- [44] Omiyi, P.E., O’Farrell, T., “Maximising spectral-efficiency in 3rd generation radio-access-networks using low-complexity multiple-access-control protocols”, *Proceedings of Third International Conference on 3G Mobile Communication Technologies (Conf. Publ. No. 489)*, pp. 520-524, May 2002.
- [45] Parsons, D., “The Mobile Radio Propagation Channel”.
- [46] Pérez-Romero, J., Sallent, O., Agustí, R., “Admission Control for Different UE-MAC Algorithms in UTRA-FDD”, *Proceedings of IEE Conference on 3G Mobile Communication Technologies*, pp. 256-260, May 2002.
- [47] Prasad, R., “Universal Wireless Personal Communications”, Artech House Publishers, 1998.
- [48] Ramakrishna, S., Holtzman, J. M, “A Scheme for Throughput Maximization in a Dual-Class CDMA System”, *IEEE Journal on Selected Areas in Communications*, vol. 16, No. 6, August 1998.
- [49] Rapeli, J., “UMTS: Targets, System Concept, and Standardization in a Global Framework”, *IEEE Personal Communications*, vol. 2, no. 1, pp. 20-28, February 1995.
- [50] Rappaport, T., “Wireless Communications, Principles and Practice”, IEEE Press, 1996.

- 
- [51] Sallent, O., Rérez-Romero, J., Agustí, R., Casadevall, F., “Provisioning Multimedia Wireless Networks for Better QoS: RRM Strategies for 3G W-CDMA”, *IEEE Communications Magazine*, pp. 100-104, February 2003.
- [52] Sallent, O., Pérez-Romero, J., Casadevall, F. J., Agustí, R. “An Emulator Framework for a New Radio Resource Management for QoS Guaranteed Services in W-CDMA Systems”, *IEEE Journal on Selected Areas in Communications*, Volume 19, No. 10, pp. 1893-1903, October 2001.
- [53] Sánchez, J., Pérez-Romero, J., Sallent, O., Agustí, R., “Mixing Conversational and Interactive Traffic in the UMTS Radio Access Network”, *4th International Workshop on Mobile and Wireless Communications Networks*, pp. 597-601, September 2002.
- [54] Schwartz, M., “Telecommunication Networks, Protocols, Modelling and Analysis”, Addison-Wesley Publishing Company, 1988.
- [55] Sørensen, T., B., “Correlation Model for Slow Fading in a Small Urban Macro Cell”, *Proceedings of the 9th IEEE International Symposium on Personal, Indoor and Mobile Radio Communications*, vol. 3, pp. 1161-1165, September 1998.
- [56] Tanenbaum, A. S., “Computer Networks”, Prentice Hall, 1999.
- [57] Villier, E., Legg, P., Barrett, P., “Packet Data Transmissions in a WCDMA Network - Examples of Uplink Scheduling and Performance”, *Proceedings of 51st IEEE Conference on Vehicular Technology (VTC Spring 2000)*, May 2000.
- [58] Viterbi, A. J., “CDMA: Principles of Spread Spectrum Communication”, Addison-Wesley, 1995.
- [59] Walke, B. H., “Mobile Radio Networks - Networking and Protocols”, John Wiley and Sons, 1999, ISBN 0-471-97595-4.
- [60] Wigard, J., “Uplink Traffic Models”, presentation slides, June 2002.
- [61] “Quality of Service (QoS) Concept and Architecture; Release 5”, 3rd Generation Partnership Project, 3GPP TS 23.107, V5.7.0 (2002-12).
- [62] “UE Radio transmission and Reception (FDD); Release 5”, 3rd Generation Partnership Project, 3GPP TS 25.101, V5.7.0 (2003-06).
- [63] “UTRA (BS) FDD; Radio transmission and Reception; Release 5”, 3rd Generation Partnership Project, 3GPP TS 25.104, V5.7.0 (2003-06).
- [64] “Requirements for Support of Radio Resource Management (FDD); Release 5”, 3rd Generation Partnership Project, 3GPP TS 25.133, V5.8.0 (2003-09).
- [65] “Physical Layer - General Description; Release 5”, 3rd Generation Partnership Project, 3GPP TS 25.201, V5.2.0 (2002-09).
- [66] “Physical channels and mapping of transport channels onto physical channels (FDD); Release 5”, 3rd Generation Partnership Project, 3GPP TS 25.211, V5.4.0 (2003-06).

- 
- [67] “Multiplexing and channel coding (FDD); Release 5”, 3rd Generation Partnership Project, 3GPP TS 25.212, V5.6.0, (2003-09).
  - [68] “Spreading and Modulation (FDD); Release 5”, 3rd Generation Partnership Project, 3GPP TS 25.213, V5.4.0 (2003-09).
  - [69] “Physical layer procedures (FDD); Release 5”, 3rd Generation Partnership Project, 3GPP TS 25.214, V5.6.0 (2003-09).
  - [70] “Physical layer - Measurements (FDD); Release 5”, 3rd Generation Partnership Project, 3GPP TS 25.215, V5.5.0 (2003-09).
  - [71] “Radio Interface Protocol Architecture; Release 5”, 3rd Generation Partnership Project, 3GPP TS 25.301, V5.2.0 (2002-09).
  - [72] “Services Provided by the Physical layer; Release 5”, 3rd Generation Partnership Project, 3GPP TS 25.302, V5.6.0 (2003-09).
  - [73] “Medium Access Control (MAC) protocol specification; Release 5”, 3rd Generation Partnership Project, 3GPP TS 25.321, V5.6.0 (2003-09).
  - [74] “Radio Link Control (RLC) protocol specification; Release 5”, 3rd Generation Partnership Project, 3GPP TS 25.322, V5.6.0 (2003-09).
  - [75] “Packet Data Convergence Protocol (PDCP) specification, Release 5”, 3rd Generation Partnership Project, 3GPP TS 25.323, V5.2.0 (2002-09).
  - [76] “Broadcast/Multicast Control (BMC) specification; Release 5”, 3rd Generation Partnership Project, 3GPP TS 25.324, V5.3.0 (2003-03).
  - [77] “Radio Resource Control Protocol Specification; Release 5”, 3rd Generation Partnership Project, 3GPP TS 25.331, V5.6.0 (2003-09).
  - [78] “Feasibility Study for Enhanced Uplink for UTRA FDD; Release 6”, 3rd Generation Partnership Project, 3GPP TR 25.896, V1.0.0 (2003-09).
  - [79] “Radio Resource Management Strategies; Release 5”, 3rd Generation Partnership Project, 3GPP TR 25.922, V5.1.0 (2003-09).
  - [80] “RF System Scenarios”, 3rd Generation Partnership Project, 3GPP TR 25.942, V5.1.0 (2003-06).
  - [81] “Mandatory speech CODEC speech processing functions; AMR speech CODEC; General Description; Release 5”, 3rd Generation Partnership Project, 3GPP TR 26.071, V5.0.0 (2002-06).
  - [82] “Common Test Environments for User Equipment (UE); Conformance Testing; Release 4”, 3rd Generation Partnership Project, 3GPP TS 34.108, V4.8.0 (2003-09).
  - [83] “Universal Mobile Telecommunications System (UMTS); Selection procedures for the choice of radio transmission technologies of the UMTS”, ETSI Technical Report 101 112 (UMTS 30.03).

# List Of Publications

1. Dimou, K., Godlewski, P., “MAC Scheduling For Uplink Transmission in UMTS WCDMA”, *Proceedings of 53rd IEEE Conference on Vehicular Technology (VTC Spring 2001)*, Volume 4, pp. 2625-2629, May 2001.
2. Dimou, K., Godlewski, P., “Transport Format Combination Selection Procedure in Uplink in MAC UMTS: Algorithms and Performance”, *Proceedings of International Conference on Third Generation and Beyond, 3G Wireless*, May 2001.
3. Dimou, K., Godlewski, P., “Scheduling Issues For Uplink Transmission in WCDMA UMTS”, *Proceedings of 4th Symposium on Wireless Personal Multimedia Communications, WPMC'01*, Volume 2, pp. 991-995, September 2001.
4. Dimou, K., Godlewski, P., “Decentralized Uplink Packet Data Transmission in WCDMA Based Systems”, *Proceedings of IST Mobile and Wireless Telecommunications Summit*, Volume 1, pp. 719-723, May 2002.
5. Dimou, K., Rosa, C., Sørensen, T., B., Wigard, J., Mogensen, P., “Performance of Uplink Packet Services in WCDMA”, *Proceedings of the 57th IEEE Conference on Vehicular Technology (VTC Spring 2003)*, Volume 3, pp. 2071-2075, April 2003.